Water holding characteristics of pumice fragments in New Zealand Pumice Soils

---

A thesis
submitted in partial fulfilment
of the requirements for the Degree of
Master of Science

at
Lincoln University
by
Julie Danielle Gillespie

Lincoln University
2020

Abstract of a thesis submitted in partial fulfilment of the requirements for the Degree of Master of Science.

Water holding characteristics of pumice fragments in New Zealand Pumice Soils

by

Julie Danielle Gillespie

Nutrient budget models are used throughout New Zealand to monitor the movement of water and nutrients in farm systems. Currently there is limited knowledge pertaining to the water release and water holding characteristics of a variety of coarse fragments within soils, and of the influence that some clasts, such as pumice, have on nutrient and water movement through the soil.

The role of pumice clasts in soil has been largely unstudied in New Zealand, with studies focusing on the physical and chemical characteristics of the soil profile. International studies on the physical properties of pumice clasts have found that the characteristics of pumice in different deposits vary. Due to the variability in the results of international studies and lack of data on the physical properties of pumice fragments in New Zealand soils, the properties of New Zealand pumice clasts cannot be derived or assumed. To fill this knowledge gap, the water holding capacity of pumice clasts produced in a mid-Quaternary New Zealand volcanic eruption has been quantified through the development of a water release curve. The curve, from a matric potential of -3 kPa to -1500 kPa has been produced from data obtained in a trial using suction plates under vacuum and a WP4C dewpoint hygrometer.

The study found that:

The assumption that the behaviour of soil fines as a matrix is consistent as the ratio of pumice clasts to soil fines changes is false. At any given matric potential, the water content of the soil fines in relation to the proportion of the pumice clasts was variable.

The method developed to determine the water content of the pumice clasts between saturation and -80 kPa was most effective when matrix variability was minimised by adding glass fragments to keep the total clast content of the core constant.

Keywords: pumice, New Zealand, water release, available water content, water holding capacity, Pumice Soil, coarse fragments, Overseer, S-map.

Acknowledgements

Firstly I would like to acknowledge my supervisors; Associate Professor Peter Almond, Dr Henry Chau and Dr Sam Carrick, for your guidance and support. Thank you Peter for all of the time and effort you have put in to help me work through this project and develop my thesis.

To Balin Robertson. Thank you for your mentorship in the lab and the extensive amount of time you put into troubleshooting to get this experiment going. I am very grateful for all of your work, I couldn't have don't it without you.

Thank you to John Payne and Graeme Rogers at Landcare Research for your technical support in getting the experiment up and running.

To Judith, Josh and the Soil Judging Team. Thank you for your encouragement and all the great times preparing for and away at the competitions.

Thank you Fiona for being a sounding board, supporter and great friend over this time.

To my incredible mentor, Paula. Thank you for helping me to organise my thoughts, develop my time management, grow my confidence and especially for taking the time to read my thesis.

And finally to my family. Thank you for all of your support, encouragement, care and tolerance over the last year and for your interest in my work.

Table of Contents

Abstract ..... **ii**

Acknowledgements ..... **iv**

Table of Contents ..... **v**

List of Tables ..... **vii**

List of Figures ..... **viii**

Abbreviations **10**

Chapter 1 Introduction **11**

1.1 Aims 16

1.2 Hypothesis 16

Chapter 2 Review of the Literature **17**

2.1 Introduction 17

2.2 Water storage in soils 17

2.2.1 Matric potential 17

2.2.2 Water content 19

2.2.3 Measuring soil water 20

2.2.4 Water retention curve 22

2.2.5 Soil moisture status 22

2.2.6 Soil water storage and rock fragments 23

2.3 Pedotransfer functions 24

2.3.1 Overseer 26

2.4 Pumice 27

2.4.1 Formation 28

2.5 Pumice Soil (NZSC) 34

2.6 Pumice clast physical properties 36

2.7 Determining pumice water content 41

2.7.1 Pressure plates 41

2.7.2 Suction plates 42

2.7.3 Time domain reflectometry 43

Chapter 3 Methods **45**

3.1 Equipment 45

3.2 Experiment 1 47

3.2.1 Analysis 1 50

3.2.2 Analysis 2 51

3.3 Experiment 2 53

3.3.1 Experimental design and mathematical analysis 54

3.3.2 Set up 57

3.3.3 Analysis 3 62

3.3.4 Analysis 4 62

Chapter 4 Results **65**
4.1 Experiment 1 65
4.1.1 Analysis 1 67
4.1.2 Analysis 2 68
4.2 Experiment 2 70
4.2.1 Analysis 3 70
4.2.2 Analysis 4 70

Chapter 5 Discussion **77**
5.1 Method evaluation 77
5.1.1 Experiment 1 77
5.1.2 Experiment 2 80
5.1.3 Soil water release curve 82
5.2 Comparison to other studies of water release from Taupō pumice 84
5.3 S-map 87

Chapter 6 Conclusions **88**
6.1 Limitations 89
6.2 Further research 89

References **91**

Appendix A Core weight – Experiment 1 ..... **101**
A.1 Analysis 1 102
A.2 Analysis 2 104

Appendix B Experiment 2 ..... **108**
B.1 Analysis 4 110

Appendix C Equations relating to bulk density error **112**

List of Tables

Table 2.1: Physical properties of pumice clasts used in various international studies. ρ_p – particle density, ρ_b – bulk density, ϕ_T – total porosity, FC – Field capacity, PWP – Permanent wilting point, AWC – Available water content, EAW - easily available water. 38
Table 3.1: Experimental design of Experiment 2, using glass to enable to soil matrix to remain at a constant volume. 55
Table 3.2: Proportions of soil fines, pumice clasts and glass fragments packed in each core. 57
Table 4.1: R^2 values of the linear trend lines fitted to the raw data and scaled data for each level of suction applied to the cores. 71

Table A.1: Soil weight at equilibrium - analysis 1 and 2 101
Table A.2: Gravimetric water content of pumice clasts, determined using Equation 3.3. Proportion of pumice used in each core is presented gravimetrically (0.05 = 10%). 102
Table A.3: Volumetric water content of pumice, determined using Equation 3.4. 103
Table A.4: Linear regression analysis of gravimetric water content of Pumice Clasts 10-40%. 104
Table A.5: Linear Regression analysis of gravimetric water content of Pumice Clasts 10-30%. 105
Table A.6: Statistical analysis of Linear Regression for 10-40% clast content. Ws – water content of the soil, Wp – water content of pumice, θw – gravimetric water content, SE – standard error, ρb – bulk density (of fines packed in core/pumice clasts), θv – volumetric water content. 106
Table A.7: Statistical analysis of Linear Regression for 10-30% clast content. Ws – water content of the soil, Wp – water content of pumice, θw – gravimetric water content, SE – standard error, ρb – bulk density (of fines packed in core/pumice clasts), θv – volumetric water content. 107

Table B.1: Soil weight at equilibrium for suction plate experiment. 109
Table B.2: Volumetric water content of the soil cores used on the suction plates and Dewpoint potentiometer. 110
Table B. 3: Volumetric water contents at matric potentials determined using the Dewpoint Potentiometer for pumice clasts and soil fines 110
Table B.4: Statistical analysis of Analysis 4, where each data point was individually scaled. 111

List of Figures

Figure 1.1: GDP ($m) produced by forestry activities and services per region for 2016 (From Nixon, Gamperle, Pambudi, & Clough, 2017). 14
Figure 1.2: The 2016 contribution of dairy farming and processing to regional GDP in $ million (From Ballingal & Pambudi, 2017). 15
Figure 2.1: Soil water characteristic curves for soils of three different textural classes. pF= log(-ϕ_m) where ϕ_m is the matric potential in cm, θ is the volumetric water content, WP is the wilting point and FC is field capacity (From Shukla, 2014). 22
Figure 2.2: The Pacific Ring of Fire is made up of a series of volcanic arcs and ocean trenches that partially encircle the Pacific Basin (From Jacquelyne & Tilling, 1999). 29
Figure 2.3: Phases of the 232 ± 10 AD Taupō eruption. The 'V' shaped incision into the Hatepe Ash indicates a break in the eruption lasting approximately 3 weeks, in which erosion (E) caused by torrential floods from high rain carved gullies into the soft ash deposit (Lowe & King, 2015). 31
Figure 2.4: The Taupō Volcanic Zone, a 300 km long volcanic depression in the Central North Island of New Zealand and the extent of the area covered by the Taupō Ignimbrite and 10 cm isopach for airfall material (From Hogg et al., 2012). ... 31
Figure 2.5: Soil groups of the Pumice Soil order found in the Central North Island of New Zealand. A further small area of Orthic Pumice soils are found to the south east of Mt Taranaki (Map created in QGIS with soil data from Landcare Research, 2010). 34
Figure 3.1: Gauze secured to the base of the PVC core to prevent soil loss when moving the packed cores. 45
Figure 3.2: Shut-off valve (red and black) used to isolate the plate from the vacuum. The manifold is the white PVC pipe connected to each plate through the shut-off valve and 6 mm tube and to the vacuum pump and collection flask (Figure 3.4, Figure 3.10). 47
Figure 3.3: A silica flour and RO water slurry was applied to the entire surface of the plate and smoothed to provide an even coating to ensure contact between the base of the soil core and the suction plate. 49
Figure 3.4: Arrangement of the components of Experiment 1 including the 5 boxes containing the soil cores, grey and blue vacuum pump, water collection flask and computer with tensioVIEW controlling the vacuum. 49
Figure 3.5: Location of source of pumice clasts used in soil cores. The pumice pit is located within the extent of the Taupō ignimbrite, shown by the red outline, on the lilac coloured map units which represent non-welded ignimbrite (Adapted from GNS, n.d.; Hogg, Lowe, Palmer, Boswijk, & Ramsey, 2012). 53
Figure 3.6: Split glass fragments packed into the soil cores to enable the matrix to remain at a constant volume. 54
Figure 3.7: Glass bead method to determine the bulk density of pumice clasts. 56
Figure 3.8: Packed soil core containing soil matrix, pumice clasts and glass fragments. ... 58
Figure 3.9: 1 mm high, 110 mm diameter silica layer on the suction plate to ensure connectivity between the base of the core and the suction plate. 59
Figure 3.10: Layout and set up of manifold system used in Experiment 2. 59
Figure 3.11: Lay out of relocated experimental set up. 60

Figure 3.14: Iterations of the scaling of each data point to determine the water content of the soil at pumice at a matric potential of -10 kPa. The notation 10 kPa (blue) is the unscaled data and 10 kPa' (green) is the scaled data. 64
Figure 4.1: New Zealand texture triangle with fractions of fine earth present in the Acacia Bay soil used in Experiment 1 indicated in red. (From Milne, Clayden, Singleton, & Wilson, 1995). 65
Figure 4.2: Condensation gradient present as both distance from pump increases and clast content increases. The vacuum pump is situated to the left of the 0% pumice content core and the 40% pumice clast core is closest to the lab wall. 66
Figure 4.3: Total gravimetric water content of soil cores. 67
Figure 4.4: Volumetric water content of pumice clasts at different suctions determined using Analysis 1. 67
Figure 4.5: Linear regression for cores containing 10-40% clast contents. 68
Figure 4.6: Plot of gravimetric water contents for the different matric potentials applied against the gravimetric content of pumice clast for 10% – 30% pumice clast treatments. 69
Figure 4.7: Volumetric water release curve for pumice clasts and soil fines, with error included for each matric potential for 10-30% pumice clast treatments. 69
Figure 4.8: Comparison of the volumetric water contents of the pumice clasts and soil fines. 72
Figure 4.9: Volumetric water content of pumice clasts determined using individually scaled regression analysis data from the suction plate experiment and Dewpoint Potentiometer data. 73
Figure 4.10: Soil water release curve for scaled pumice clasts, with four unimodal equations developed using SWRC Fit (Seki, 2007). 74
Figure 4.11: Soil water release curve for scaled pumice clasts, fitted with the Kosugi equation using SWRC Fit (Seki, 2007). 74
Figure 4.12: Soil water release curve for scaled pumice clasts, with the data point of the volumetric water content at 100 kPa removed, fitted with four unimodal equations using SWRC Fit (Seki, 2007). 75
Figure 4.13: Soil water release curve for scaled pumice clasts, with the data point of the volumetric water content at 100 kPa removed, fitted with the Kosugi model using SWRC Fit (Seki, 2007). 75
Figure 4.14: Comparison of the volumetric water content of the pumice clasts and soil fines for data collected using suction plates and Dewpoint PotentiaMeter. .. 76
Figure 5.1: Estimated ratio of the true soil bulk density to target soil bulk density against the proportion of pumice clasts for Experiment 1. 79
Figure 5.2: Estimated ratio of the true soil bulk density to the target soil bulk density against the proportion of pumice clasts for Experiment 2. 81

Figure B.1: Temperature of garage that Experiment 2 was run in from March 24 2020 to May 28 2020, recorded using HOBO datalogger. Temperature was recorded every 30 minutes for the duration of the time in the garage. Prior to relocation, the experiment was run in a temperature controlled room, kept at 22°C. 108

Abbreviations

AD	Anno Domini
AWC	Available water content
BP	Before present
C	Constant (total proportion of pumice and glass)
EAW	Easily available water
FC	Field capacity
Fe	Iron
GDP	Gross Domestic Product
ID	Internal diameter
KCl	Potassium chloride
kPa	Kilopascal
Ma	Million years ago
N	Nitrogen
NSD	National Soils Database
NZSC	New Zealand Soil Classification
OD	Outside diameter
PAW	Plant available water
PTF	Pedotransfer function
PWP	Permanent wilting point
RO	Reverse osmosis
TDR	Time domain reflectometry
Ti	Titanium
TVZ	Taupō Volcanic Zone
WHC	Water holding capacity
θ	Volumetric water content

Chapter 1

Introduction

Soil is the interface between the lithosphere and the atmosphere, supporting all forms of terrestrial life. It is a non-renewable resource that is prone to degradation and loss, requiring careful management to ensure economic and environmental sustainability (Lal & Shukla, 2004; Shukla, 2014). Soils across the world face many stresses that result in their degradation. These include erosion, leaching, compaction, salinity and the destruction of soil structure as a result of both natural and anthropogenic factors (Hillel, 2011). A range of management practices are used across the world to enable soil health to be maintained. A healthy soil has the capacity to function within ecosystem boundaries, sustaining productivity and promoting growth of plants and animals (Doran, 2002). Soil health is related to aspects of the soils' biological, chemical and physical properties (Arriaga, Guzman, & Lowery, 2017). The physical properties of a soil that relate to soil health are largely focused on the storage and movement of water through the profile. These physical properties are interrelated, and include the soil structure, particle size distribution, porosity and bulk density (Shukla, 2014).

A balance of water and air filled pore space is required for high productivity in plant growth (Shukla, 2014). This balance is able to be achieved in a soil with good structure, high porosity and low bulk density. Soil structural aggregates are formed as individual, fine textured, soil particles bind together. Soils with large stable aggregates have a high porosity, which is inversely related to a low bulk density. Water in the soil adheres to the surface of the soil aggregates and is held in the pores of the soil. Under saturated conditions, all pores in the soil are water filled and as drainage occurs, the pores empty from largest to smallest, until the water is held against gravity at which stage it can only be removed by external forces.

To ensure that the physical properties relating to water movement and storage in the soil are maintained and improved, soil management practices are implemented. While different locations across the world face different challenges, such as climate, soil types present and land use, a number of the management practices to mitigate these issues are widely used (Davies, Eagle, & Finney, 1997; Hatfield & Sauer, 2011). There has been a shift in soil management best practices from traditional farming methods including tillage/cultivation, burning plant residue, flood irrigation and generalised fertiliser application to techniques of precision agriculture, green mulching and no-till (Hatfield, Parkin, Sauer, & Prueger, 2012; Hillel, 2011; Steiner, 1994). Limiting activities that result in

soil degradation and replacing them with practices that improve soil quality reduces the amount of leaching, erosion and the associated nutrient loss through improvements to the physical properties of the soil (Reicosky, Sauer, & Hatfield, 2011).

The physical properties of a soil are degraded when practices such as tillage and the use of heavy machinery are employed. When the soil is cultivated, the natural soil structure is destroyed, reducing the interconnecting pores that form natural pathways for water movement and gas exchange (Al-Kaisi, Lal, Olson, & Lowery, 2017). As a result of destroyed soil structure, the porosity of the soil is reduced, while the bulk density is increased. The impact on porosity and bulk density is also exacerbated by compaction as a result of heavy vehicle movements across the soil surface. The results of these changes to the physical properties of the soil include limited water and nutrient movement through the soil, decreased infiltration leading to erosion through greater surface run off and lower productivity.

Management practices to improve the soil structure, porosity and bulk density include retaining organic matter from previous crops and replacing tillage with practices such as direct drilling. The addition of organic matter, such as plant residues and manure, increases the stability of soil aggregates. Using direct drilling to sow crops, removing the need to plough the soil, prevents the soil structure from being destroyed, the porosity being reduced and the bulk density from being increased. It also ensures that the organic inputs remain in high concentrations at the soil surface, which is important for its role in the development of soil structure (Shepherd, Harrison, & Webb, 2002).

Some physical properties of soils can be complex and hard to measure, and as such are not always easily obtainable. The physical properties of the soil are parameters that are key inputs into the Overseer nutrient budgeting model. Overseer is used to aid farmers in managing the inputs and outputs for their farming systems to achieve target economic and environmental outcomes (Watkins & Selbie, 2015; Watkins, Shepherd, & Ledgard, 2015). Pedotransfer functions (PTFs) are used to enable the physical properties of the soil that are complex and hard to measure to be estimated using easily obtainable data (Webb, 2003; Wheeler, 2018). The properties produced using PTFs are then used within the Overseer model, from which nutrient losses from the soil system are determined. To enable appropriate land and nutrient management practices to be implemented, accurate data for the parameters used is required; however, a lack of knowledge of certain soil properties may be resulting in incorrect outputs being generated. In addition to the parameters used in Overseer, there are a number of assumptions involved. These relate to the data included in the model and reliability of user inputs (Ridler, 2017). Assumptions related to the data used in the PTFs

include the assumption that rock fragments in soil have no water holding capacity (WHC), and as such the water content of each soil layer is decreased proportional to the amount of stones present, with the exception of pumice clasts (Landcare Research, 2018a).

Until recently pumice clasts in New Zealand Pumice Soils were regarded the same as all other rock fragments, essentially void space in the soil (Landcare Research, 2018a). It was recognised that this assumption was likely to be incorrect, and an alternative assumption was adopted, namely that pumice clasts behave hydraulically like the soil fines they are found in (Landcare Research, 2018a). This alternative assumption has been implemented in recent PTFs developed for use in S-map (McNeill, Lilburne, Carrick, Webb, & Cuthill, 2018), which aligned with the findings of Will and Stone (1967) on a study of the Taupō pumice.

Pumice is a vesicular, extrusive igneous rock, produced during plinian volcanic eruptions (Allaby, 2013; Flores-Ramírez, Abel, & Nehls, 2018; Lowe, Balks, & Laubscher, 2014; Schmincke, 2004). It is used widely in horticulture, including as a lightweight building material, for filtration in wastewater treatment and for various other uses. Pumice clasts produced in different eruptions around the world have variations in their physical properties. While the general trends of their behaviour are relatively comparable, they are sufficiently distinct in their behaviour that characteristics from one deposit cannot be extrapolated to another (Bilardi, Calabrò, Caré, Moraci, & Noubactep, 2013; Boertje, 1995; Celik, Family, & Menguc, 2016; Gizas & Savvas, 2007; Raviv, Wallach, Silber, & Bar-Tal, 2002; Raviv, Wallach, Silber, Medina, & Krasnovsky, 1999).

In New Zealand, pumice deposits are restricted to the Central North Island and are the parent material of Pumice Soils (Hewitt, 2010). Pumice Soils are free draining and have low concentrations of a number of essential plant and animal nutrients (Hewitt, 2013; Landcare Research, n.d.-b). To ensure maximum productivity occurs with minimal negative environmental impacts when the land is used for pastural farming, thorough knowledge of the soils and landscapes is required to carefully manage the nutrient and physical limitations of these soils.

New Zealand's Central North Island regions, where Pumice Soils are located, hold significant economic and cultural values. Within the Waikato region, 52% of the land area is dedicated to agriculture and a further 14% is used for commercial forestry (Waikato Regional Council, n.d.). In the Bay of Plenty, 24% of the land is used for farming and 20% is under commercial forestry (Bay of Plenty Regional Council, n.d). These two regions make a significant economic contribution to the country in both forestry and agricultural industries, with a large amount of production occurring on Pumice Soils.

Forestry activities in the Waikato and Bay of Plenty regions contributes 33% of the national GDP generated by this industry. Figure 1.1 identifies the Bay of Plenty and Waikato as the two largest generators of income from forestry and its related services (Nixon et al., 2017). Figure 1.2 demonstrates the contribution of dairy farming and processing to regional GDP. In 2016, the dairy industry in the Bay of Plenty contributed over $430 million to the regions' GDP. The significance of dairy related activities is obvious for the Waikato Region, contributing over $2 billion to regional GDP in 2016 (Ballingal & Pambudi, 2017).

Initially, agricultural productivity on Pumice Soils was limited due to low concentrations of essential elements. This resulted in New Zealand Pumice Soils being the focus of a number of studies relating to their chemical properties. A large portion of these studies occurred between 1900 and the early 1930's with a focus on diagnosing the cause of the animal wasting disease 'bush sickness'. A smaller number of studies have looked at the physical properties of the soil to assess their suitability for pastoral farming and forestry (Packard, 1957; Read, 1974; Watkins et al., 2015; Will & Stone, 1967). As a result of these intensive early studies on the chemistry of the soil, management practices in relation to fertilisation were developed and the land has since enabled high productivity.

In addition to being valuable assets for primary industries, the Waikato and Bay of Plenty regions are also tourism hot spots. For the year ending February 2019, tourism spend for the Waikato totalled $2.7 billion and $1.89 billion for the Bay of Plenty, contributing a combined total of 16% of the national market share for tourism (Ministry of Business Innovation and Employment, 2019). Tourists are attracted by the unique geothermal setting, diverse landscapes, high water quality of abundant

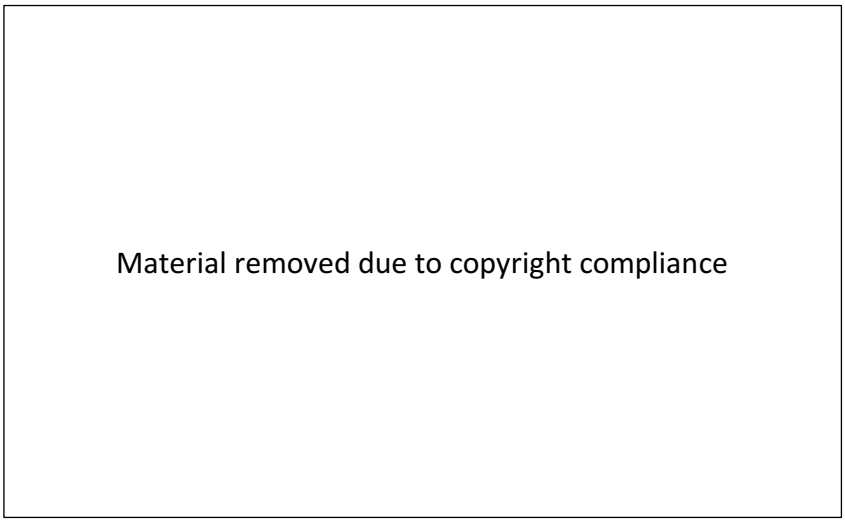

Figure 1.1: GDP ($m) produced by forestry activities and services per region for 2016 (From Nixon, Gamperle, Pambudi, & Clough, 2017).

nearby lakes and the rich cultural history of the area (Rawlings-Way, Atkinson, Bennett, Dragicevich, & Slater, 2016).

Lake Taupō, New Zealand's largest lake (Land Air Water Aotearoa, n.d.), is renowned for its pristine waters. Reductions in the water quality of the lake may have negative impacts on tourism to the area. Excess nutrients in lakes lead to algal blooms, some of which can be harmful to humans and animals as well as degrading the aesthetic qualities of the lakes (Parliamentry Commissioner for the Environment, 2012).This may have a more significant impact in summer, when tourist numbers are highest and the lake is used for recreational activities, as the cyanobacterial populations that cause the blooms increase due to the warmer temperatures (Wood, Hamilton, Paul, Safi, & Williamson, 2009).

In addition to the economic importance of the Bay of Plenty and Waikato regions, the land, water and environment are of significant cultural and historical importance. There are a number of Iwi with ancestral lands located within the areas where Pumice Soils are found, including Ngāti Tuwharetoa, Te Arawa, Tūhoe and Ngāti Awa (Te Puni Kōkiri, n.d.). These Iwi all have strong connections to the natural resources found within the Central North Island (NIWA, 2019; Wikaira, 2017). Degrading water quality, including the occurrence of toxic algal blooms and low dissolved oxygen levels caused by increased amounts of nutrients in water bodies also impacts freshwater ecology (Parliamentry Commissioner for the Environment, 2012). Low dissolved oxygen levels have been recorded in several Rotorua lakes within the Bay of Plenty Region, with Lake Okaro recorded as nearly completely deoxygenated (Landman, Van Den Heuvel, & Ling, 2005). The increased nutrient levels

Figure 1.2: The 2016 contribution of dairy farming and processing to regional GDP in $ million (From Ballingal & Pambudi, 2017).

and low oxygen levels cases stress within lake ecosystems, which can result in events such as significant fish kills, including of Kōura, a valued mahinga kai (Landman et al., 2005; NIWA, n.d.).

A delicate balance is needed to achieve the economic gains of the primary industries and tourism to be met, while retaining the cultural value of the regions. Plans to improve the water quality within the two regions have been developed and implemented to reach a balance between agricultural productivity and environmental protection (Barnes, 2013; Bay of Plenty Regional Council, n.d.; Council, 2011; Waikato Regional Council, 2011). These include planning at a district and regional level. For this planning to be effective an accurate estimate of the extent of diffuse pollution of nutrients from agricultural and forestry land needs to be obtained so appropriate land management strategies can be implemented to achieve the targets that have been identified.

1.1 Aims

The aim of this research is to develop a method that enables the hydraulic properties of pumice clasts to be obtained. This includes determining the water retention and water release characteristics of pumice clasts compared with current estimates that are used in New Zealand's soil information systems. Ensuring the accuracy of information within the soil information systems and models used will result in farming system outputs becoming more reliable, allow for areas of concern to be correctly identified and the development and implementation of appropriate land management practices.

1.2 Hypothesis

It is hypothesised that:

1) Pumice clasts have a water content that is greater than that of the matrix it is found in due to the higher vesicularity of pumice clasts than the surrounding matrix.

Chapter 2

Review of the Literature

2.1 Introduction

Water stored in soils is an important part of the hydrological cycle, forming the interface between the lithosphere and atmosphere through interactions with the various components of the cycle (Shukla, 2014). Soil hydrology influences the transport, storage and release of water through the soil. Important aspects of water management central to horticulture and agriculture includes accounting for drainage, leaching and percolation, groundwater recharge, capillary rise, root and plant uptake, evaporation from the soil and transpiration from plants (Lal & Shukla, 2004). Knowledge of the hydraulic properties of unsaturated soils is an important part of understanding the role of soil in the hydrological cycle and establishing soil management practices appropriate for each land use, soil type and climate regime. Numerical models are an important part in determining the water storage of soils through predictions of field capacity (FC) and permanent wilting point (PWP) (Shukla, 2014).

2.2 Water storage in soils

The water content of a soil at any given time is the net result of positive and negative forces that are in action within the soil system. Positive forces include those that enable the soil to retain water, including adhesion, cohesion and capillarity while negative forces remove water from the soil, such as gravity, water uptake by plant roots and evaporation (Lal & Shukla, 2004).

2.2.1 Matric potential

Water stored in soils has potential energy, which describes the movement of the water within the soil. Water moves from areas of high potential to low potential due to gravity, or from zones of wet soil to zones of dry soil. Soil water potential is determined as a relative measure of the energy of soil water with respect to the energy of water at a reference state. The reference state of the soil water potential is a standard state in which no solutes are present and the only external force present is gravity at a reference pressure, temperature and elevation. Measurement of soil water potential is a reliable indicator of soil water availability and is an important aspect of irrigation scheduling to enable optimal plant growth (He & Weber, 2019; Leib, Grant, & McClure, 2019; Leib, Grant, & Raper, 2019; Marco, 2010; METER Environment, n.d.-a; Nolz, Kammerer, & Cepuder, 2013). Total soil water potential is determined as the sum of the four soil water potentials, gravitational, matric, pressure

and osmotic. The matric potential, which results from the forces of adhesion and cohesion that occur in the soil, is commonly used in soil water experiments and is a key variable in the soil water release curve (Campbell & Campbell, 2005; Marco, 2010).

There are different methods which are used to lower the matric potential of a soil sample, from which the water content of the sample can be determined. Other methods are able to be used *in situ* to measure the matric potential of a soil.

Pressure plates

Pressure plate extraction is used when water contents below -100 kPa are needing to be achieved. Cores that are less than 10 mm deep are packed with a soil slurry and placed on a porous plate in the pressure chamber. The chamber is pressurised above the porous plate and unpressurised below the plate, and the soil water is mobilised across membrane using positive pressure. The air pressure in the pressurised section is able to be increased, which in turn lowers the matric potential of the sample (Soilmoisture equipment corp, n.d.).

Suction plates

Suction plates are generally limited to being used to derive the wet end (low suctions) of the water release curve (Tokunaga, Olson, & Wan, 2003). Suction plates require a hanging water column, often limited to 5 m of suction (Dane & Hopmans, 2002), or a vacuum pump, which is limited to a matric potential of -85 kPa, equivalent to a water column depth of 8.7 m (METER Group Inc, 2012). That limitation is dictated by cavitation effects in water at greater suctions.

Unlike the requirement for cores to be no deeper than 10 mm for pressure plate methods (Dane & Hopmans, 2002), there is less restriction on core size for suction plate methods. This enables 'raw' coarse fragments, that have not been ground, crushed or altered, to be included in measurement. Dane and Hopmans (2002) advise that cores should be within the height range of 10 - 60 mm for most practical purposes to reduce the time it takes for the soil to reach equilibrium. Analysis has shown that the time required for a core to reach equilibrium is proportional to the square of the height of the sample (Dane & Hopmans, 2002).

Dielectric permitivity

Soil water potential can be measured *in situ* using a device such as the Teros21, which measures the dielectric permittivity of a soil. The sensor is installed in the soil during packing and attached to a datalogger. Sensors come with factory calibrations for a use in a number of soil mediums, including those with perlite and rockwool included.

Teros21 devices have limitations at both the wet and dry ends of the range. At the wet end, the Teros21 may not respond until the potential is lowered due to the air-entry potential of the ceramic discs of -9 kPa. Between -9kPa and -100 kPa the device is calibrated using 4 calibration points, providing a level of accuracy ± 10%. Beyond -100 kPa, the device has a lower level of accuracy because the device extrapolates beyond the range of calibration, assuming a linear relationship between the logarithms of water content and water potential. While this does not produce results as accurate as the calibration between -9 and -100 kPa, the accuracy up to PWP at -1500 kPa is still sufficient, with low variability between sensors to this matric potential (METER Group Inc, 2019b).

Dewpoint

A dewpoint psychrometer, such as the WP4C Dewpoint PotentiaMeter manufactured by METER, is a method for determining the water potential of a sample. Samples are placed in a stainless steel cup and inserted into the device, which measures the sum of the osmotic and matric potentials of a sample from the vapour pressure of air in equilibrium (METER Group Inc, 2019c). Samples inserted into the device are required to be of a known water content, with the most common method being to fully saturate the sample and then place it in a constant temperature chamber with a set relative humidity to evaporate until equilibrium is reached (Dal Ferro, Pagliarin, & Morari, 2014; Ferrari, Favero, Marschall, & Laloui, 2014; Parajuli, Sadeghi, & Jones, 2017).

Manufacturer instructions state that the sample is required to cover the entire base of the sample cup and the cup should not be more than half full for an accurate measurement to be taken, to avoid damaging the device and contaminating following samples (METER Group Inc, 2019c). The requirement for a sample to cover the entirety of the cup base was found to be unnecessary when measuring the water potential of rock fragments in a study by Ferrari et al. (2014). In additional analysis to assess the appropriateness of using the device to determine the matric potential of shale fragments, an average accuracy of 3% was determined, and evaluated to be satisfactory for the study (Ferrari et al., 2014). The dewpoint method has low accuracy at matric potentials above -10 kPa, but is able to be used below -1500 kPa (METER Group Inc, 2019c). This makes this method suitable for use in conjunction with other methods, such as with the suction plates, to develop a full water release curve.

2.2.2 Water content

Water is held in soils by forces of adhesion and cohesion, causing water films to form on the surface of soil particles and in large pores. Adhesion is the attraction of water to the soil surfaces. Cohesion occurs due to the shearing strength of a film of water that separates individual soil particles, in

which the water molecules are attracted to each other due to their polar nature. (Allaby, 2013; Cooper, 2016). Capillarity is the way in which water is held in soil pores (Cooper, 2016), when a hydraulic head gradient is present across the curved air-water interface (Shukla, 2014). Water rises up inside the pores of a substrate, with smaller pores facilitating greater capillary rise and holding the water tighter than in larger pores (Cooper, 2016). This enables water to be able to move through the soil in all directions and be held against gravity (Shukla, 2014). Soil water content is a measure of the mass or volume of water contained per mass or volume of soil (Campbell & Campbell, 2005).

2.2.3 Measuring soil water

Quantifying the moisture content of soils is an important aspect of understanding their ability to modulate water fluxes in the landscape and support plant growth. This information is used to assist with irrigation scheduling, assessing plant water uptake, depth of water infiltration and evaluating soil physical properties and processes such as strength, water storage capacity and rate of water movement (Lal & Shukla, 2004).

There are a number of methods used to determine the water content of a soil, each with benefits and limitations under different conditions. These methods are grouped as direct and indirect methods.

Direct methods of determining the water content of a soil are based on processes of physically removing the water from a sample, followed by the measurement of the water that is removed. While these methods can be low cost, such as the gravimetric method, they require destructive sampling and are not instantaneous (Lal & Shukla, 2004).

Indirect methods for determining the water content of a soil are based on water induced changes in soil properties that can be measured. These methods all require specialist equipment; however, can be carried out in less time than direct methods and are less destructive (Lal & Shukla, 2004).

Gravimtric

The determination of the gravimetric water content is a method that is often carried out to enable the water content of soil to be determined at the end of an experiment (Dal Ferro et al., 2014; Jackson, 1974; Packard, 1957; Will & Stone, 1967).

Determining the gravimetric water content involves destructive sampling, in which the whole or a portion of the samples being studied are weighed to determine the mass of the soil when wet (M_w) before air drying the sample at 105°C followed by weighing again to get the dry weight of the sample (M_d). From this, the gravimetric water content (WC) is determined using the following equation

$$WC = \frac{M_w - M_d}{M_d} \quad (2.1)$$

From the gravimetric water content the bulk density of the sample ($\boldsymbol{\rho}_b$) and the density of water ($\boldsymbol{\rho}_w$) which is equal to 1 g cm^{-3} (Shukla, 2014), the volumetric water content (θ) can be calculated

$$\theta = WC \frac{\rho_b}{\rho_w} \quad (2.2)$$

Determining the water content of a sample using the gravimetric method is simple and low cost. However; it is often not used as a stand-alone method, with other methods used to bring the sample to a certain matric potential before the gravimetric method can be used to determine the water content.

Time domain reflectometry

As an alternative to gravimetric methods, time domain reflectometry (TDR) devices may be installed in the soil to measure dielectric permittivity. Dielectric permittivity is the charge storing capacity of the soil, a function of the volumetric water content (θ), obtained by measuring the return-time of an electric charge sent down conductive rods (METER Environment, n.d.-b).

Coarse fragments present difficulties when using TDR to determine θ of soils, including refusal of the soil to the probes; and if the probes are able to be inserted, compensation of measurements to account for the coarse fragment content is required (Coppola et al., 2013).

TDR sensors, such as the METER Group 5TM, require specific calibration for accuracy from which a transfer equation is developed. Detailed instructions on calibration of the sensors to specific soils are provided in the METER product operating manual (METER Group Inc, 2019a, n.d.-a). The transfer equation used for most soil types is known as Topp's equation (Equation 2.3), in which the measured apparent dielectric constant (K_a) is converted to θ (Topp, Davis, & Annan, 1980).

$$\theta = -0.053 + 0.0292K_a - 5.5 \times 10^{-4}K_a^2 + 4.3 \times 10^{-6}K_a^3 \quad (2.3)$$

2.2.4 Water retention curve

Soil water potential and soil water content are related through the soil moisture characteristic curve (Campbell & Campbell, 2005; Ferrari et al., 2014; METER Group Inc, 2019b; Shukla, 2014). The soil moisture characteristic curve, also known as the water release or retention curve, characterises the relationship between soil water content and matric potential. As the pressure or suction applied to a soil increases soil matric potential declines, and progressively smaller soil pores become air-filled while soil water content decreases (Shukla, 2014).

2.2.5 Soil moisture status

Soil water that is stored in pores of the size range 0.2 – 30 µm, is released at matric potentials of -10 - --1,500 kPa. These two matric potentials are key points on the soil water release curve, FC at – 10 kPa and PWP at – 1,500 kPa, which describe the moisture status of the soil (Figure 2.1). The difference between the water content at FC and PWP is known as the available water content (AWC) of the soil (Shukla, 2014). This provides a key data input for quantitative assessment of water storage and drainage in agricultural soils for purposes such as irrigation management (Haghverdi, Leib, Washington-Allen, Ayers, & Buschermohle, 2015).

FC is the amount of water stored in a soil after it has drained freely under gravity, with no evaporation following full saturation. At FC, all of the macropores have drained and become air

Figure 2.1: Soil water characteristic curves for soils of three different textural classes. pF= log(-ϕ_m) where ϕ_m is the matric potential in cm, θ is the volumetric water content, WP is the wilting point and FC is field capacity (From Shukla, 2014).

filled. FC is the upper limit of the amount of water that a soil can store (Lal & Shukla, 2004), and is often determined at a matric potential of -10 kPa in laboratory settings (Silva, Kay, & Perfect, 1994), which under natural conditions occurs after 1 – 2 days of drainage following an irrigation or precipitation event that saturates the soil (Kirkham, 2005).

The PWP is the lower limit of the soil moisture content, where adhesion and cohesion forces are greater than the forces that are exerted by plant roots to extract soil moisture. At this point, the water in the soil is unavailable to plants, causing plant leaves to wilt and unable to regain turgidity as the retention pores are depleted of water (Lal & Shukla, 2004). In most laboratory studies, the PWP is determined at a matric potential of -1500 kPa (Shukla, 2014; Webb, 2003), however; there are some plants that are able to grow at matric potentials beyond this point (Kirkham, 2005).

The soil water stress point is the point at which plant growth is slowed due to limited water availability. While this point varies for different plants, plants become stressed when about half of the AWC has been used (Bloomer, Curtis, & Reese, n.d.; Brown, Martin, & Craigie, 2010). This is often used as a trigger point for irrigation, as plant water is no longer readily available. In laboratory based studies, the soil water stress point is recorded at a matric potential of -100 kPa (Bloomer et al., n.d.; Webb, 2003).

Using the FC, PWP and stress point values determined for a soil, the AWC and plant available water (PAW) contents of a soil can be calculated. AWC is determined as the difference between FC and PWP values for a soil and is a key parameter used in irrigation scheduling, which is an important aspect of precision agriculture (Haghverdi et al., 2015). PAW is the amount of water in a soil that is able to be extracted by plants without growth limitations. Growth limitations begin to occur once soil moisture reaches the stress point, and as such, PAW is the difference between FC and the stress point (Bloomer et al., n.d.; Webb, 2003).

2.2.6 Soil water storage and rock fragments

It is assumed that rock fragments within a soil have no WHC, and as such the water content of a horizon is reduced by the proportion of rock fragments present. The effects of the presence of rock fragments on nutrient movement through the soil has been studied widely in relation to increasing preferential flow paths in soil as the proportion of rocks present increases (Beibei, Ming'an, & Hongbo, 2009). In New Zealand, rock fragments in the soil are commonly treated as having a dominant influence on soil hydrology by way of preferential flow paths as opposed to having any intra-particle water holding capacity, with no contribution to the total water holding capacity of the soil (Bouwer & Rice, 1984; Pollacco, 2016). This is accounted for in predictions of the WHC of stony

soils by reducing the water content by the proportion of stones present. This has been recognised as being a false assumption for pumice clasts, found in Central North Island Soils, and models have been updated to the assumption that pumice clasts have a water holding capacity equal to that of the surrounding soil matrix (Landcare Research, 2018a).

2.3 Pedotransfer functions

Pedotransfer functions (PTFs) are simulation models that take raw, easily obtainable soil field data and translate it into predictions of more complex and useful soil information (Lilburne, Hewitt, & Webb, 2012; McNeill et al., 2018; Odeh & McBratney, 2005). PTFs are statistical models that describe a relationship between soil properties and mathematical models and have been used widely to predict some soil properties from measured data since the 1970's (McNeill et al., 2018; Odeh & McBratney, 2005; Rawls, Brakensiek, & Saxtonn, 1982). A large number of PTF models have been developed to predict soil properties in different locations around the world. The models developed for each location are not transferable to other locations due to differences in the properties of the soil data used in the simulations (McNeill et al., 2018).

Soil hydraulic PTFs are used in a range of applications in New Zealand, including irrigation scheduling, soil leaching losses and soil management (McNeill et al., 2018). An estimate of θ of a soil is the main aim of hydrological PTFs used in New Zealand. The θ is measured as a function of tension and ranges from 0%, when the soil is completely dry, to 100% which represents the soil at saturation, with the relationship between θ and tension known as the water release curve (McNeill et al., 2018). Models are required to determine the water content of different soils for various tensions, to enable the AWC and PAW to be determined. Determining the water contents of soils at different tensions is time consuming and difficult to measure, but is required when calculating the water holding capacity and the related limitations of a soil. The data required for the models is sourced from the National Soils Database (NSD) and S-map and includes functional horizon descriptors, which are explanatory variables that include soil order, texture and structure (Landcare Research, 2019a; McNeill et al., 2018). The NSD contains profile data for over 1,500 soil profiles, of which 52 are Pumice Soils (Landcare Research, n.d.-a). The data stored in the NSD for each profile includes a soil description and soil physical and chemical laboratory analysis data (McNeill et al., 2018). S-map is the soil information system used in New Zealand. It is operated by Manaaki Whenua Landcare Research (Lilburne et al., 2012) and provides functional horizon information that is used in PTFs. Functional horizons are groups of horizons that have similar properties, enabling PTFs to cover soils with similar hydrological properties (McNeill et al., 2018).

The soil hydraulic PTF model that is used in New Zealand is the logit model, in which the θ at a given tension or tension range is fitted using a linear model where the logit-transformed θ at a given tension is the response variable and properties including soil order, rock of fines, the presence of top soil and texture are the explanatory variables (McNeill et al., 2018).

To determine the θ at 1500 kPa, the equation below is used

$$logit(\theta_{1500kPa}) = f(\cdots) + \varepsilon \quad (2.4)$$

Where $f(\cdots)$ is the linear function of the explanatory parameters and ε is the uncertainty.

The equation is then transformed to cover the constraining interval of 0 – 100% by calculating the θ as differences between tension ranges, such as 100 kPa – 1500 kPa using the equation below

$$\Delta = \frac{(\theta_{100\ kPa} - \theta_{1500kPa})}{(1 - \theta_{1500kPa})} \quad (2.5)$$

Where Δ is the difference calculated, making the regression model

$$logit(\Delta) = f(\cdots) + \varepsilon \quad (2.6)$$

Equations 2.2 and 2.3 are repeated throughout the range until the difference of 0 kPa to 5 kPa has been calculated and regression completed (McNeill et al., 2018).

From the θ at different tensions produced, derived values, such as PAW (Equation 2.4), can be produced.

$$\theta_{PAW} = \theta_{FC} - \theta_{PWP} \quad (2.7)$$

In which θ_{FC} is the water content at FC (10 kPa) and θ_{PWP} is the water content at PWP (1500 kPa) (McNeill et al., 2018).

Prior to June 2013, PAW was calculated using a simple correlation between functional soil horizons and measured soil water data from the National Soils Database (NSD), with the soil water content at PWP subtracted from the soil water content at FC. If soil horizons contained stones, the water content of the horizon was reduced by the proportion of stones present in that horizon, including pumice clasts. Since 2013, the PAW of soil horizons has been estimated using hydrological PTFs, using soil sand, silt and clay contents, soil type, structure, consistence and topsoil vs subsoil. The new method used to estimate PAW found that pumice clasts hold significant amounts of water that is available to plants. The output of these PTFs indicate that the water content of the pumice clasts is as much as the soil fines that the clasts are found in, with this applied to clasts in Pumice Soils as an assumption. While laboratory data in the NSD indicates that this is likely, there is no field experimental data for this to be compared with to allow for confirmation (Landcare Research, 2018a).

2.3.1 Overseer

Overseer is a nutrient budgeting and management tool that enables farmers to examine nutrient use and movement within a farm (Watkins & Selbie, 2015; Watkins et al., 2015). Overseer is an important tool used by Regional Councils in New Zealand to set Resource Management Act (1991) limits and objectives related to the National Policy Statement for Freshwater Management (Murray & Freeman, 2017). It is currently the best tool available for modelling and estimating nutrient movement (Maseyk, Brown, & Taylor, 2018). However, it does have limitations including not being able to provide reliable and accurate outputs in some scenarios, such as farming systems on Pumice Soils (Watkins et al., 2015). Soil properties entered into Overseer include broad inputs, such as soil classification which define default values for a range of soil properties, and site specific properties that can be entered to override default values (Pollacco, Lilburne, Webb, & Wheeler, 2014). The values used and entered into Overseer are part of the production of a range of estimates, including soil water content, leaching and greenhouse gas emissions (Overseer, n.d.). To improve estimations of the soil water contents in stony soils, non-standard layers were developed to be used as subsoil profile descriptors. There are three non-standard layer categories, defines as:

- Sandy - where the subsoil profile is sandy (not applicable to Pumice Soils),

- Stony - when there is ≥50% stones in a sandy matrix, or
- Stony Matrix - when there is ≥50% stones in a loamy or clayey matrix (Roberts et al., 2015; Wheeler, 2018).

A stony non-standard layer was used in a study of two Rotorua dairy farms, situated on Pumice Soils, which compared the Overseer estimates for drainage and leaching with values determined using the daily water balance model from Woodward, Barker, and Zyskowski (2001) (Equation 2.5).

$$W(t+1) = \min(0, W(t) + rain(t) - AET(t)) \quad (2.8)$$

in which *W* is the soil water deficit in mm, *t* is time in days, *rain* is the daily rainfall in mm d^{-1} and *AET* is actual evapotranspiration in mm d^{-1} (Woodward et al., 2001).

The results of this study indicate that work is still needed to improve the non-standard layer as the estimated drainage values produced using Overseer were much less than the drainage values produced using the values obtained using the Woodward et al. (2001) model, which were regarded as the measured values in the study (Watkins et al., 2015). This corresponds to the N leaching estimates also being underestimated for Pumice Soils, where a non-standard layer is used. Further research is needed into the properties involved in a non-standard layer to ensure better representation of the water contents of soil types that require the use of a non-standard layer for water content estimates (Watkins et al., 2015).

2.4 Pumice

Pumice clasts are used in many places throughout the world as a popular horticultural growing medium (Boertje, 1995; Flores-Ramírez et al., 2018; Gizas & Savvas, 2007; Gunnlaugsson & Adalsteinsson, 1995; Papadopoulos, Bar-Tal, Silber, Saha, & Raviv, 2008; Raviv et al., 1999; Sahin, Ercisli, Anapali, & Esitken, 2004a, 2004b). Consequently, pumice's physical properties have been the focus of a number of laboratory studies. These studies have shown that while the physical characteristics of pumice from different deposits generally have a high porosity and low bulk density, there is significant variability (Boertje, 1995; Flores-Ramírez et al., 2018; Gizas & Savvas, 2007; Gunnlaugsson & Adalsteinsson, 1995; Papadopoulos et al., 2008; Raviv et al., 1999; Sahin et al., 2004a, 2004b).

In New Zealand, pumice produced in eruptions between 1,700 – 3,500 years ago is the parent material in which Pumice Soils are formed (Hewitt, 2013). Pumice Soils cover 7% of New Zealand's land area, largely confined to the Waikato and Bay of Plenty regions of the Central North Island (Landcare Research, 2018b). These regions are where a number of New Zealand's significant lakes are located, including Taupō, Rotorua and Rotoiti (Land Air Water Aotearoa, n.d.). Trends over the past 50 years have indicated that the water quality in a number of Central North Island lakes has declined (Vant, 2013). As a result of intensifying land use and development, elevated concentrations of nitrate within most streams feeding into Lake Rotorua have been observed, and in Lake Taupō the nitrate levels in the bottom waters of the lake have also increased (Carter, 2018; Morgenstern et al., 2015; Waikato Regional Council, 2011). Action has been taken to prevent the lake water quality from declining further. Within the Lake Taupō catchment, a target to reduce the amount of human-generated nitrogen (N) entering the lake by 20% was enacted (Waikato Regional Council, 2011), with the plan including stock exclusion from water bodies, the introduction of a N 'cap-and-trade' scheme (Barnes & Young, 2013), removal of N from wastewater (Waikato Regional Council, 2011), and nutrient management through the development of nutrient budgets (Bay of Plenty Regional Council, n.d.). To ensure that the outputs obtained from the nutrient budgets are an accurate representation of reality, further investigation into the reliability of model inputs is required, particularly the water holding capacity of pumice clasts.

2.4.1 Formation

Pumice deposits are distributed around the Pacific Ring of Fire (Figure 2.2) at subduction zones, where one tectonic plate is forced beneath another (Lowe et al., 2014). Rhyolitic volcanism has been a dominant part of volcanism in the Taupō Volcanic Zone (TVZ) (Figure 2.3) since 0.7 million years ago (ma). Between 2 ma and 0.9 ma, the volcanism in the TVZ was dominantly andesitic, characterised by drier pyroxene-plagioclase liquid lines of descent. Approximately 0.9 ma, an acceleration in rifting of the volcanic arc in which the TVZ is located occurred. This rifting triggered a change in the composition of magma in the TVZ, with a shift occurring from being dominantly andesitic to the dominant eruptives being rhyolitic since ~0.7 ma (Deering, Bachmann, Dufek, & Gravley, 2011; Wilson et al., 1995). An increase in water in the magma as a result of the rifting appears to have caused a shift in the composition of the magma from the drier andesitic liquid lines of descent, to a wetter liquid line of descent that reflects the presence of hornblende and Fe – Ti oxides found in the rhyolite (Deering et al., 2011). The change in the liquid lines of descent first produced a dacitic magma, which became trapped under the mantle, where the magma would crystallise to >50%, forming an upper crust mush. This stored large amounts of rhyolitic melt that was later erupted (Deering et al., 2011).

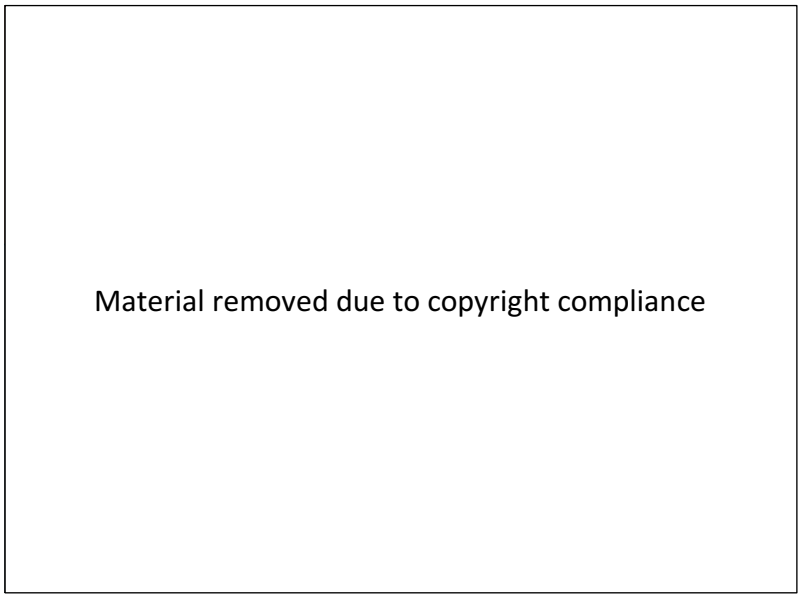

Figure 2.2: The Pacific Ring of Fire is made up of a series of volcanic arcs and ocean trenches that partially encircle the Pacific Basin (From Jacquelyne & Tilling, 1999).

Other theories that have attempted to explain the process of rhyolite formation in the TVZ include advanced fractional crystallisation of basalt in the mantle then assimilation of andesitic lower crust and massive heat transfer from the mantle to the crust causing crustal fusion (Graham, Cole, Briggs, Gamble, & Smith, 1995). These processes have been discounted following more recent analysis of the mineral phases which do not record a compositional gap, which would be expected if melting and mixing of rhyolite with andesite had occurred (Deering et al., 2011).

Pumice is formed as the gasses in gas rich magmas expand due to a decrease in pressure in the magma chamber. This causes the gas to froth as it is expelled from the volcano. This more commonly occurs when the composition of the magma is rhyolitic, which is more viscous than basaltic and andesitic magmas.

There are a number of different volcanic centres across the North Island of New Zealand that have produced pumice that constitutes the parent material from which the existing pumice soils and the paleosols beneath them have formed.

The composition of the magma is an important factor that drives the physical properties of the pumice. Pumice can be formed from andesite when the magma is supersaturated with gas, as was the case in the 1655 AD eruption at Mt Taranaki, which produced the Burrell Lapilli (Efford, Clarkson, & Bylsma, 2014; Topping, 1972). Andesitic pumice differs from rhyolitic pumice due to its lower SiO_2 content, the presence of more early formed crystals, such as olivine, and has a higher bulk density and lower porosity. The clasts of the Burrell pumice deposit are a higher bulk density than what is found in rhyolitic pumice, recorded as having a bulk density of 0.9 g cm^{-3} for the clasts and 1.3 g cm^{-3}

for the pumice flow (Platz, 2007). This is higher than TVZ pumice which is not generally greater than 0.8 g cm^{-3}. These pumice clasts are very firm and angular and are of the lapilli size fraction (Allaby, 2013).

Pumice Soils in the Central North Island Regions of the Waikato and Bay of Plenty are predominantly formed from material produced in the 232 ± 10 AD Taupō eruption and the 1314 AD Kaharoa eruption (Hogg et al., 2012; Nairn et al., 2004). The more recent Kaharoa eruption overlies tephras from the Taupō eruption in the northern extent of the Pumice Soils near the Bay of Plenty, while the Taupō ignimbrite and the Taupō pumice layer are the parent material of a majority of the rest of the Pumice Soils (Nairn et al., 2004). There are a number of earlier eruptions that also deposited material across the Central North Island, such as the 26.5 BP Oruanui eruption, also centred in Lake Taupō; however, the eruptive material and the paleosol soils that have formed from these eruptions have since been buried by material deposited in more recent eruptions. The WHC of this material may be of interest in studies in locations such as the Galatea Basin, where soil flipping has been trialled to increase the WHC of the soil, with paleosols brought to the surface, which contain pumice from older eruptions (Laubscher, 2014).

The Kaharoa eruption from the Horohoro caldera at Mt Tarawera consisted of 11 phases, most of which produced rhyolitic pumiceous material. These pumices have a moderate vesicularity of 40 – 60%, are a white/cream colour and have a high SiO_2 content of 76 – 78%. The tephras were first blown south – east before the wind changed and the material was deposited to the north – west of the caldera, covering a large portion of the Bay of Plenty region.

The 232 ± 10 AD Taupō eruption consisted of 6 phases, of which two are of particular importance to the formation of soils, the Taupō plinian pumice and the ignimbrite. Material produced during the Taupō plinian pumice phase of the eruption was carried east by the prevailing wind over parts of the Waikato, Bay of Plenty, Gisborne and Hawkes Bay regions, while the collapse of the eruption column triggered the Taupō ignimbrites, a flow of pyroclastic material that moved rapidly across the landscape, placing a layer of pumiceous material in an 80 km radius around the caldera.

The 232 $\pm$ 10 AD Taupō eruption produced 105 km^3 bulk volume of volcanic material that mantled the surrounding landscape (Wilson & Walker, 1985). The eruption consisted of six phases, including a number of ash and pumice eruptions (Figure 2.3) ejecta from which were transported eastward by the prevailing wind, covering the eastern Central North Island, as shown in (Figure 2.4). These plinian eruption phases were followed by a series of pyroclastic flows, which emplaced ignimbrites covering an area of 20,000 km^2 around the vent (Figure 2.4) (Hogg et al., 2012; Wilson, 1985; Wilson & Walker, 1985). The tephra and ignimbrite flows deposited by this eruption sequence provided the

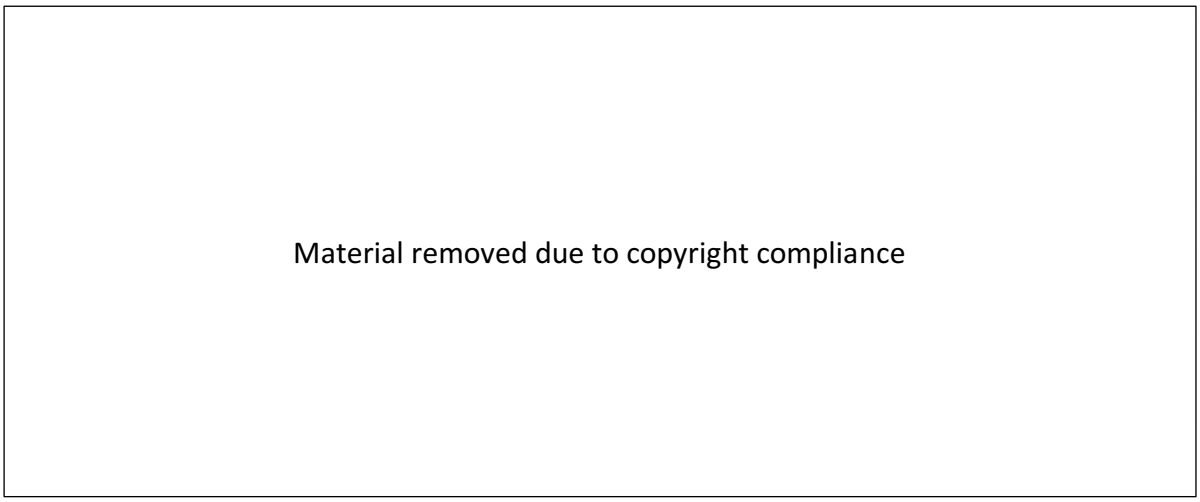

Figure 2.3: Phases of the 232 ± 10 AD Taupō eruption. The 'V' shaped incision into the Hatepe Ash indicates a break in the eruption lasting approximately 3 weeks, in which erosion (E) caused by torrential floods from high rain carved gullies into the soft ash deposit (Lowe & King, 2015).

parent material in which a large amount of the Pumice Soils have formed from. These soils are pedogenically young, in which the clasts present have undergone little weathering (Cowie, 1974; Schaetzl, 2015).

The volcanic material that the soils surrounding Lake Taupō, and a large portion of the wider region, are formed from was produced in the 232 ± 10 AD Taupō eruption (Hewitt, 2013; Hogg et al., 2012). This mid-Quaternary eruption was the largest explosive eruption to occur globally in the last 7000 years (Wilson & Walker, 1985), consisting of six different phases from a caldera situated in Lake Taupō, where the Horomatangi Reefs are today (Hogg et al., 2012; Wilson & Walker, 1985). The

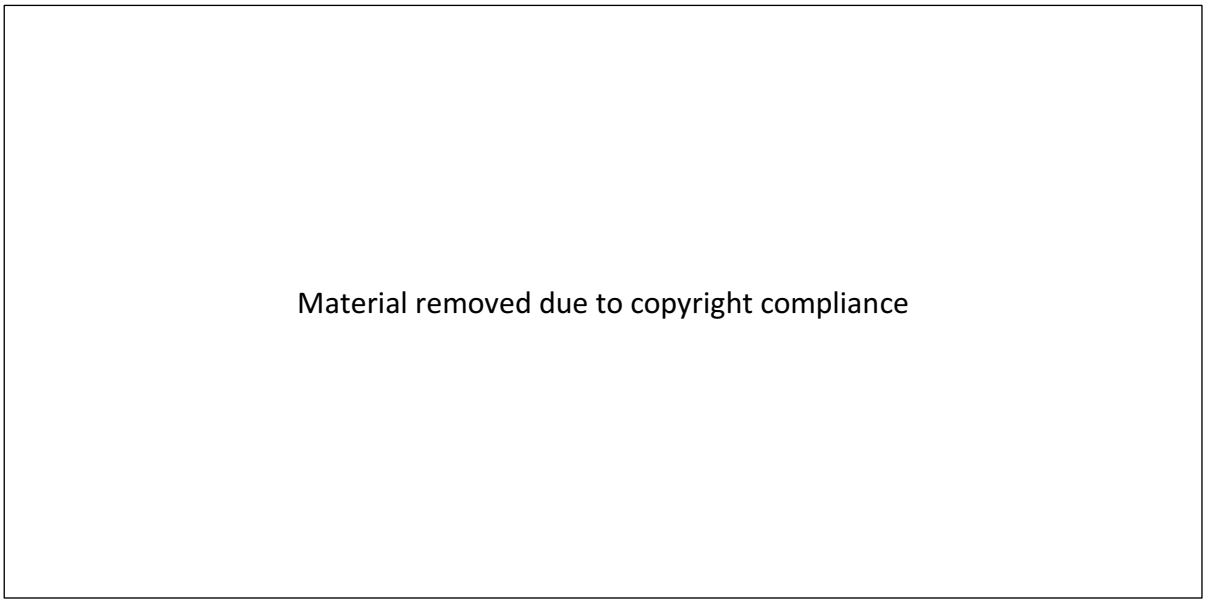

Figure 2.4: The Taupō Volcanic Zone, a 300 km long volcanic depression in the Central North Island of New Zealand and the extent of the area covered by the Taupō Ignimbrite and 10 cm isopach for airfall material (From Hogg et al., 2012).

eruption sequence began with an initial phreatomagmatic ash, generated from the interaction between the hot magma and water that was in the vent. The top of the crater is thought to have been at, or just below, the surface of the lake, producing the minor plinian eruption. Due to the limited dispersion of the ash, reaching an extent of 20 – 25 km around the vent, it is thought that the eruption column reached a height of 10 km, with the ash carried eastwards by a south westerly wind. This initial ash stage of the eruption is thought to have only lasted a few hours and it appears to have cleared the vent of water, as indicated by the dry plinian phase that followed (Wilson & Walker, 1985)

The Hatepe plinian pumice was produced by a continuous gas blast, with coarse pumiceous material produced. This stage of the eruption had a greater mass eruption rate than the preceding ash phase, with the pumice material produced being more widely dispersed than the initial ash. The tephra produced in this eruption phase was deposited predominantly to the east of the vent. This eruption stage is thought to have lasted for around 10 – 30 hours, with the eruption column reaching 30 km high, which was maintained by a discharge rate of 13,000 – 40,000 m^3 s^{-1}. The Hatepe plinian pumice was followed by the Hatepe phreatoplinian ash. This phreatoplinian eruption phase has characteristics that indicate that the ash interacted with a large amount of surface water, as opposed to with the water inside the vent which occurs in most phreatoplinian eruptions. The pumiceous characteristics of the ash indicates that the vesiculation and fragmentation levels were occurring at a considerable depth inside the vent, producing a denser deposit than the underlying pumice (Wilson & Walker, 1985).

Following this stage of the eruption was a pause in the sequence, which may have lasted from a few hours to several weeks. During this stage, a considerable amount of water entered the vent and penetrated deeply. A large amount of erosion resulting in deep gullies forming in the Hatepe ash also occurred during this break (Figure 2.3) concentrated near the vent and the surrounding area. The cause of this erosion is likely to have been from a water source that was not uniform, such as widespread rain, however, it is more likely to be from a water spout that was ejected from the vent, as the degree of gullying decreases with increasing distance from the vent. The pause in the eruption and the period of erosion was followed by the Rotongaio phreatoplinian ash, composed of poorly and non-vesiculated obsidian glass. This eruption was of phreatoplinian nature and may have lasted from a few hours to tens of hours. The ashes dispersed by the phreatoplinian eruptions are much less than that of the dry plinian eruptions, indicating that the eruption columns of the dry plinian events were much higher. The water that penetrated into the vent during the break was expelled

during the Rotongaio ash phase, leaving the vent dry for the Taupō plinian pumice phase that followed (Wilson & Walker, 1985).

The pumice produced in the Taupō plinian pumice phase of the eruption is of very low density as the vesiculation and fragmentation surfaces moved down within the vent rapidly (Wilson & Walker, 1985). The Taupō plinian pumice event is the most powerful plinian eruption event documented and the term ultraplinian was developed in the 1980's to indicate that the eruption column was thought to have reached a height of 50 km. Recent research has concluded that the eruption column was unlikely to have reached this height, with a height range of 35 - 40 km considered to be more likely, which does not fulfil the criteria of the title ultraplinian (Houghton, Carey, & Rosenberg, 2014). While this eruption is likely to not be as violent as first thought, it is still the most powerful eruption to have occurred in the last 7000 years (Hogg et al., 2012; Houghton et al., 2014). The high eruption rate of the Taupō plinian pumice dropped in the fragmentation levels in the vent resulting in the magma chamber being unsupported and causing a caldera collapse, widening the vent significantly. This widening may have caused the eruption column to collapse, triggering the Taupō ignimbrite flows (Wilson & Walker, 1985).

Ignimbrites are pyroclastic flows emplaced across the landscape (Allaby, 2013). The early ignimbrite flow is imbedded with the Taupō plinian pumice within 15 km of the vent. The proximal early flow units are composed of lithic fragments and pumice clasts up to 20 cm across. Beyond 15 km, in the distal regions, clast size reduces to 10 cm and the flows are absent of coarse pumice. Interbedding layers are also thinner than what is found at the proximal outcrops. The Taupō ignimbrite is separated from the early ignimbrite flow both genetically and stratigraphically. The distribution of the ignimbrite flow was not influenced by the topography as the ignimbrite covers a near circular area with the outer limit reaching 80 ± 10 km from the vent, covering an area of around 20,000 km^2 (Figure 2.2). In some locations the flows have followed valleys and river channels, extending flows beyond the 80 km boundary, which have formed aggregational terraces. The flows have been identified to have climbed over 700 m and there is evidence that the outer limit of the ignimbrite is where the flow ran out of material as opposed to energy. The velocity of the ignimbrite flows were able to be derived from the height of the relief that the flow traversed and it has been estimated that the minimum velocity was greater than 150 m s^{-1}, while it may have exceeded 250 – 300 m s^{-1} near the vent (Wilson & Walker, 1985).

The Taupō ignimbrite is made up of two main layers, layer 1 and layer 2, which have significant distinguishing properties. Layer 1 was generated by the processes that occurred in or ahead of the pyroclastic flow head, whereas layer 2 was deposited by the body of the flow. There are two other

layers of ignimbrite also emplaced which are of less significance; layer 3, an airfall of ash that was above the flow, and the distant facies, found at the outer most extent of the flow where velocity was high but the material was depleted (Wilson, 1985). The ignimbrites are entirely non-welded and are of low-aspect ratio, thinly covering a large area (Wilson & Walker, 1985).

2.5 Pumice Soil (NZSC)

Pumice Soils are dominated by pumiceous and glassy skeletons, have low soil strength and are susceptible to erosion. Pumice Soils typically have clay contents of less than 10%, of which this fraction is dominated by allophane, a non-crystalline amorphous mineral (Allaby, 2013; Hewitt, 2010, 2013). The Pumice Soil order in the New Zealand Soil Classification is divided into three groups, Orthic, Impeded and Perch-Gley Pumice Soils (Hewitt, 2010), shown in Figure 2.5. Orthic Pumice Soils are often free draining and deep rooting. Impeded Pumice Soils are characterised by the presence of a layer, such as welded ignimbrite, in the soil profile that severely restricts the movement of water and root penetration. Perch-Gley Pumice Soils occur under periodic saturation due to the presence of a perched water table on a slowly permeable subsurface layer (Hewitt, 2010). In the U.S. Soil Taxonomy, Pumice Soils are part of the Andosol soil order, which encompasses soils

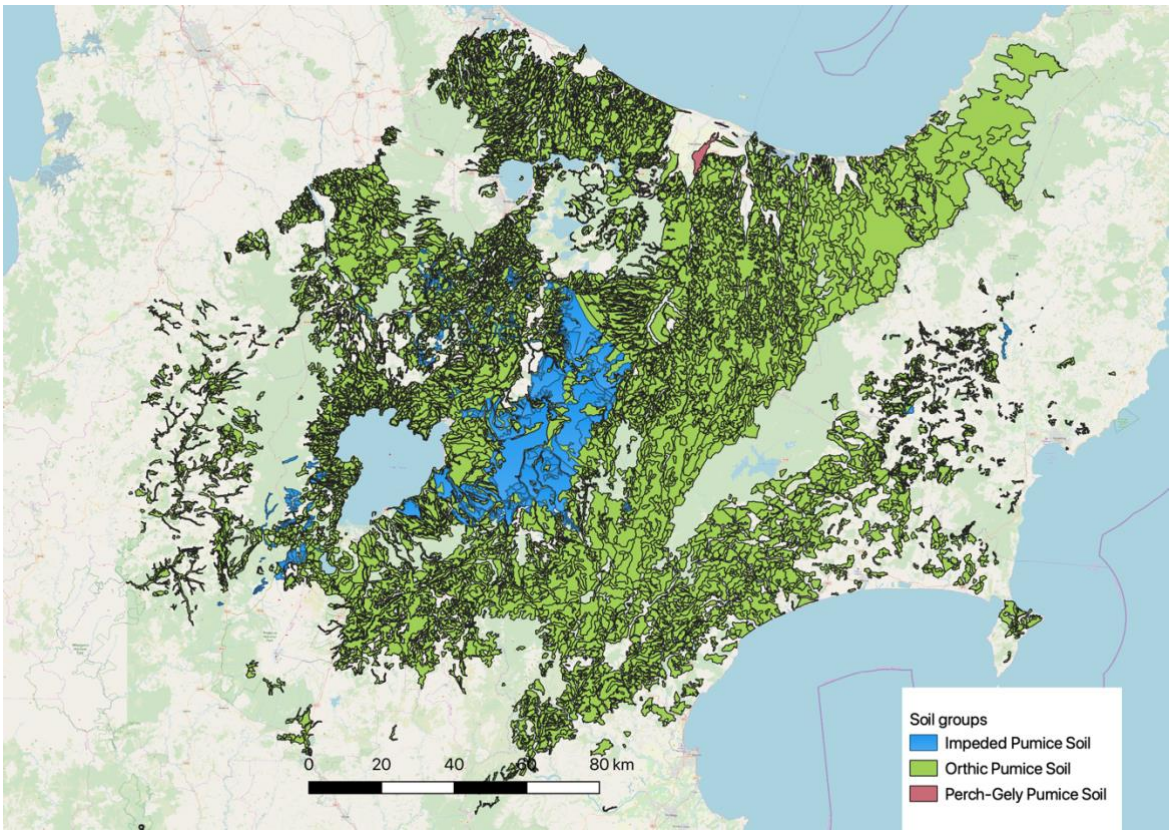

Figure 2.5: Soil groups of the Pumice Soil order found in the Central North Island of New Zealand. A further small area of Orthic Pumice soils are found to the south east of Mt Taranaki (Map created in QGIS with soil data from Landcare Research, 2010).

that have formed in volcanic ash (Soil Survey Staff, 1999; Takahashi & Shoji, 2002). Within the Andosol soil order, Pumice Soils are most closely aligned with the Vitriaquand and Vitricryand great groups of the Vitrand suborder (Hewitt, 2010; Soil Survey Staff, 1999; Takahashi & Shoji, 2002).

While there have been no studies on the role of pumice clasts in water storage in New Zealand Pumice Soils, there have been a number of studies focused on other aspects of these soils. The chemistry of these soils was studied in the first half of the 1900's to determine the cause of 'Bush Sickness', an animal wasting disease. In the early 1930's it was found that the disease was caused by a deficiency of cobalt in the soil as a result of high concentrations of molybdenum. Other studies of the chemistry of Pumice Soils during the 20th century came as a result of other animal health issues, including white muscle disease in lambs and calves, infertility in ewes and unthriftiness in all stock, which were attributed to a deficiency in selenium in the soil (Andrews, 1974; Clare, 1999).

The physical properties of Pumice Soils have also been the focus of studies to determine the suitability of the land for agriculture and forestry. A majority of agricultural studies have found that the soils are free draining with low drought tolerance and rapid onset of moisture stress for pasture species (Gordon, 1971; Noble, 1974).

To improve the readily available water content of Pumice Soils used for pasture production, the Galatea Soil Flipping Project in the Bay of Plenty was implemented. In this trial, the soils were mixed using a digger, bringing developed paleosols (buried soils) to the surface, with WHC, soil heat transfer properties, pasture root development and soil fertility quantified in comparison to undisturbed Pumice Soils. The trial occurred over two years, one of which was the longest drought since 2007. While the pasture on the control soil did not survive the drought, the pastures on the flipped soils remained green, and over a 12 month period the flipped soil treatments produced more dry matter per hectare than the control treatments. The flipped soils had considerably more readily available water than the undisturbed soils and more even temperatures throughout the soil (Laubscher, 2014; Lowe et al., 2014).

In contrast to the pasture based studies that are largely concerned with the properties and characteristics of the upper soil profile where the root zones of pasture species are located, forestry based studies have concluded that there is sufficient available water to sustain growth through periods of low rainfall (Will & Stone, 1967). This water is stored in the deeper subsurface horizons, accessible by the roots of the main forestry species, *Pinus radiata*. In a study of the suitability of

Pumice Soils for forestry on the Kaingaroa plateau, Will and Stone (1967) found that growth in *P. radiata* continued steadily through periods of drought which affected pasture production and under

conditions that slowed *P. radiata* growth on other soil types. The deep root systems of forestry species enables the trees to access water stored in deeper horizons that is unavailable to pasture species (Will & Stone, 1967). Pumiceous material is found in greater amounts in sub-soil layers in the soil profile (Landcare Research, 2019b, 2020), potentially impacting the water availability of the soil for forestry species. The location of the studies are also likely to have affected the results observed, with a majority of pastural studies occurring on areas dominated by free draining Orthic Pumice Soils, while forestry and its related studies have mainly occurred on the Kaingaroa Plateau, an area covered by Impeded Pumice Soils (Landcare Research, 2018b). The latter is characterised by a subsoil layer that is slowly permeable, restricting water movement or roots within 90 cm of the soil surface (Hewitt, 2010; Landcare Research, 2018b). This is often due to compaction or the presence of welded ignimbrite layers (Hewitt, 2010).

2.6 Pumice clast physical properties

Pumice is formed in explosive volcanic eruptions from silicic magmas that are rich in gasses and volatiles. When the pressure in the magma chamber is released rapidly during an eruption, the volatiles exsolve and gasses expand in the magma resulting in the formation of low density pumice. This causes the magma to bubble and froth, forming low density rock once cooled (Challinor, 1996; Papadopoulos et al., 2008). The use of pumice clasts in a range of applications has led to the physical properties of the clasts being the focus of a number of studies internationally, as outlined in Table 2.1. The majority of these studies have focused on the use of pumice clasts in horticulture and have found that the physical properties of pumice clasts are influenced by the size of the clast, subsequently influencing plant growth and yield. Gizas and Savvas (2007) found that as clast size increased, the bulk density decreased and total porosity increased. This relationship between clast size, bulk density and porosity was also found by Dal Ferro et al. (2014). The bulk density of pumice is typically low, ranging from 0.3 – 0.8 g cm^{-3} (Dal Ferro et al., 2014; Papadopoulos et al., 2008; Raviv et al., 1999). As indicated by the relationships described by Gizas and Savvas (2007) and Dal Ferro et al. (2014), pumice porosity is high, ranging from 0.64 – 0.85 m^3 m^{-3} (Boertje, 1995; Challinor, 1996; Gizas & Savvas, 2007; Lockwood & Hazlett, 2010; Raviv et al., 1999). Pumice porosity has been determined to be bimodal, with dual-porosity models used to fit parameters to water release curves developed for pumice clasts to accurately describe water movement within the clast (Blonquist, Jones, Lebron, & Robinson, 2006; Dal Ferro et al., 2014). Using dual-porosity when describing water movement in horticultural studies, in which pumice only treatments of varying size fractions were used, ensures that both intra-aggregate pore space (within the clast) and interaggregate pore space (between clasts) is accounted for (Blonquist et al., 2006; Dal Ferro et al., 2014). It is unclear if this

model has been applied when pumice clast and soil fines mixes have been used. Blonquist et al. (2006) presents a hydraulic critical point when discussing dual-porosity, in which intra-aggregate pore space is water filled and interaggregate pore space is air filled. This is an important aspect of water availability from pumice clasts, which is affected by hydraulic conductivity. As the suction applied to a core containing pumice is increased, the unsaturated hydraulic conductivity of the core decreases rapidly, resulting in a steep drop in the water content at matric potentials just below 0 kPa. This is more pronounced in larger clasts, which typically have larger pores that drain rapidly, with small clasts having smaller pores (Dal Ferro et al., 2014; Gizas & Savvas, 2007; Raviv et al., 2002; Raviv et al., 1999). While larger pores and lower hydraulic conductivity would correspond to improved root zone aeration, the AWC is decreased to a greater extent than occurs in smaller clasts. This is supported by the findings of Özhan, Özcan, and Gökbulak (2008), in which ground pumice sourced from Turkey was added to different soil textural classes. Treatments in which pumice ground to 2 mm was added improved the WHC of coarse textured soils (sand and sandy loam) (Özhan et al., 2008), indicating a high WHC of small clasts. In contrast to this, Sahin, Ors, Ercisli, Anapali, and Eistken (2005) found that strawberry plant growth in a soil-pumice mix was greatest in treatments with clast size between 4-8 mm, as opposed to 2-4 mm, attributed to greater root aeration.

Table 2.1: Physical properties of pumice clasts used in various international studies. ρ_p – particle density, ρ_b – bulk density, ϕ_T – total porosity, FC – Field capacity, PWP – Permanent wilting point, AWC – Available water content, EAW - easily available water.

Author	Origin	Size grade	ρ_p	ρ_b	Φ_T	FC	PWP	AWC	EAW
		mm	g cm^{-3}	g cm^{-3}	%	%	%	%	%
Flores-Ramírez et al. (2018)	Germany	2-12 mm	2.12	0.57	73%	11	2	9	
Gizas and Savvas (2007)	Greece	4-8 mm		0.62					1.07
Dal Ferro et al. (2014)	Italy	6-14 mm	2.42	0.3	39%			10	
	Italy	7-12 mm	2.47	0.32	45%			10	
Lockwood and Hazlett (2010)					64-85%				
Gabriel, Altland, and Owen (2009)	Oregon	<9.5 mm		0.41	77%				
Boertje (1995)	Iceland			0.4	85%				5
Raviv et al. (1999)	Italy			0.71	70%				3.8
	Greece			0.64	75%				2.1
Sahin et al. (2005)	Turkey	2-4 mm	2.24	0.38					

Author	Origin	Size grade	ρp	ρb	ΦT	FC	PWP	AWC	EAW
		mm	g cm^{-3}	g cm^{-3}	%	%	%	%	%
Özhan et al. (2008)	Turkey	<2 mm				32	11	21	
Parajuli et al. (2017)	Various	25 mm		0.96					
Marinou, Chrysargyris, and Tzortzakis (2013)	Greece	<8 mm		0.63	68%				
Gunnlaugsson and Adalsteinsson (1995)	Iceland	0-6 mm		0.4	80%				
	Iceland	1-4 mm		0.4	82%				
	Iceland	0-1 mm		0.4	85%				
Pérez-Urrestarazu, Fernández-Cañero, Campos-Navarro, Sousa-Ortega, and Egea (2019)	Spain	0.0625-4 mm		0.83	56%				3.8
Maloupa, Abou Hadid, Prasad, and Kavafakis (2001)	Greece	0-5 mm		0.85	55%				
	Greece	5-8 mm		0.63	67%				
	Greece	8-16 mm		0.54	69%				
Banitalebi, Mosaddeghi, and Shariatmadari (2019)	Iran	<2 mm	2.48	0.98	60%				

Author	Origin	Size grade	ρ_p	ρ_b	Φ_T	FC	PWP	AWC	EAW
		mm	g cm^{-3}	g cm^{-3}	%	%	%	%	%
Grzegorz et al. (2018)	Poland	3-6	1.28	0.69		31	14	17	
Seoane, Vence, Svartz, and Barbaro (2018)	Argentina	0.062 - 2		0.28	89				
Blok, De Kreij, Baas, and Weaver (2008)				0.43	83				
Flint and Childs (1984)	Oregon	2-4.75	2.33	1.11	52			12.1	
	Oregon	2-4.76	2.13	0.84	60			20.2	
Blonquist et al. (2006)	Washington	3.2-9.5	2.1	0.36	83				

2.7 Determining pumice water content

Different methods have been used to determine the water content of pumice clasts in international and domestic studies. These studies have included methods to alter the matric potential of the clasts and measurement of the water contents at the different matric potentials reached. Methods used have included pressure plates, suction plates, TDR and gravimetric methods.

2.7.1 Pressure plates

In international studies using pressure plates to determine the water content of graded, whole pumice clasts, repacked cores were often used, enabling specific treatments to be implemented and replicated. When packing samples containing pumice clasts in increments to a target bulk density, the size of the fragments included are limited to less than the height of each packing layer; however, the size of the pumice clasts being studied is in most situations is likely to be greater than the 10 mm height used for packing cores for use with pressure plates. Pumice clasts found in New Zealand Pumice Soils range in size from <2 mm to >70 mm, with the bulk density of clasts increasing as clast size decreases. This relationship is demonstrated in the reverse – grading effect seen in lacustrine environments, where the denser, smaller clasts sink before the larger pumice clasts (White et al., 2001). As a result of the size requirement when packing cores for use with this method, whole and unaltered clasts are unlikely to be representative and provide a reliable indication of the water content of pumice clasts found in New Zealand Pumice Soils.

Two international studies used pressure plates with repacked soil cores for studies where the limitation of clast size due to the shallow depth of the cores were not an issue. The first study, by Volterrani and Magni (2012), on the suitability of different porous volcanic materials, sourced from Italy, for use in root zone mixes for sports fields and turfs, used unaltered pumice clasts up to 4 mm in diameter. The material was packed into 10 mm deep cores with a diameter of 52 mm, saturated and placed in the pressure chamber with matric potentials from -33 kPa (FC) to -1,500 kPa (PWP) applied for a soil water release curve to be developed (Volterrani & Magni, 2012). This study found that pumice clasts between 2 – 4 mm had a AWC that was greater than clast size fractions below 2 mm (Volterrani & Magni, 2012). The second study, by Özhan et al. (2008) on pumice sourced from Turkey, used repacked soil cores of an unspecified size for use in a pressure chamber. The cores were packed with mixtures of pumice ground to 2 mm and soils of different textural classes. This study found that a mixture of 50% ground pumice and 50% soil fines significantly increased the AWC of all soil textural classes, with the exception of clay loam (Özhan et al., 2008). Grinding the pumice destroys the natural structure and porosity of the fragments and although this may be useful in

horticultural applications, it does not provide a representation of the WHC of natural pumice fragments *in situ*.

The main advantage of the pressure plate method when developing a full soil water release curve is the range of 0 kPa to 1500 kPa that is able to be covered using a single method (Soilmoisture equipment corp, n.d.; Volterrani & Magni, 2012). Care must be taken, as while retaining soil structure is not important when developing the wet end of the soil water release curve, it is important when determining the water content of samples near saturation, as this is where the large pores in the soil are drained (Cooper, 2016). This is not likely to have an impact in situations such as the study by Özhan et al. (2008), in which ground pumice is used, eliminating the need to consider the natural structure of the pumice, as should be a consideration in studies involving unaltered clasts, as were used by Volterrani and Magni (2012).

The dry end of the soil water release curve for a range of aggregated porous media was developed using pressure plate extraction with cores 10 mm deep. Of the four porous media types used in this experiment, pumice were the largest clasts used, measuring 3.2 – 9.5 mm, while the next largest material analysed was turface at 2.0 – 5.0 mm and the smallest material, profile, at 0.25 – 0.85 mm (Blonquist et al., 2006). To avoid variation in the physical properties of each of the media, the same size fraction was used when developing the wet end of the soil water release curve using a suction method, despite deeper cores used for the wet end experiment.

Pressure plate apparatus were used in two New Zealand based studies on Pumice Soils. These two studies used the pressure plates to assess the PWP of the soils at -1,500 kPa, to compare with PWP values obtained using dwarf sunflowers in glasshouse trials. The first study by Packard (1957), used repacked soil cores with material that had been sieved to 2 mm. Packard (1957) found that the soil fines required longer than a week to reach saturation and greater than 2 weeks for equilibrium to be reached at -1,500 kPa. The study by Will and Stone (1967) on Pumice Soils on the Kaingaroa Plateau included a horizon of the Taupō lapilli. The size of the cores and grade of the lapilli included in this experiment were not stated; however, Will and Stone (1967) note that all horizons required 10 days to reach equilibrium at -1,500 kPa, as opposed to the 14 days determined by Packard (1957).

2.7.2 Suction plates

A number of different suction methods have been used when determining the water content of pumice and other coarse fragments at the wet end of the soil water release curve. This includes sandboxes, tension tables and suction plates with vacuum.

Small soil cores that were 20 mm deep were used with the hanging water column method, described by Dane and Hopmans (2002), in the study by Blonquist et al. (2006) on aggregated porous media, including pumice. Using this method, 0.0 and -0.3 meters of head, the equivalent of 0.0 and -2.9 kPa, were applied to the cores. When using suction methodology, the limitation of core height present when using pressure plate apparatus does not apply, enabling larger samples and clasts to be analysed. The small cores used in the experiment by Blonquist et al. (2006) were selected as the size of the clasts used were small and so the variation in head from the top of the core to the bottom could be neglected.

In a study on the moisture characteristics of the porous Hanford Gravels, Tokunaga et al. (2003) used gravels packed into 30 mm deep modified large Tempe cells. Prior to packing, the gravels were saturated overnight at subatmospheric pressure (2.3 kPa). The cell was placed on a fritted glass plate and an outflow pipette was attached (Tokunaga, Wan, & Olson, 2002). While this study did not involve pumice clasts, the porous nature of the Hanford Gravels indicate the suitability of suction plates when developing the wet end of the water release curve for other porous materials.

The water retention curve in a horticultural study on the hydraulic properties of pumice as a growing medium by Gizas and Savvas (2007) was developed through the use of a sandbox apparatus. After 5 days of saturation, a head of 100 cm of suction was applied using this method, equivalent to -9.8 kPa.

2.7.3 Time domain reflectometry

The transfer equation used for most soil types is known as Topp's equation (Topp et al., 1980); however, this equation is not suitable for use with Pumice Soils (Regalado, Muñoz Carpena, Socorro, & Hernández Moreno, 2003; Topp & Ferré, 2005). Volcanic soils exhibit atypical dielectric behaviour, attributed to their low bulk density and high total porosity, resulting in these soils not obeying the universal relationship of ε_c- θ described by Topp et al. (1980). Tomer, Clothier, Vogeler, and Green (1999) attempted to determine a more appropriate equation to apply to New Zealand Pumice Soils. Three equations were developed for the volcanic soils with physical characteristics such as low bulk density, high porosity and abundant coarse fragments (Tomer et al., 1999). The equation that was most suited to soils with high sand contents of 86 – 91% and gravel contents of 8.7 – 40.9 % is

$$\theta = 0.0215 + 0.0226K_a - 3.02 \times 10^{-4}K_a^2 + 1.1410^{-6}K_a^3 \qquad (2.9)$$

where K_a is the soils apparent dielectric constant (Tomer et al., 1999).

This method for determining the water content of Pumice Soils is useful for horizons that do not contain a large amount of clasts. As mentioned in section 2.2.3, coarse fragments in a soil present difficulties, including the refusal of probes in the soil when they come into contact with fragments, including pumice clasts. Some Pumice Soils have horizons that contain <35% clasts contents (Landcare Research, 2019b), which would be likely to cause difficulties when inserting the probes.

Chapter 3

Methods

A method to quantify the moisture content of pumice clasts has been developed for laboratory based studies using repacked soil cores. Repacked cores are used for this study, as opposed to intact soil cores, to enable the proportion of pumice clasts used to be controlled for the analysis.

3.1 Equipment

Experiments 1 and 2 use repacked soil cores on porous plastic suction plates to develop the wet end of the soil water release curve, using matric potentials between 0 kPa and -80 kPa. The cores used were rings of PVC pipe that measured 97 mm internal diameter by 50 mm high, with a total volume for each core of 369 cm^3 (V_s). A layer of gauze was secured to the base to prevent soil loss when moving the cores (Figure 3.1). The cores were packed to a desired bulk density in increments using the equation of Dane and Hopmans (2002);

$$M = V_s(1 + WC)\rho_b \qquad (3.1)$$

in which ρ_b is the target bulk density of the soil matrix accounting for the prescribed volumetric proportion of clasts; WC is the gravimetric water content (Equation 2.1) of the soil matrix; and V_s is the volume of the increment being packed.

Figure 3.1: Gauze secured to the base of the PVC core to prevent soil loss when moving the packed cores.

All soil cores were packed in two 25 mm increments and then saturated in a deep tray prior to placing on the suction plates.

The porous plastic suction plates used consisted of a polyamide membrane with a pore size diameter of 0.45 µm, a high bubble point of ≥100 kPa and an output volume of ~1000 ml/min, with the porous area measuring 230 mm x 230 mm (ecoTech, n.d.). Basal suction was applied to the plates by a VS-Pro vacuum pump (METER Group Inc, 2012), controlled by tensioVIEW V1.30 software developed by METER (METER Group Inc, n.d.-b).

Before the saturated cores were placed on the suction plates, the plates were prepared. Preparation applying a suction of 1 kPa to 3 kPa to each plate while spraying reverse osmosis (RO) water on as a fine mist to saturate the plate surface. Plates were considered saturated when no air bubbles in the tubing attached to the base of the plate were present. A slurry of silica flour and RO water was then applied to the surface of each plate to ensure contact between the base of the core and the plate. The excess water was drained from the slurry at a low suction before the excess water from the edges of the plates was wiped away. Suction was then applied to all of the plates, increasing incrementally from 0 kPa to 80 kPa to remove any excess water from the plate, to ensure it did not interact with the soil cores. The plates were then placed in large plastic clip-top containers (Sistema™ brand), with self-adhesive sealant applied to the lid to prevent evaporation, and the 6 mm tubing passed through a small hole and sealed. The plate and box unit was then weighed prior to the core being placed in it. Once the cores were deemed to be saturated, each core was removed from the water bath, allowed to drain at a 45° angle for 10 seconds and then weighed, to determine the saturated weight, prior to pacing the core on its plate. Once all the cores were situated on their plates, the box lids were replaced and the starting suction applied.

Each plate was able to be isolated from the vacuum using the shut-off valves connecting each plate to the main vacuum line (Figure 3.2). The core and box units were all weighed daily by turning off all of the valves connecting the vacuum to the plates; the plates were unplugged from the manifold (Figure 3.2) at the shut off valve and weighed, without removing the plates from the boxes. The plates were then plugged back in and vacuum applied. Once equilibrium was reached at each matric potential, the matric potential was lowered to the next pre-determined set point. Finally, when equilibrium was reached at -80 kPa, the soil cores were weighed for the last time. To determine the final bulk density of the soil fines, a layer of plastic wrap was laid over the surface of each core and gently pressed down until the surface of the soil in the core was covered. The core was then placed on a tared balance and water was added until the surface of the water was flush with the top of the PVC ring. The volume of water used was calculated and then subtracted from the total volume of the

Figure 3.2: Shut-off valve (red and black) used to isolate the plate from the vacuum. The manifold is the white PVC pipe connected to each plate through the shut-off valve and 6 mm tube and to the vacuum pump and collection flask (Figure 3.4, Figure 3.10).

core (369 cm^3) and the bulk density was recalculated. The water was then siphoned off using a syringe to prevent any water entering the core. Following this, the soil was transferred from the PVC ring into a tared drying tin and weighed, before being air dried for 24 hours at 105°C. The soil and tin were then weighed again when dry to enable the gravimetric water content to be determined (Equation 2.1). The box and plate units and PVC rings were weighed to enable the weight of the soil in each core to be determined at each metric potential.

3.2 Experiment 1

In Experiment 1, five soil cores were packed with soil matrix and pumice clasts sourced from Acacia Bay, Lake Taupō. The soil was an Immature Orthic Pumice Soil, from the Taupo soil family (Sibling 48) (Landcare Research, 2019b), from which air dried pumice clasts (2 – 20 mm) and soil fines (<2 mm) were used.

The cores were packed with clast concentrations of 0%, 10%, 20%, 30% and 40% as a ratio of pumice to the total volume of the soil core (χ_v). These concentrations were based on the proportions of pumice clasts found within the profile of the Taupō soil family, which ranges from 5% to 35% (Landcare Research, 2019b).

Equation 3.1 was rearranged to Equation 3.2 to account for both the soil fines and pumice clasts in the total volume. The target soil fines bulk density (ρ_b) used was 0.95 g cm $^{-3}$. This value was used based on the result of preliminary trials carried out to determine a suitable packing bulk density to limit sinking and cracking in the repacked soil cores. This value is higher than what is commonly found in Immature Orthic Pumice Soils under natural conditions (Landcare Research, 2019b), but it avoided the sinking and cracking observed when a lower target bulk density was used.

The mass of pumice clasts and soil fines (M) required to pack into each core was determined using

$$M = ((1 + w_s)V_s(1 - \chi_v)\rho_b) + ((1 + w_p)V_s\chi_v\rho_p) \quad (3.2)$$

in which the gravimetric water contents of the soil (w_s) and pumice clasts (w_p) were calculated using Equation 3.2 following the drying and weighing of known amounts of moist soil or pumice. The dry bulk density of the pumice clasts (ρ_p) was determined by weighing individual dry pumice clasts and then submerging them while wrapped tightly in plastic in a measuring cylinder to determine their volume. This was repeated with 20 pumice clasts, from which an average bulk density of 0.4 g cm^{-3} was calculated using the following equation from (Shukla, 2014);

$$\rho_p = \frac{dry\ clast\ weight}{clast\ volume} \quad (3.3)$$

Once the cores were packed, they were left to saturate, while covered to limit evaporation, for two weeks before being weighed and placed on the prepared porous suction plates.

In Experiment 1, the silica flour slurry was used to cover the entire surface of the saturated suction plates (Figure 3.3). The matric potentials applied in this experiment were; -2 kPa, -4 kPa, -6 kPa, -8 kPa, -10 kPa, -20 kPa, -40 kPa, -60 kPa and -80 kPa.

The configuration of the suction plates used in Experiment 1 consisted of five plates lined up at increasing distance from the vacuum pump (Figure 3.4). The plates were connected using 4 mm ID (6mm OD) tubing through which vacuum was applied to the base of each plate (Figure 3.4). The

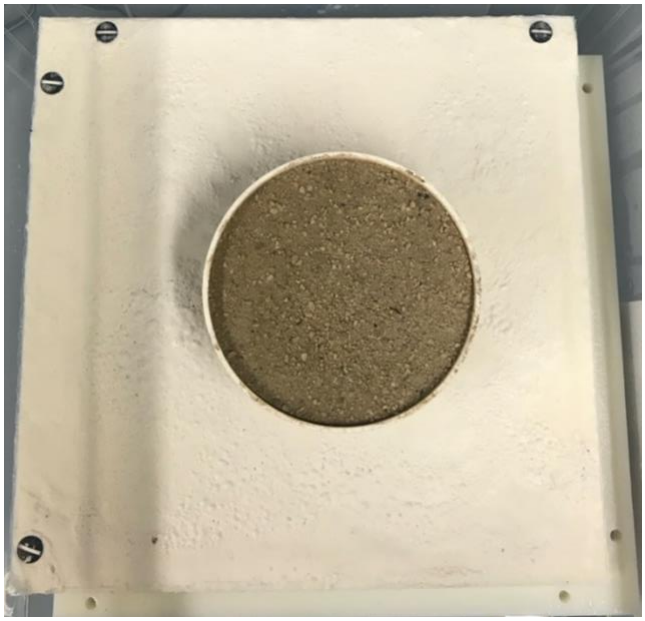

Figure 3.3: A silica flour and RO water slurry was applied to the entire surface of the plate and smoothed to provide an even coating to ensure contact between the base of the soil core and the suction plate.

water was sucked from the plates, through the tubing and into a collection flask located on the bench. Vacuum was applied to the flask and to the plates through a connection to the vacuum pump (white tubing in Figure 3.4).

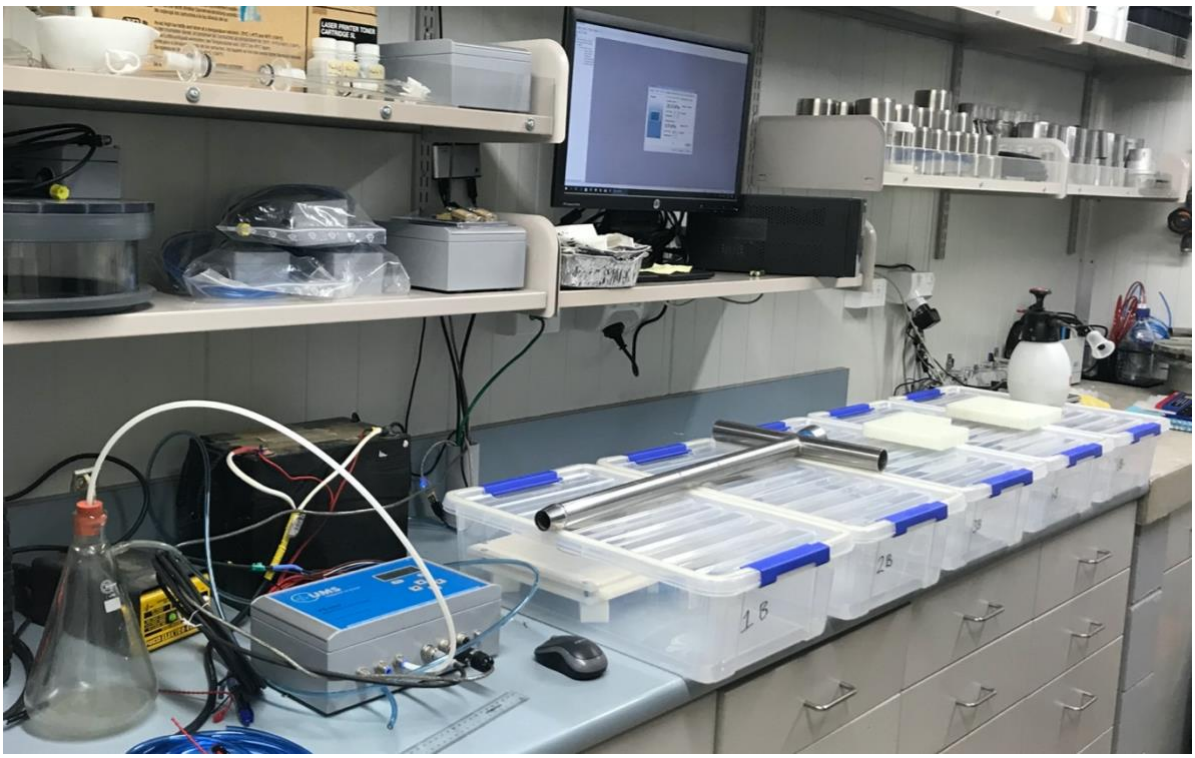

Figure 3.4: Arrangement of the components of Experiment 1 including the 5 boxes containing the soil cores, grey and blue vacuum pump, water collection flask and computer with tensioVIEW controlling the vacuum.

Following weighing of the cores each day, the valves were turned on in a random order, restoring vacuum to the plates.

To determine the particle size distribution of the soil fines that the cores in Experiment 1 were packed with, the pipette method (Day, 1965) (method 190 (ii)) was used at the Manaaki Whenua Landcare Research Soil Physics Laboratory. In this method, a soil suspension is placed in a column and shaken. A pipette is then used to withdraw samples from a set depth at various times, as described by (Claydon, 1989).

3.2.1 Analysis 1

The water content of the soil matrix and pumice clasts were determined volumetrically using the following steps. First it was assumed that the water content of the soil fines at any suction does not vary with pumice clast content, so the gravimetric water content of the soil fines (w_s) was given by

$$w_s(h) = \frac{M_{s,w}(h) - M_{s.d}}{M_{s,d}} \tag{3.4}$$

where h refers to the suction imposed, M_s refers to the mass of the soil in the soil-only (0% pumice clast) core, and subscripts w and d refer to wet and dry, respectively. The gravimetric water content of the pumice clasts (w_p) at suction h was then

$$w_p(h) = \frac{M_{s+p,w}(h) - (1-\chi)M_{s+p,d}w_s(h)}{\chi_m M_{s+p,d}} \tag{3.5}$$

where χ_m is the ratio of mass of dry pumice to the mass of dry soil fines and subscript p refers to the pumice clasts.

The gravimetric water content of the pumice clasts at suction h were then converted θ using

$$\theta_p(h) = w_p(h)\left(\frac{\rho_p}{\rho_w}\right) \tag{3.6}$$

The bulk density (ρ_p) value used was the average dry bulk density of the pumice clasts included in the core, 0.4 g cm^{-3}, and the density of water was assumed to be 1.0 g cm^{-3} (Shukla, 2014).

The θ values of the pumice clasts were then plotted against suction *h* to develop a water release curve.

3.2.2 Analysis 2

Based on the findings of Analysis 1, Equation 3.5 must be rearranged as it is clear that the soil-only core overestimated the water content of the fines of the cores containing pumice.

Equation 3.5 can be rearranged to

$$w_{s+p} = (w_p - w_s)\chi + w_s \tag{3.7}$$

where w_{s+p} is the total water content of the core, in which subscript *p* refers to the pumice clasts, subscript *s* refers to the soil fines and χ is the ratio of mass of dry pumice to mass of dry soil.

The water content of the core (w_{s+p}) was plotted against χ and regression applied to derive the line of best fit for each matric potential.

Using Equation 3.7, it is clear that a plot of w_{s+p} against χ will yield a straight line with the slope ($w_p - w_s$) and intercept (w_s) so long as assumptions of the derivation hold true. The key assumption is that w_s is a constant at any given matric potential across different pumice clast concentrations. Thus, this analysis is a test of that assumption: if the data fall on a line, the assumption holds true. The water content of the pumice is given by the sum of the slope and the intercept of the regression equation. Statistical analysis of the water content of the soil and clasts was carried out in excel using the LINEST function, calculating the standard error, R^2 values and F statistic (Microsoft, n.d.).

To determine the θ value of the pumice clasts, Equation 3.6 was used. To determine the water content of the soil fines, Equation 3.6 was adapted to

$$\theta_s(h) = w_s(h)\left(\frac{\rho_b}{\rho_w}\right) \tag{3.8}$$

in which ρ_b is the average bulk density of the soil fines. The bulk density of the soil fines was recalculated at the end of the experiment to account for the sinking that occurred in each core throughout the experiment, increasing it from the target bulk density the cores were packed to.

The standard error (SE) was then calculated for the volumetric water contents of the soil fines and the pumice clasts using Equation 3.9,

$$SE = \sqrt{SE_w^2 + SE_{\rho b}^2} \tag{3.9}$$

where SE_w is the standard error of the water content of the pumice clasts/ soil fines and SE_{pb} is the standard error of the bulk density calculated for each constituent.

The θ of the soil fines and the pumice clasts were then plotted against the suctions applied to develop a water release curve.

3.3 Experiment 2

Experiment 2 aimed to address limitations of the methods used in Experiment 1 induced by changes in the water retention properties of the fines caused by different volumetric proportions of clasts. In this experiment, ten repacked soil cores, all intended to have a constant volumetric proportion of fines, were constructed. The soil fines fraction was sourced from Taupō Landscape Supplies and was sieved to 2 mm. Pumice clasts of the size fraction 6 - 20 mm, sourced from a pumice quarry near Atiamuri, 40 km from Lake Taupō (Figure 3.5), were packed in increments from 2% to 22%, shown in Table 3.1. These clasts are likely to be from the Hatepe plinian pumice phase of the 232 ± 10 AD Taupō eruption. The clasts had not been air dried and were saturated in RO water for three weeks prior to packing to ensure that accurate pumice water contents were able to be determined. When pumice has been air-dried and re-saturated, it is possible that not all of the pores that may release water when suction is applied are able to refill.

To create the range in pumice clast volumetric proportion necessary to derive pumice water content while maintaining a constant volumetric proportion of fines, glass fragments were introduced as an inert coarse clast content. The glass fragments used were 17 – 20 mm Nouveau garden glass gemstones that were split in half (Figure 3.6) to better match the characteristic size of pumice clasts

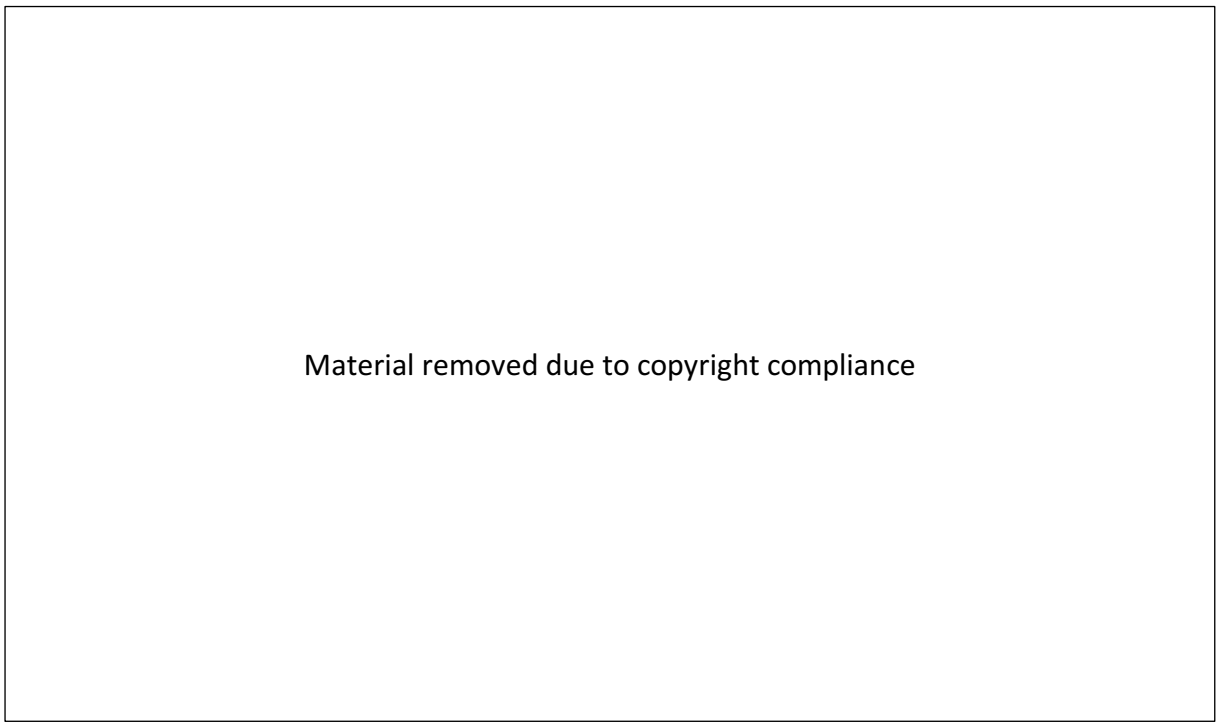

Figure 3.5: Location of source of pumice clasts used in soil cores. The pumice pit is located within the extent of the Taupō ignimbrite, shown by the red outline, on the lilac coloured map units which represent non-welded ignimbrite (Adapted from GNS, n.d.; Hogg, Lowe, Palmer, Boswijk, & Ramsey, 2012).

Figure 3.6: Split glass fragments packed into the soil cores to enable the matrix to remain at a constant volume.

and thereby create similar packing effects. The glass fragments were assumed to be inert with respect to water retention characteristics of the soil; i.e., they had a volumetric water content of 0% and did not induce water storage via surface effects or lacuna porosity.

3.3.1 Experimental design and mathematical analysis

The cores were packed to a target volumetric proportion of coarse clasts (C = $\chi_p + \chi_g$, Table 3.1) of 30%, and a fines bulk density of 0.85 g cm^{-3}. This lower target bulk density than what was used in Experiment 1 is more aligned with the bulk density of Pumice Soils under natural conditions (Jackson, 1974; Landcare Research, 2019b; McLeod, McGill, Thronburrow, & Fitzgerald, 2016; Nanzyo, 1993). To pack the cores, the gravimetric water contents of the moist soil fines (w_s) and saturated pumice clasts (w_p) were determined and the bulk density of the glass and pumice calculated. A sample of 20 randomly selected glass fragments were weighed and submerged in a measuring cylinder partially filled with water. The weight of the dry glass fragments was divided by the displacement volume to determine the dry bulk density. To determine the bulk density of the pumice clasts, 40 dry clasts were each weighed and submerged in a measuring cylinder partially filled with water, while tightly wrapped in plastic wrap to determine the displacement volume of the clast, from while the dry bulk density was calculated as for the glass fragments.

Cores were packed using pumice clast bulk densities as derived by the method outlined above. However, on further consideration it became clear that the bulk densities derived this way were both inaccurate and imprecise. An Archimedean glass bead method was used as an alternative.

Errors arising from the inaccurate bulk density propagated through to the volumetric proportion of fines and clasts, but these errors were accounted for mathematically as described below. At the

Table 3.1: Experimental design of Experiment 2, using glass to enable to soil matrix to remain at a constant volume.

Core #	Soil matrix (1-C)	Pumice (χ_p)	Glass (χ_g)	C
1	70	3	27%	30%
2	70	6	24%	30%
3	70	9	21%	30%
4	70	12	18%	30%
5	70	15	15%	30%
6	70	18	12%	30%
7	70	21	9%	30%
8	70	24	6%	30%
9	70	27	3%	30%
10	70	30	0%	30%

completion of the suction plate experiment, the bulk density of the pumice clasts was determined using the Archimedean glass bead method. The volume of a small measuring vessel (v_r) was determined by filling it with water until the water sat flush with the top of the vessel and recording the volume of water required. Next, the vessel was dried thoroughly before determining the density of 400 µm gas chromatography beads from BDH Chemicals Ltd. The density of the beads was determined by filling the vessel with beads, tapping incrementally, until the vessel was overflowing, then levelled to flush with a ruler and weighing on a balance tared to the vessel mass. The density of the beads (ρ_{gb}) was calculated using the following

$$\rho_{gb} = \frac{m_b}{v_b} \tag{3.10}$$

Figure 3.7: Glass bead method to determine the bulk density of pumice clasts.

where m_b is the mass of beads required to fill the vessel and v_b is the volume of beads, equal to the volume of the vessel.

Following the determination of the density of the beads, 10 randomly selected, oven dried, pumice clasts from a sieved core were weighed together to determine their mass (m_p) and placed into the vessel that was partially filled with the beads. The vessel was tapped 20 times to ensure contact around the clasts. This was repeated in three increments for each core to enable all ten clasts to be placed in the vessel with no contact between clasts. The vessel was then filled almost to the top with the beads and tapped 20 times before filling the rest of the way and levelling with a ruler before weighing. The volume of the pumice (v_p) was then determined using the following steps

$$m_b = m_t - m_p \tag{3.11}$$

where m_t is the combined weight of the glass beads and pumice clasts. Once the mass of beads was known, the volume of beads could be calculated (Equation 3.12) and the volume of the pumice can be determined (Equation 3.13)

$$v_b = \frac{m_b}{\rho_b} \tag{3.12}$$

$$v_p = v_r - v_b \quad (3.13)$$

From this information, the bulk density of the pumice clasts was determined by adapting Equation 3.10 to calculate the bulk density of the pumice (ρ_p) by dividing the mass of the pumice by the volume calculated in Equation 3.13. This procedure repeated 20 times with 10 clasts at a time, with 200 clasts in total analysed.

From the more reliable pumice bulk density the volumetric proportions of pumice clasts and glass was recalculated (Table 3.2).

Table 3.2: Proportions of soil fines, pumice clasts and glass fragments packed in each core.

Core #	Soil matrix (1-C)	Pumice (χ_p)	Glass (χ_g)
1	71	2	27%
2	72	4	24%
3	72	7	21%
4	73	9	18%
5	74	11	15%
6	75	13	12%
7	76	15	9%
8	76	18	6%
9	77	20	3%
10	78	22	0%

3.3.2 Set up

Equation 3.2 was adapted to determine the mass of material (*M*) to be packed into each core, accounting for the soil fines (subscript *s*), pumice clasts (subscript *p*) and glass fragments (subscript *g*) (Equation 3.14).

Figure 3.8: Packed soil core containing soil matrix, pumice clasts and glass fragments.

$$M = \left((1 + w_s)V_s(1 - C)\rho_b\right) + \left(\left(1 + w_p\right)V_s\chi_v\rho_p\right) + (1 + V_s\left(1 - \chi_g\right)\rho_g) \qquad (3.14)$$

Once the cores were packed (Figure 3.8), they were placed in a large container with degassed water poured carefully around the cores, before being left to stand for one week in order to saturate. Once saturated the cores were drained and weighed before placing on the prepared suction plates. In contrast to Experiment 1 where the whole surface of the plate was covered in the silica slurry, a 110 mm annulus was placed in the centre of the saturated plate and a silica flour slurry comprising 11 g of silica flour mixed with RO water was poured in to provide a 1 mm high layer of silica (Figure 3.9). Suction up to 4 kPa was applied to the plate to remove excess water before the annulus could be removed. This was repeated for all 10 suction plates. Following this the saturated cores were placed in the centre of the silica circle. Unlike Experiment 1, where the cores were set out in order, a random order was generated for the placement of the soil cores layout on the suction plates.

Adjustments were made to the set-up of the vacuum system used in Experiment 1. It was observed that water plugs often formed in the 4 mm tube, potentially influencing the matric potential imposed at different positions along the system. To prevent this occurring, a manifold system was developed, using 53.65 mm ID PVC pipe and 8 mm ID tubing to reduce the opportunity for water plugs to form in long sections of tube. The water collection flask was also moved to a position below

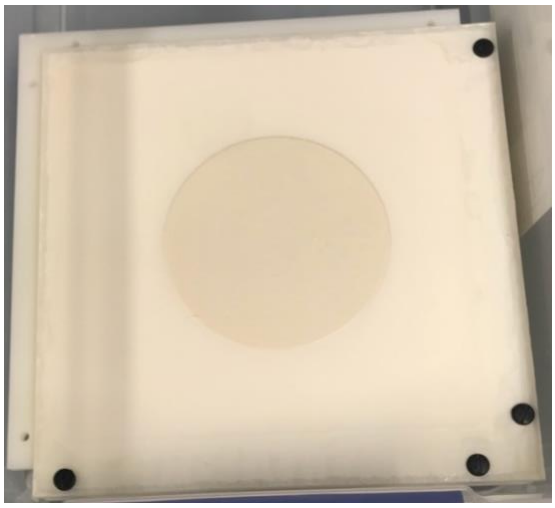

Figure 3.9: 1 mm high, 110 mm diameter silica layer on the suction plate to ensure connectivity between the base of the core and the suction plate.

the water outlet from the plates, enabling the water to drain down into the flask, without having to overcome a pressure head. To allow the water to drain out of the manifold, each length of pipe was angled downward towards the centre of the set up. For the water to flow straight out of the plate and into the manifold, a ramp with steps was set up to keep the plates level while on an inclining platform (Figure 3.10 and 3.11).

Once all cores were in placed and the boxes sealed, the first matric potential of -3 kPa was applied. Matric potentials imposed were -3 kPa, -6 kPa, -8 kPa, -10 kPa, -20 kPa, - 40 kPa, -60 kPa and -80 kPa.

Figure 3.10: Layout and set up of manifold system used in Experiment 2.

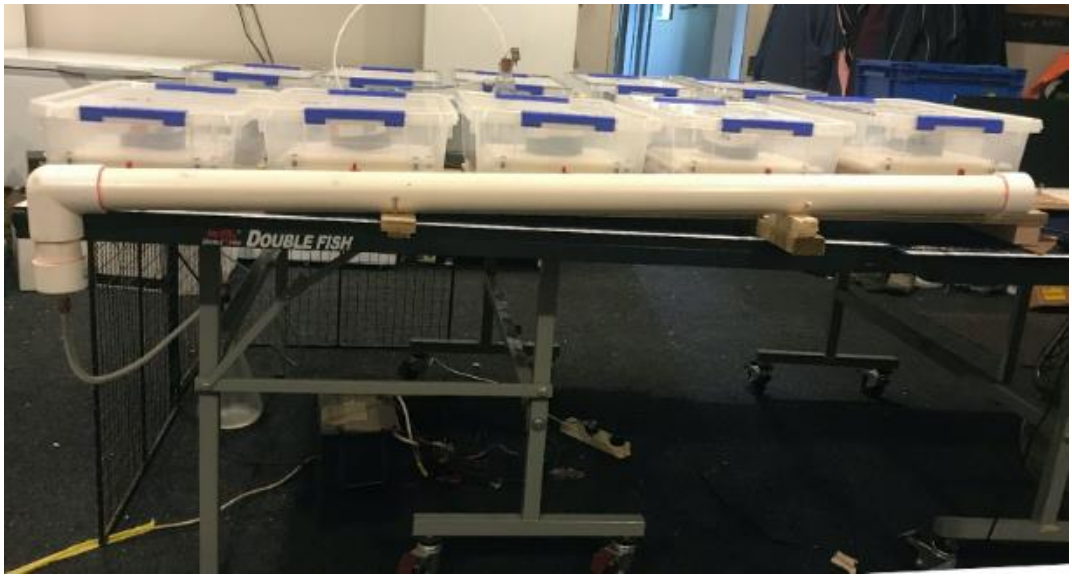

Figure 3.11: Lay out of relocated experimental set up.

Weighing occurred daily to determine when equilibrium had been reached at each matric potential. The shut-off valves were used to stop vacuum being applied to each plate and in tensioVIEW the set point was reduced from the pre-determined matric potential to a matric potential of 0. The plate units were then disconnected, weighed and reconnected to the manifold, with the shut-off valves returned to the open position. Once all of the cores were weighed and reconnected, the set point was then increased to the required matric potential. For matric potentials less than -10 kPa, the set point was increased in -5 kPa increments to reduce stress on the vacuum pump and the possibility of it going to a matric potential less than the required point.

When equilibrium was reached at each matric potential, the condensation that had built up on the lid and walls of each box was wiped off using high absorbency cloths (Figure 3.12). The plate units were then weighed again and the mass of water wiped off was subtracted from the plate unit so that the amount of water lost in condensation was not attributed to the final water content of the core at each matric potential. Once equilibrium was reached at -80 kPa, the final volume of the cores was measured and the cores were air dried.

Using the suction plates and repacked soil cores, a water release curve was developed from near saturation to -80 kPa. To complete the water release curve to a matric potential of -1500 kPa (PWP) a WP4C Dewpoint PotentiaMeter was used to develop the dry end of the curve (Figure 3.13). The device was calibrated using a 0.5 mol KCl standard in a stainless steel sample cup (Decagon Devices, 2013).

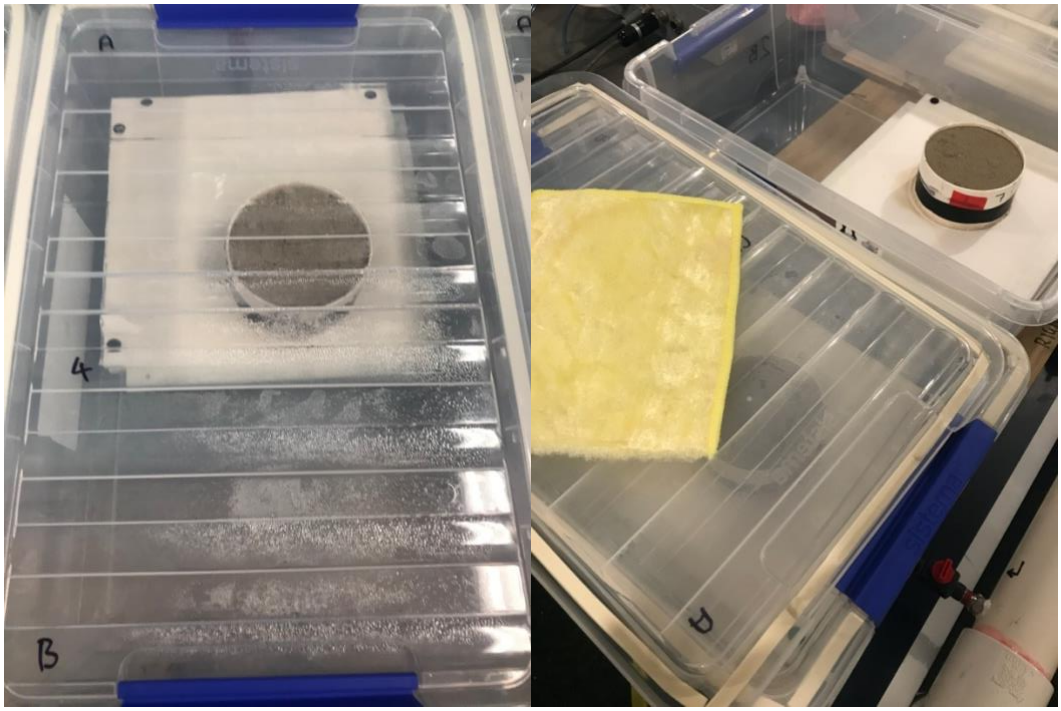

Figure 3.12: Condensation in box that is wiped away using absorbent cloths once equilibrium is reached at suction(h).

Saturated pumice clasts were placed in a constant temperature chamber at 25°C with a relative humidity of 60% for up to 20 hours to dry the clasts to between plant stress point at -100 kPa and PWP. The clasts were removed from the chamber, placed in a stainless-steel sample cup and inserted into the calibrated device with analysis run using the precise mode. The matric potential

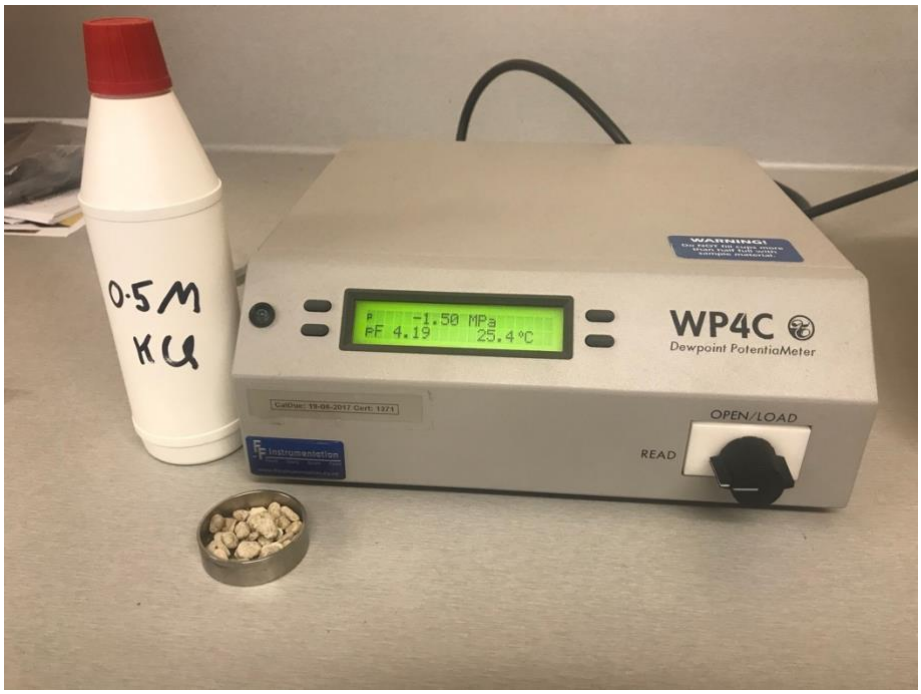

Figure 3.13: WP4C Dewpoint PotentiaMeter device used to develop the dry end of the water release curve at matric potentials lower than -80 kPa.

was recorded and the sample was removed and air dried for 24 hours at 105°C to enable the gravimetric water content of the clasts to be determined. Equation 3.7 was used to convert the gravimetric water content of the pumice clasts to volumetric water content to be plotted as the dry end of the pumice clast water release curve.

3.3.3 Analysis 3

The following steps outline the process that was designed to determine the volumetric water content of the pumice clasts. These steps were based on the initial experimental design for Experiment 2 (Section 3.3.1). However, due to an error in the bulk density calculation, this method was not used, with Analysis 4 executed in its place. If this experiment were to be repeated following the intended methodology, this process would be used to determine the water content of the pumice clasts.

Following drying, the gravimetric water content of the core is determined using Equation 2.1. The gravimetric water content is then converted to θ and linear regression analysis run.

The volumetric water content of the whole core (fines, glass and pumice) is plotted against the volumetric content of glass and pumice included in each core (χ_{glass} and χ_{pumice}). To enable the water content of the pumice and the soil matrix to be determined, the assumption that the water holding capacity of glass is nil must be applied.

$$\theta_{Total} = \theta_{pumice}\chi_{pumice} + \chi_{glass} + (1 - C)\theta_{soil}$$

$$= \theta_{pumice}\chi_{pumice} + (1 - C)\theta_{sol} \qquad (3.15)$$

in which C is a constant representing χ_{pumice} + χ_{glass}. Equation 3.15 dictates that a linear regression of total core volume against proportion of pumice will yield a slope equal to the volumetric water content of the pumice and an intercept equal to the matric water content times 1-*C.*

3.3.4 Analysis 4

The aim of Analysis 4 was to correct for the non-constancy of total clast content (*C*) in the cores. The analysis involved an iterative scaling of the core water content to account for a change in pumice volume sufficient to achieve a constant *C*. First, the water contents of pumice and soil (θ_{pumice} and

θ_{soil}, respectively) were estimated by a regression analysis as described in section 3.3.3. The analysis used the pumice volumetric proportions and measured core water contents. The soil water content was estimated with a value of *C* equal to the average total clast content of the cores (0.26). Next, the increase in pumice content ($\Delta\chi_{pumice}$) necessary to bring each core up to the highest total clast content (0.292) was calculated. Then, the resulting change in core water content was estimated as,

$$\Delta\theta_{Total} = \theta_{pumice}\Delta\chi_{pumice} - \theta_{soil}\Delta\chi_{soil} \quad (3.16)$$

using the estimates of θ_{pumice} and θ_{soil} as described above, and where $\Delta\chi_{pumice} = \Delta\chi_{soil}$.

Next, the water content of each core was adjusted by its corresponding $\Delta\theta_{total}$ and a regression analysis conducted with the corrected pumice contents ($\chi_{pumice} + \Delta\chi_{pumice}$). Finally, the slope and intercept of the regression were used to provide better estimates of θ_{soil} and θ_{pumice}, which were refined iteratively. Iteration involved using current θ_{soil} and θ_{pumice} estimates to calculate a new core water content (Equation 3.16) and repeating the regression analysis. Iteration continued until θ_{soil} and θ_{pumice} changed less than a prescribed precision (0.001) between successive iterations. Uncertainty in θ_{soil} and θ_{pumice} was provided by the standard errors of the regression analysis. The effect of four iterations is demonstrated graphically in Figure 3.13.

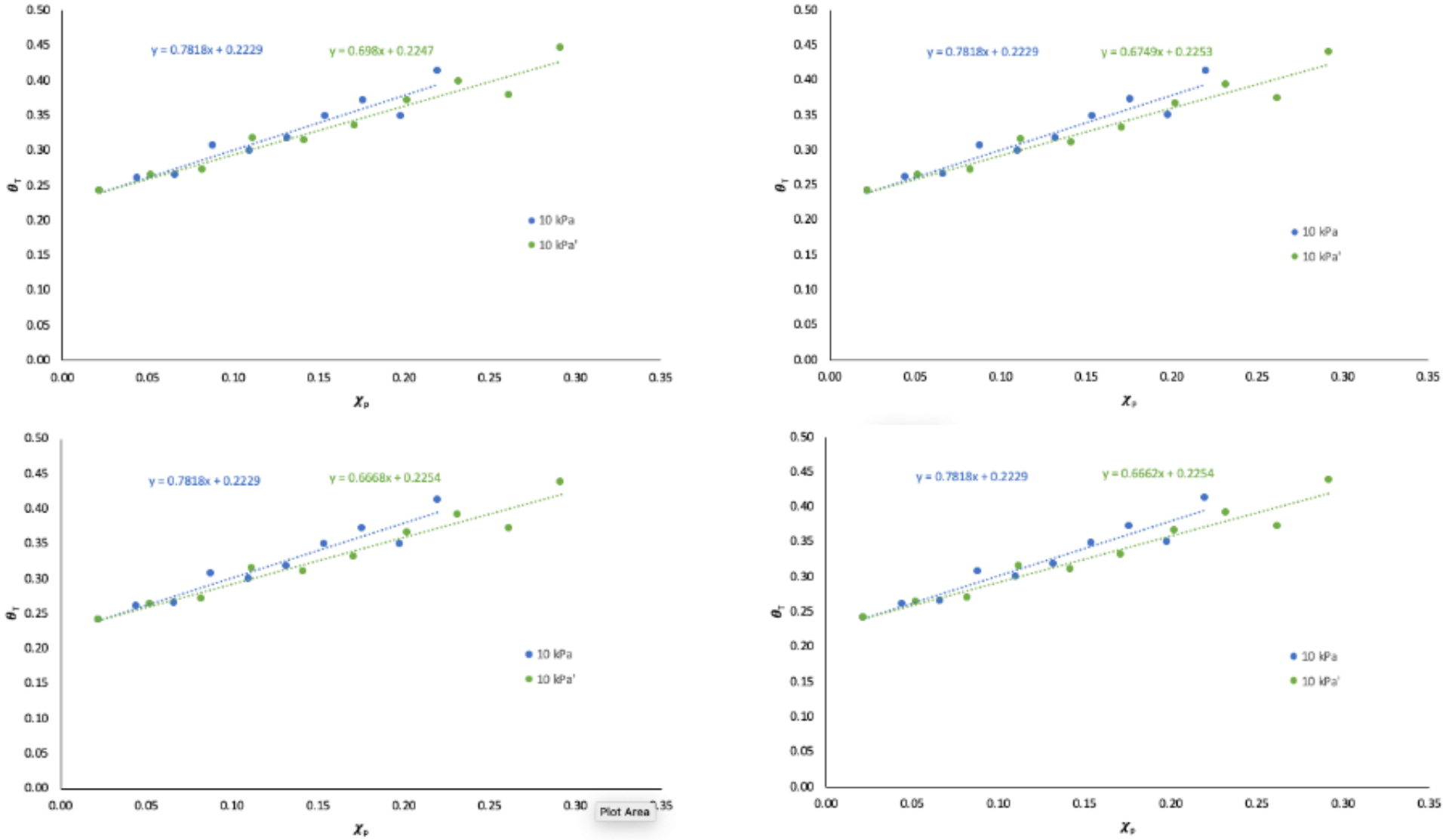

Figure 3.12: Iterations of the scaling of each data point to determine the water content of the soil at pumice at a matric potential of -10 kPa. The notation 10 kPa (blue) is the unscaled data and 10 kPa' (green) is the scaled data.

Chapter 4

Results

4.1 Experiment 1

For equilibrium to be reached at each matric potential, 7 – 10 days were required before the weights of the boxes became constant. Despite the target bulk density value that the soil cores were packed to being higher than what is often found under natural conditions (Jackson, 1974; Packard, 1957; Will & Stone, 1967); however, sinking of the soil in the cores still occurred. The effect of sinking increased the bulk density from the target of 0.95 g cm^{-3} to an average of 1.04 g cm^{-3} across all five cores, with a range of 1.00 – 1.11 g cm^{-3}. There is no pattern to which the treatments sunk the most, with the 40% pumice clast treatment showing the greatest increase in bulk density, with the least amount of change occurring in the 30% pumice clast treatment.

Particle size analysis of the soil fines material packed into the cores used in Experiment 1 was carried out at the Manaaki Whenua Soil Physics Laboratory. The material collected from a Typic Orthic Pumice Sub-soil horizon comprised 18% coarse sand, 16% medium sand, 25% fine sand, 37% silt and 4% clay, placing it in the loamy sand texture class in the New Zealand texture triangle (Figure 4.1).

The cores were set out in order of increasing pumice content, with the 0% pumice treatment at the position closest to the vacuum pump in the centre of the room and the 40% pumice treatment furthest from the pump at the far end of the room. A condensation gradient wais present across the

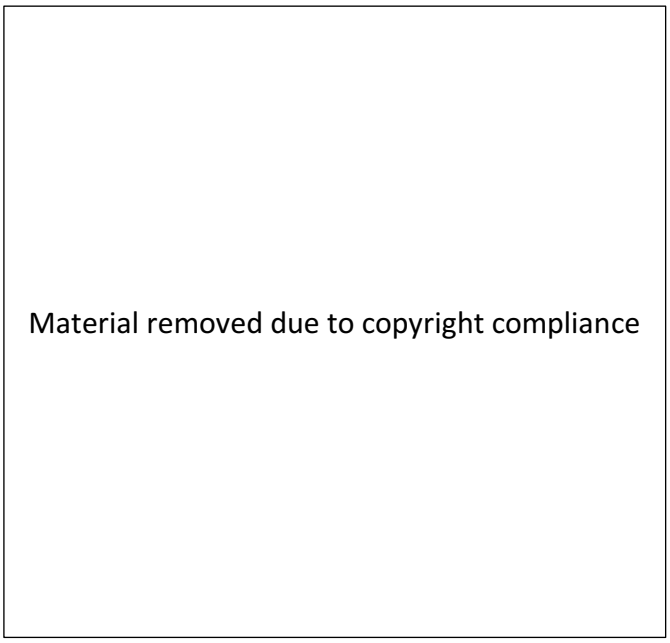

Figure 4.1: New Zealand texture triangle with fractions of fine earth present in the Acacia Bay soil used in Experiment 1 indicated in red. (From Milne, Clayden, Singleton, & Wilson, 1995).

treatments, whereby condensation on the lids and walls of the box noticeably decreased from the 0% to the 40% treatment which visibly had the least amount (Figure 4.2). The mass of condensation was not accounted for as the boxes and plates were not weighed prior to the cores being placed on the plates and the condensation was not removed at any stage during the experiment.

When looking at the water content of the cores as a whole, without isolating the pumice clasts from the soil matrix, the water content of the soil fines only core (0% pumice clasts) was the lowest of all the treatments between suctions of 0 – 10 kPa. This treatment exhibited the least amount of change as the suction increased. At suctions above 50 kPa, the 0% pumice clast core had a higher water content than all other treatments, while the 20% and 30% clast content treatments showed the greatest amount of water lost (Figure 4.2).

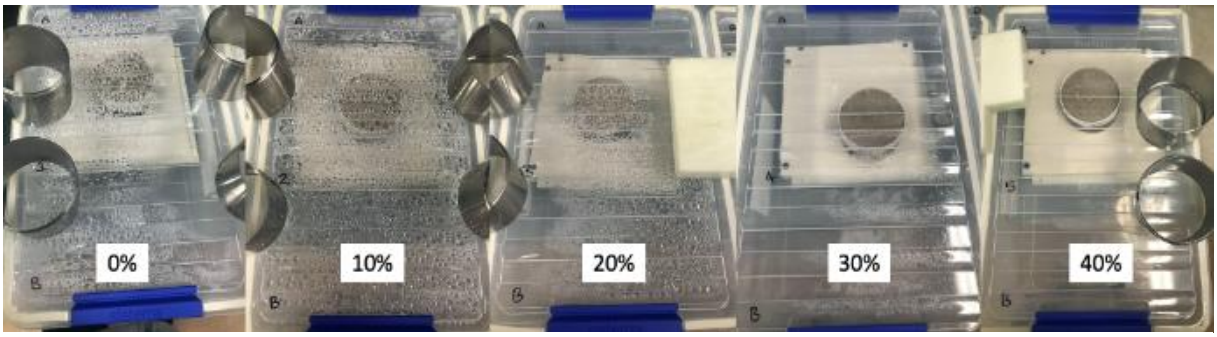

Figure 4.2: Condensation gradient present as both distance from pump increases and clast content increases. The vacuum pump is situated to the left of the 0% pumice content core and the 40% pumice clast core is closest to the lab wall.

4.1.1 Analysis 1

The assumption, that the matrix behaviour would be consistent as the proportion of pumice clasts increased, underpinning Analysis 1 was proven to be invalid. Analysis 1 used the water content of the matrix in the 0% pumice clast treatment as a proxy for the water content of the matrix in the cores that contain pumice clasts. This method appears to overestimate the water content of the matrix in the cores containing clasts. As a result, negative water contents for the treatments containing 10%, 20% and 30% pumice clasts were obtained when separating the water content of the pumice from the total water content of the core (Figures 4.3 and 4.4). While it can be observed that for most treatments containing pumice clasts that the greatest amount of water lost was between 10 kPa and 20 kPa, the absolute amounts of water lost, or indeed water contents are unreliable.

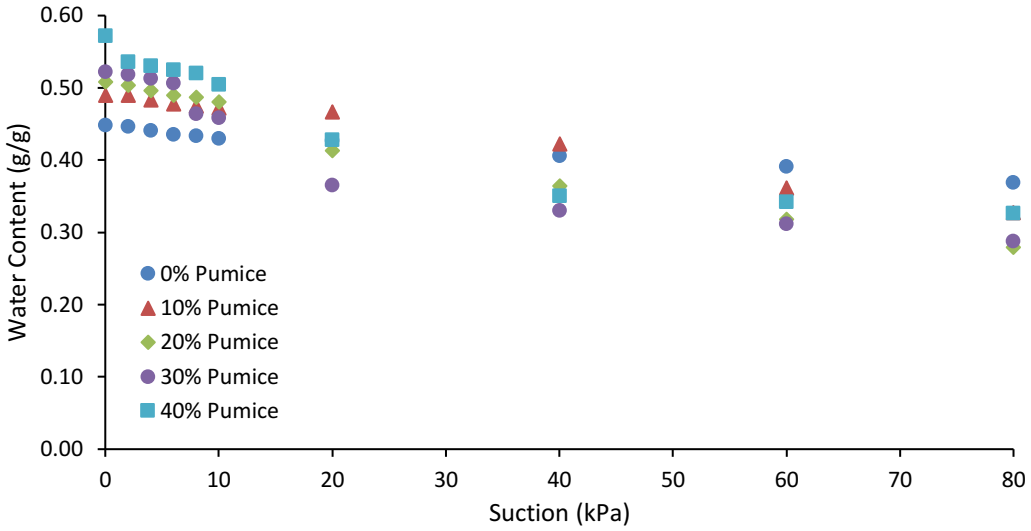

Figure 4.3: Total gravimetric water content of soil cores.

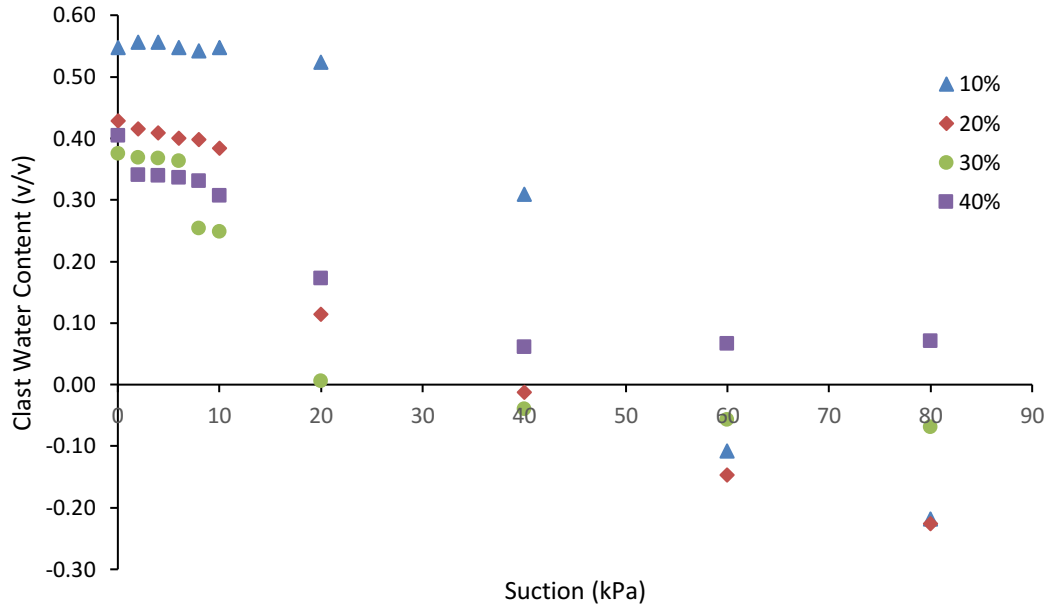

Figure 4.4: Volumetric water content of pumice clasts at different suctions determined using Analysis 1.

4.1.2 Analysis 2

The second method of analysis removed the reliance on the water content of the soil matrix in the 0% pumice clasts treatment by using a linear regression analysis for each treatment containing pumice clasts.

A positive linear relationship between the water content of the core and the volumetric proportion of pumice clasts was observed for clast abundances between 10 and 40% (Figure 4.5). However, a linear fit is poor for many matric potentials when the 40% abundance is included. Water contents at this abundance often lie below the linear trend formed by water contents from 10 – 30% abundance. This roll-off indicates this high clast abundance is influencing matrix water storage characteristics.

When the full range of treatments containing pumice clasts were included in the analysis, a poor linear fit was observed, as the water content of the 40% pumice clasts treatment was not as great as expected based on the trend of the 10% - 30% data (Figure 4.5). This indicates that the water retention characteristics are altered when the clast content is greater than 30%.

Linear behaviour existed between treatments with 10% and 30% pumice clasts (Figure 4.6), meaning that the assumption that the water content of the soil is constant at any given matric potential across the different clasts concentrations is true when the 0% pumice clasts treatment is not included. The water content of the pumice-free core was generally higher than the intercept of the regression line for the 10% to 30% pumice data. This confirms that the pumice-free cores overestimated the water content of the cores containing pumice, as was indicated by the negative water contents in Analysis 1.

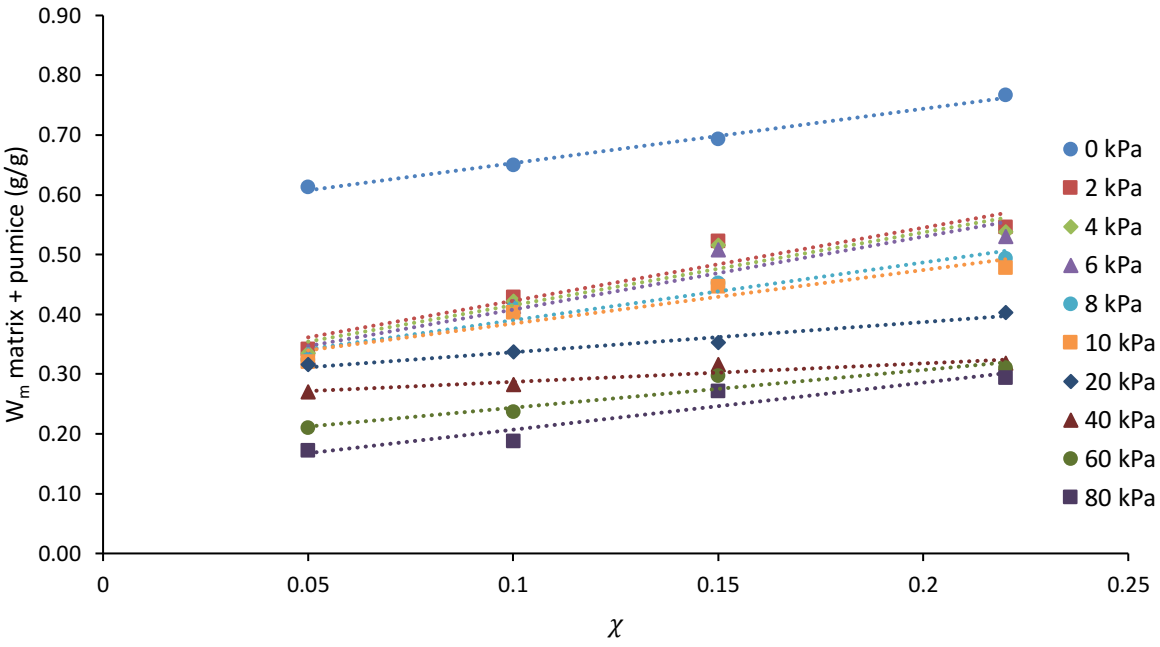

Figure 4.5: Linear regression for cores containing 10-40% clast contents.

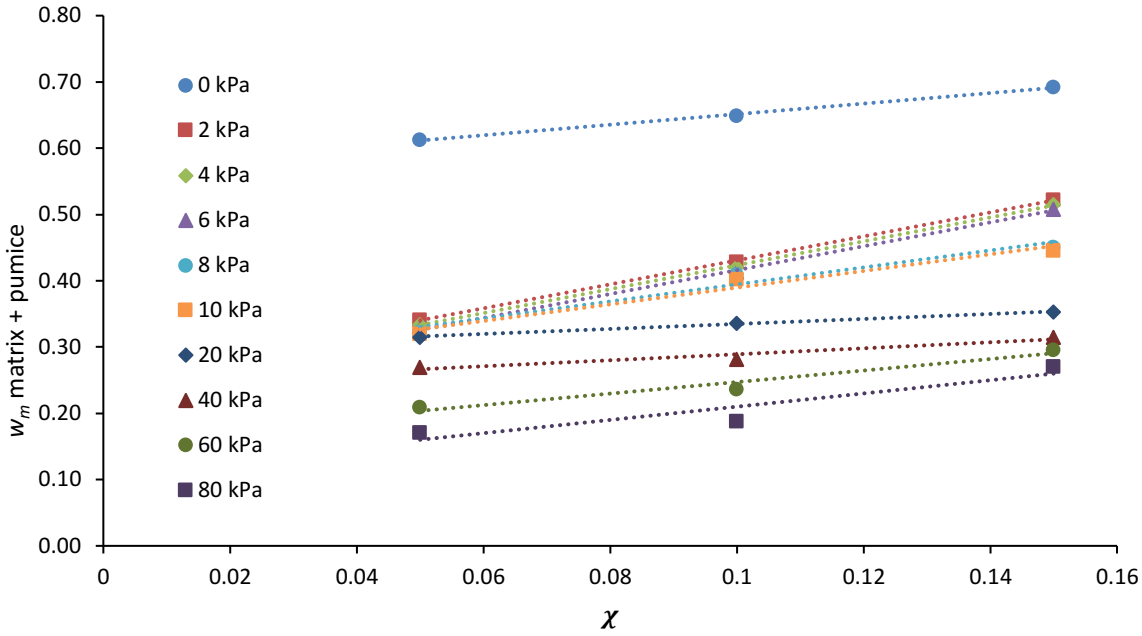

Figure 4.6: Plot of gravimetric water contents for the different matric potentials applied against the gravimetric content of pumice clast for 10% – 30% pumice clast treatments.

The results for the water release curve of pumice clasts derived from this analysis remained positive throughout the range of matric potentials applied and appear believable (Figure 4.7). However, the assumption that the soil matrix behaves the same as the ratio of pumice clasts to soil matrix changes is again brought into question by this analysis method. When the suction is greater than 40 kPa, the water content of the pumice appears to increase as the matrix water content decreases. While the extent of the error associated with the pumice fragments implies that it is possible for the water

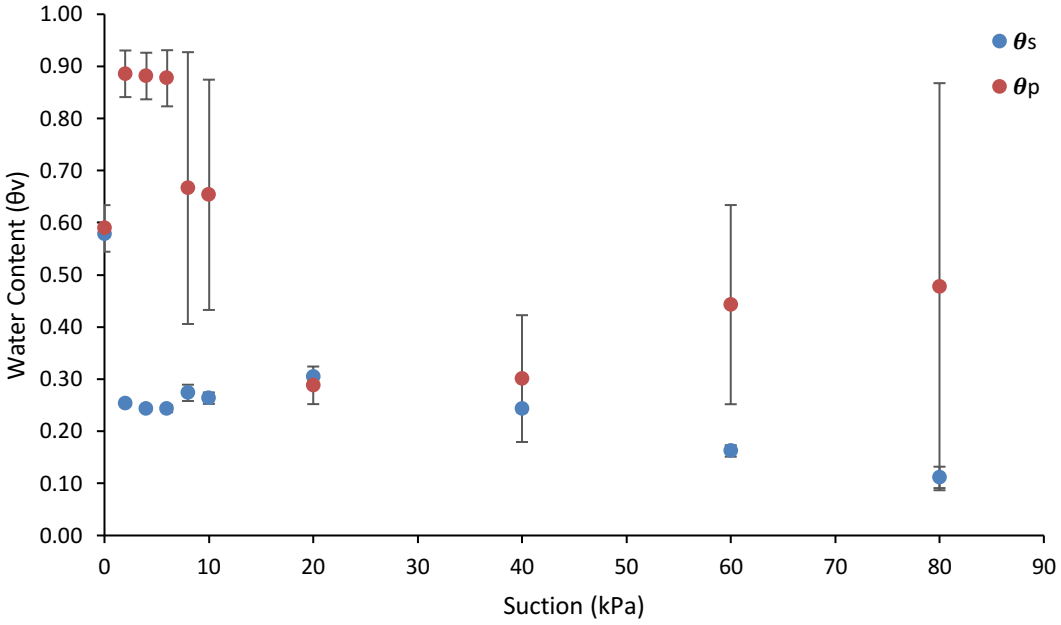

Figure 4.7: Volumetric water release curve for pumice clasts and soil fines, with error included for each matric potential for 10-30% pumice clast treatments.

content to become steady beyond 40 kPa, an increase in clast water content as the suction applied increases is unlikely.

4.2 Experiment 2

The initial submersion method used to determine the bulk density of the pumice clasts underestimated the bulk density of the clasts, and resulted in larger amounts of variability between the bulk density of the clasts that was unlikely to be present. The clast bulk density of 0.514 g cm^{-3} produced using this method was used when packing the soil cores, resulting in the amount of pumice included in the cores not reaching the target volume. The bulk density of 200 clasts used in the cores was re-evaluated at the completion of the suction plate experiment using the glass bead method. This produced an average bulk density value of 0.70 g cm^{-3} for the pumice clasts.

Due to the COVID-19 level 4 lockdown, the experimental set up was relocated from the temperature-controlled laboratory at Landcare Research to an alternative, accessible venue to enable the experiment to continue and be tended to. This relocation took place on the fourth day that the cores were at a matric potential of -3 kPa and remained in the alternative location until its completion, in order to prevent potential damage during movement. No damage appeared to have occurred to the cores or to the contact between the core and plate during the initial transport and re-start of the vacuum system. The amount of condensation removed from the container housing core 4 (9% pumice, 18% glass, 73% matrix) was the greatest of all cores at any stage throughout the experiment, with 8.03 g of water removed when equilibrium was reached at 3 kPa. This is significantly higher than any other core, with the amount of water removed once equilibrium was reached for each matric potential generally ranging from 1 g – 4 g per container.

The location the experiment was run in had little temperature control, experiencing a temperature range over the course of the experiment of 13.43°C, with the lowest temperature of 8.45°C recorded on 27/05/2020 and the highest temperature of 21.88°C on the 07/04/2020 (Figure B.1). This temperature flux is greater than what would have been experienced in the temperature-controlled lab, held at 22°C.

4.2.1 Analysis 3

Analysis 3 could not be conducted because the initial error in bulk density of pumice clasts created a non-constant total clast content, which the analysis relies on.

4.2.2 Analysis 4

To correct for the non-constancy of the total clast content of the cores, seven to eight iterations were required for the water contents to converge to the required precision of p=0.0001.

Table 4.1 presents the R^2 values of the trendlines fitted to the raw data and scaled data. For both the raw data and the scaled data, the R^2 value decreases as the level of suction increases. The R^2 value of the scaled data is always greater than the R^2 of the raw data, indicating that the scaled data is better fitted to the linear model. When the water content of the soil and water content of the pumice clasts were calculated out from the scaled linear data, the standard error of the water content of the soil was less than the standard error calculated for the water content of the pumice clasts (Figure 4.8). The standard error calculated for the water content of the pumice clasts ranged from 0.04 at saturation, 6 kPa and 20 kPa to 0.09 at 80 kPa, while the standard error of the soil fines ranged from 0.01 to 0.02.

Figure 4.8 also shows the way the water content of the pumice clasts changed with increasing suction. Irregular change in the water content of the clasts occurred between 0 kPa and 10 kPa. This change is not significant due to the overlap of the error bars. From 10 kPa to 80 kPa the change in the water content of the pumice clasts decreased monotonically.

Table 4.1: R^2 values of the linear trend lines fitted to the raw data and scaled data for each level of suction applied to the cores.

Suction (kPa)	R^2 raw data	R^2 scaled data
0	0.9638	0.9647
3	0.9237	0.9341
6	0.9501	0.9581
8	0.9262	0.9415
10	0.9308	0.9481
20	0.9362	0.9529
40	0.8037	0.8596
60	0.6431	0.7333
80	0.5778	0.6778

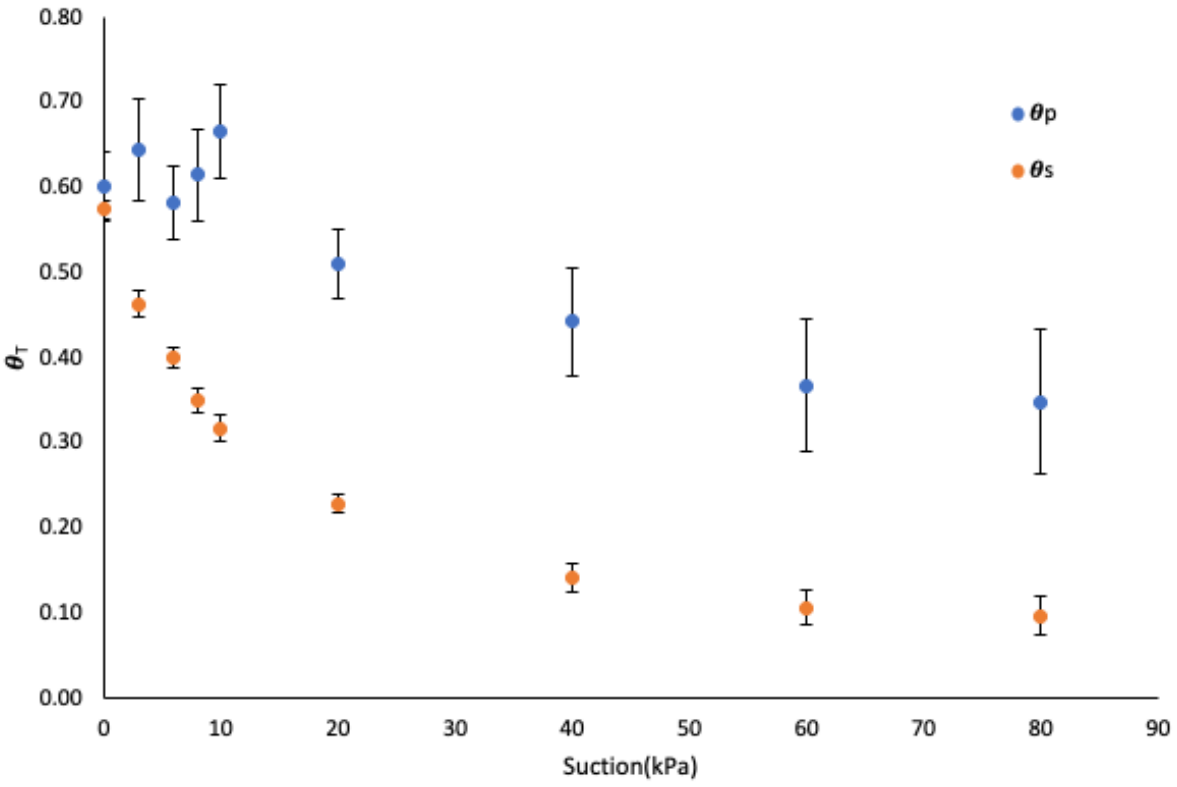

Figure 4.8: Comparison of the volumetric water contents of the pumice clasts and soil fines.

Water release curve

The water content of the pumice clasts for matric potentials from -3 kPa – -80 kPa were then plotted along with the water contents obtained for clasts at lower metric potentials using the WP4C Dewpoint PotentiaMeter (Figure 4.9). The scaled data indicated a lower water content for the pumice clasts than the water contents for the matric potentials determined using the Dewpoint Potentiometer. The water content of the pumice clasts at 100 kPa is greater, determined using the Dewpoint PotentiaMeter is greater than the water contents determined at 40, 60 and 80 kPa, determined using the suctions plates and Analysis 4.

From the θ produced for FC, stress point and PWP using the suction plates and the Dewpoint PotentiaMeter, AWC and PAW were calculated. The AWC determined using this analysis was 62% for pumice clasts and 30% for the soil fines, while PAW for the pumice clasts was 22%.

Four different empirical soil water retention models were fitted to the scaled data to describe the shape of the soil water retention curve (Figure 4.10). The four models included the popular equations proposed by Brooks and Corey (1964) and van Genuchten (1980) along with two other unimodal models proposed by Kosugi (1996) and Fredlund and Xing (1994). Of the four models, the one that

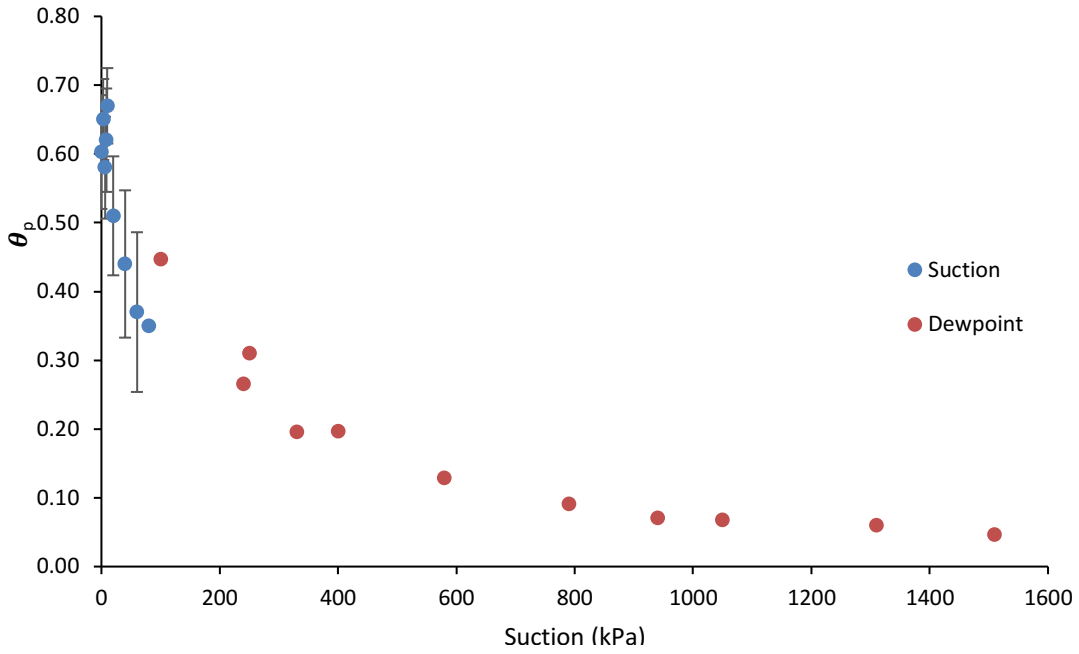

Figure 4.9: Volumetric water content of pumice clasts determined using individually scaled regression analysis data from the suction plate experiment and Dewpoint Potentiometer data.

provided the best fit was the Kosugi equation, with an R^2 value of 0.95 (Figure 4.11). The failing of the models with poor fit occurred at high suctions, with the Brooks and Corey, and van Genuchten models showing poor fit from approximately 600 kPa, while the Fredlund and Xing model differs from the Kosugi model at approximately 1,200 kPa. When the data point for the pumice water content at 100 kPa is removed from the analysis, the Kosugi model provides the best fit, with an improved R^2 value of 0.97 (Figure 4.12).

The θ determined for the pumice clasts were compared with the θ of the soil fines (Figure 4.12). The water content of the pumice clasts is greater than what was determined for the soil fines used in the experiment at all matric potentials.

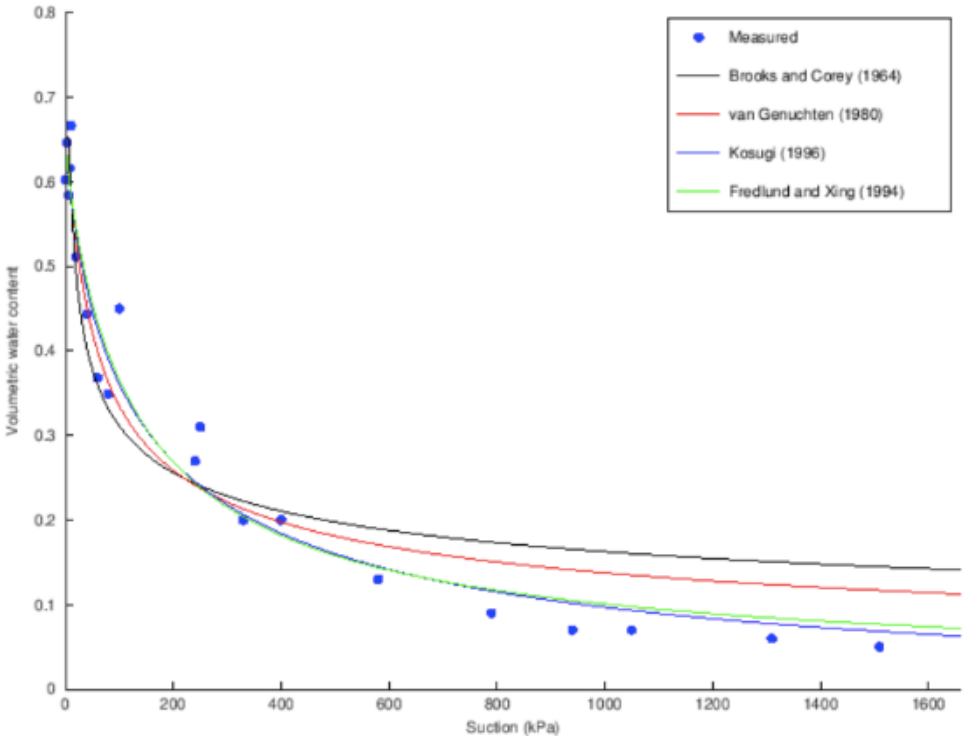

Figure 4.10: Soil water release curve for scaled pumice clasts, with four unimodal equations developed using SWRC Fit (Seki, 2007).

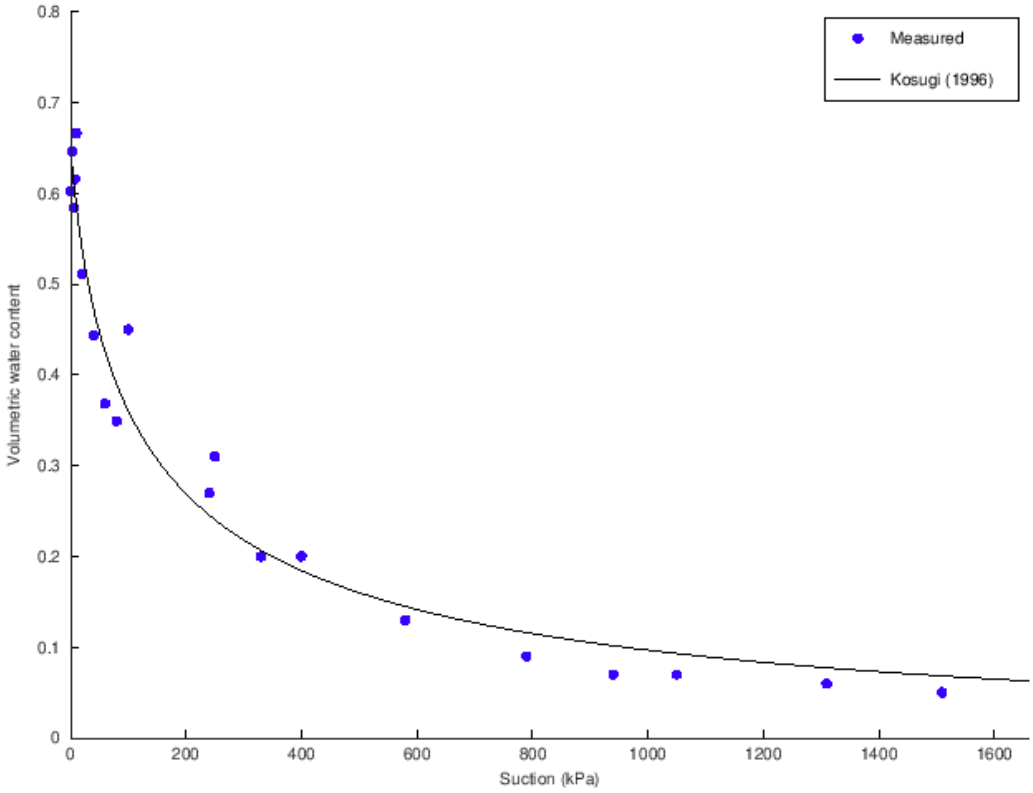

Figure 4.11: Soil water release curve for scaled pumice clasts, fitted with the Kosugi equation using SWRC Fit (Seki, 2007).

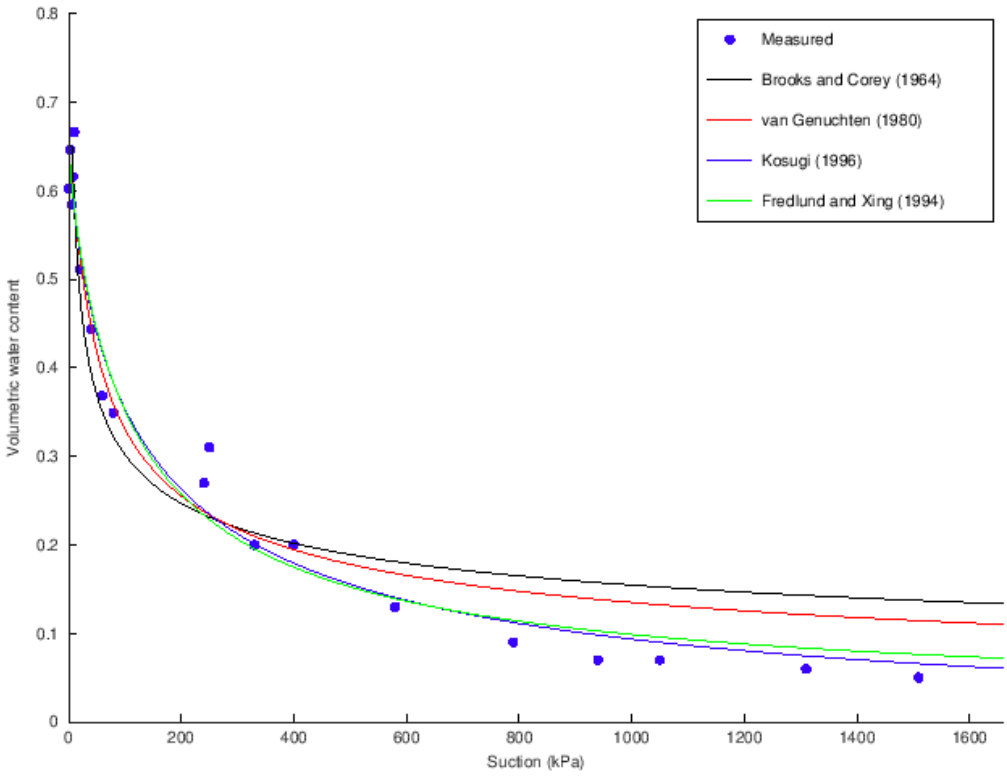

Figure 4.12: Soil water release curve for scaled pumice clasts, with the data point of the volumetric water content at 100 kPa removed, fitted with four unimodal equations using SWRC Fit (Seki, 2007).

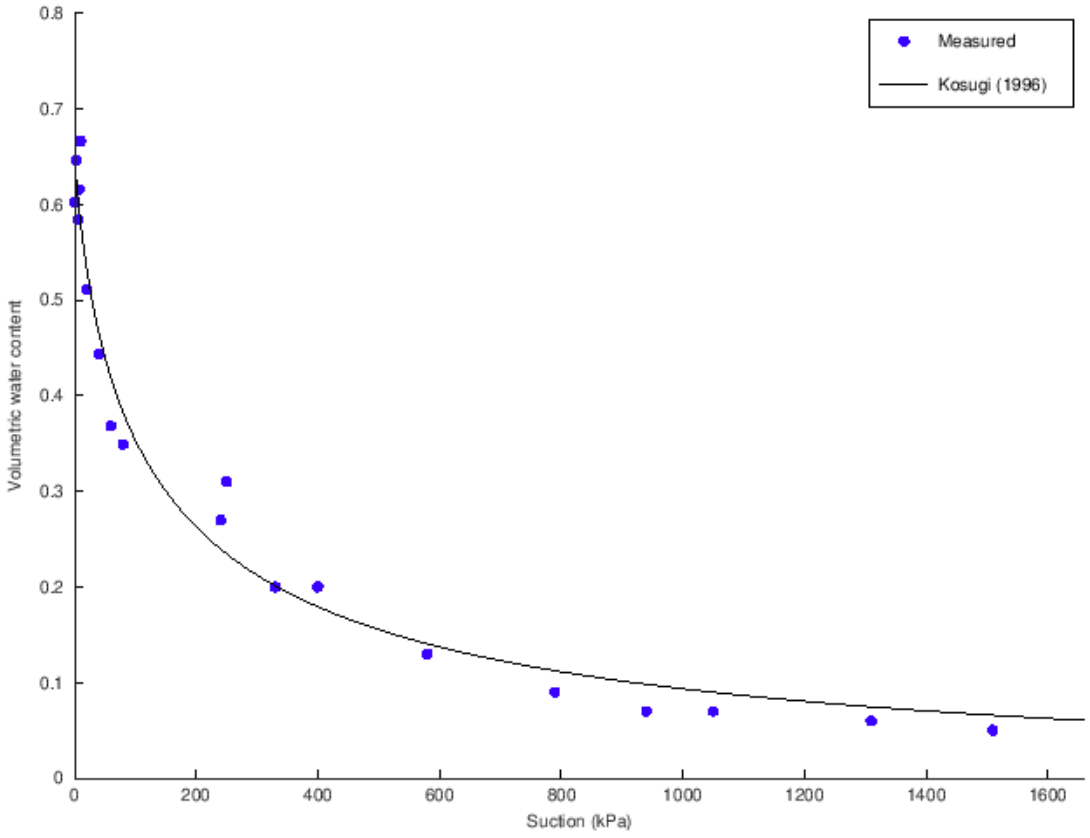

Figure 4.13: Soil water release curve for scaled pumice clasts, with the data point of the volumetric water content at 100 kPa removed, fitted with the Kosugi model using SWRC Fit (Seki, 2007).

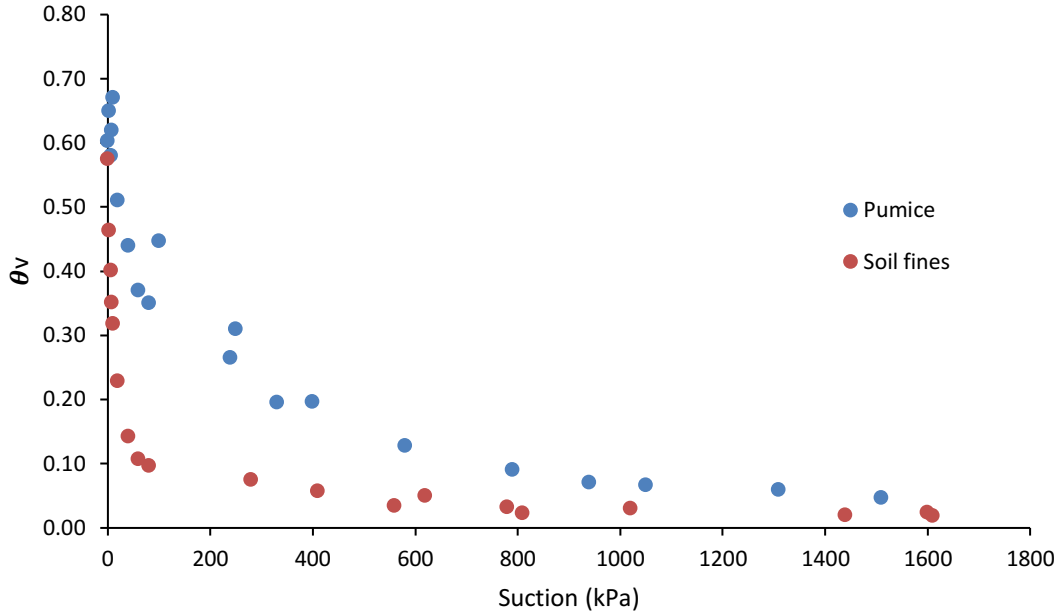

Figure 4.14: Comparison of the volumetric water content of the pumice clasts and soil fines for data collected using suction plates and Dewpoint PotentiaMeter.

Chapter 5

Discussion

5.1 Method evaluation

This research project has used novel methods to develop a water release curve for unaltered pumice clasts, ranging from 2 – 20 mm within a soil matrix. Experiments that have been carried out in various international studies to determine the water content of pumice clasts have often used isolated, graded pumice clasts, with no matrix material, or have only used ground pumice material (Blonquist et al., 2006; Dal Ferro et al., 2014; Gizas & Savvas, 2007; Özhan et al., 2008; Raviv et al., 1999; Volterrani & Magni, 2012). A small number of studies on pumice clasts have included a soil matrix, including two studies on New Zealand Pumice Soils (Flores-Ramírez et al., 2018; Packard, 1957; Will & Stone, 1967). The studies that have included a soil matrix focused on determining the water content of the constituents of the core as a whole, while the aim of this research has been to determine the water holding capacity of the pumice clasts. This has required the implementation of novel methods and analysis to derive the water content of the clasts from the water content of a whole core. Two broad approaches were used. The first aimed to characterise the behaviour of the matrix, and, assuming the matrix behaviour remained consistent, deconvolve the behaviour of pumice clasts in matrix–pumice mixes. The assumption of matrix water-release behaviour being the same between pure matrix and matrix–plus–pumice mixes proved to be invalid. Consequently, an approach based on the assumption that water release of matrix and pumice remained similar in matrix–pumice mixes was adopted and applied to the same dataset. Problems arose in this method as well, and, motivated by the suspicion that changing clast content was affecting matrix behaviour, a second approach was tested on a new set of cores. Pumice clast content was allowed to vary, but the total content of clasts was kept constant by adding in a varying volume of glass fragments, which were assumed to play no significant part in water retention. The varying core water content was modelled in terms of pumice and matrix volume and water content, and the model relationship fitted to the empirical data, from which pumice water content was extracted. The limitations and strengths of each method are discussed in more detail below.

5.1.1 Experiment 1

The underlying assumption used in Experiment 1, that the water content of the soil fines at any suction does not vary with pumice clast content, was found to be violated as shown by the negative water content of the pumice clasts. The negative clast water content calculated in Analysis 1 is the result of the difference between the water content of the treatments with and without clasts,

whereby the matrix in the 0% treatment overestimated the water content of the matrix in the treatments containing clasts.

In Analysis 2, the disagreement between the water content of the soil fines in the cores containing pumice clasts and the pumice free core is potentially due to the increasing clast content reducing the water content of the soil fines. The change in the clast content appears to have had an effect when the clast content increased from 30% – 40%, as observed in the roll off shown in Figure 4.5. The poor linear fit shown in Figure 4.5, when the 40% clast core was included in the analysis, indicated that when the clast content was greater than 30%, either the matrix or the pumice clasts hold different amounts of water, and hence the water content of the core is not solely a function of matrix to pumice ratio. This may be due to less continuity of water films between the clasts and the soils with increased potential for clasts to be touching.

A study by Fiès, Louvigny, and Chanzy (2002) found that when glass fragments were used as a proxy for coarse fragments in repacked soil cores, the water holding capacity of the soil fines decreased as the clast content increased. This was attributed to a decreased bulk density as clast content increased with modification of the pore space in the soil, notably an increase in coarse lacunar pores (Fiès et al., 2002). Decreasing water content of soil fines as clast content increases was also found in a study by Chow, Rees, Monteith, Toner, and Lavoie (2007). The moisture content of the core containing no coarse fragments was greater than that of the treatments containing clasts. The clast contents used in the study by Chow et al. (2007) were 10, 20 and 30% and the water content of the soil for each of the treatments was 2.1, 8.4 and 13.2% lower, respectively, than the water content of the 0% clast treatment of 27.9% at field capacity (-33.3 kPa). The change in water content of the fines in this research was found to be due to an increase in the proportion of the macropores in the cores as the clast content increased (Chow et al., 2007).

The effects discussed above relate to inherent clast–matrix interactions that affect matrix water holding capacity. It is possible that in Experiment 1 there was also an effect due to incorrect packing that stemmed from an error in pumice density. The cores were packed to a target soil fines bulk density of 0.95 g cm^{-3}. This was done by using the bulk density of the pumice clasts to calculate the mass of pumice needed to achieve the desired pumice volume. The mass of the soil fines required to fill the rest of the core was calculated by multiplying the remaining volume, determined by subtracting the volume of pumice from the total volume of the core, by the target bulk density of the soil fines. However, from the results of Experiment 2, it seems likely that the bulk density assumed for the pumice was an underestimate. The effect of the underestimated pumice bulk density was that the pumice volume was overestimated and hence the mass of fines used to fill the remainder of the core was too little. This would have resulted in under-achievement of the target bulk density of

the soil fines, which would have got worse as the pumice volume increased. The magnitude of this error, expressed as a ratio, *R*, of true bulk density to target bulk density is given by

$$R = \frac{1-\chi_p}{1-\chi_p\frac{\rho_p}{\rho_p'}} \quad (5.1)$$

where ρ_p and ρ_p' are the assumed and true fines bulk densities, respectively. The potential error was estimated by using the bulk density of the pumice determined at the completion of Experiment 2 (0.7 g cm^{-3}) as the true density, and the density used in the original calculations (0.4 g cm^{-3}) (Figure 5.1). This relationship shows that as the proportion of the pumice clast included in the cores increased from 10% to 40%, the ratio of the bulk density achieved to the bulk density target may have decreased from about 0.95 to 0.77. Although the error is significant, it is likely to be a worst case because the pumice used in Experiment 1 was taken from deposits closer to the eruption vent, and from a different unit of the Taupo eruption to that of Experiment 2. Hence, it is likely to have a density less than 0.7 g cm^{-3}.

Consistent with the anticipated error described above, sinking and cracking of the soil matrix was observed in all four of the soil cores containing pumice, and the effect was worst for the 40% pumice core: The 40% core sunk by 68 cm^3, while the other cores containing pumice sunk between 28 – 33 cm^3. All cores containing pumice sunk to an average soil fines bulk density of 1.04 g cm^{-3}, with a range of 1.00 – 1.11 g cm^{-3}.

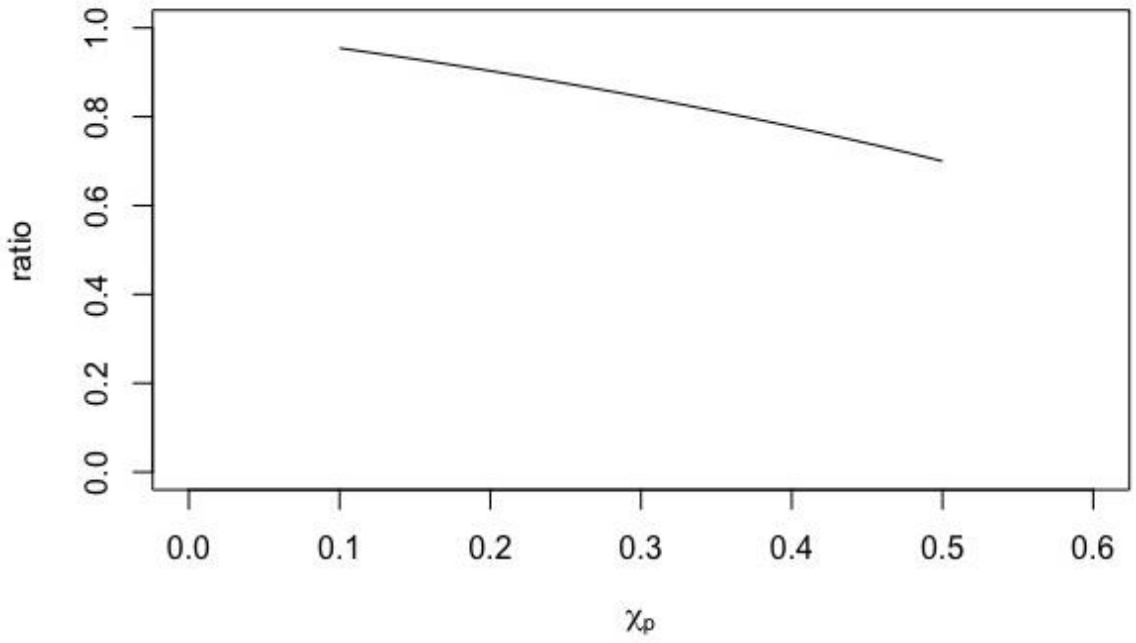

Figure 5.1: Estimated ratio of the true soil bulk density to target soil bulk density against the proportion of pumice clasts for Experiment 1.

A similar approach to Experiment 1 (Analysis 1) to determine the water storage of porous materials, including pumice, was adopted by Flores-Ramírez et al. (2018). Also relying on an assumption of matrix water content constancy with different clast abundance, they subtracted the water content of the fines derived from fines-only cores from the total water content of the composite cores to determine the water content of the porous material. Parajuli et al. (2017) conducted a similar experiment to Experiment 1 where a consistent fines bulk density was achieved. Pumice clast contents of 0, 5, 10, 20, 30 and 40% were packed with a sandy soil matrix of bulk density 1.70 g cm^{-3}. Using an equation similar to what was used in Analysis 1, the water contents of the pumice clasts and soil fines were able to be determined, based off the water content of the fines only treatment (Parajuli et al., 2017). In both of these studies, the authors make no reference to problems associated with a dependence between the water content of the soil fines and the abundance of pumice clasts. This may indicate that the behaviour change of the soil fines that occurred during Experiment 1 was related to the variation in the bulk density of the soil fines.

5.1.2 Experiment 2

Limitations of Experiment 1 were aimed to be addressed in Experiment 2. These included potential errors in the re-saturated pumice clasts that were packed, the physical layout of the experiment and potential problems associated with inconsistent soil matrix water release characteristics.

In Experiment 1, air dried pumice was re-saturated once the cores had been packed, with the dried pumice used to enable accuracy when packing. This potentially prevented the clasts from being completely saturated, as some of the pores in the clasts may have been unable to refill following drying. To avoid potential inaccuracies in the water release as a result of the clasts not having fully re-saturated, the clasts packed into the cores for Experiment 2 were not air dried, and were saturated in a water bath for a number of weeks prior to packing them into the cores. The packed cores were then left to stand in a water bath for 2 weeks until the soil was saturated.

The lay out of the experiment was also altered after Experiment 1. In that experiment, a second set of five soil cores were packed and placed on a set of suction plates; however, the water contents of these cores were unable to be included in the analysis. The data were omitted because water in the 6 mm tubing that had drained from the four cores distal to the collection flask flowed into the core closest to the collection flask. This occurred because the water had to overcome a hydraulic gradient to enter the flask whose inlet was higher than the water outlet from the suction plates. To prevent this from occurring in Experiment 2, the water collection flask was placed on the ground, allowing water to drain down into the flask, removing the risk of water from any of the cores entering another core. Another problem related to the physical layout of experiment 1 was inconsistency in suction experienced by different plates, despite them being all connected to the same vacuum pump. The

problem arose as a result of water plugs forming in the tubing. To solve the problem a manifold system was developed for Experiment 2, which used a gently inclined PVC pipe that was attached to each of the cores through a small length of 6 mm tubing. This ensured short, straight runs of pipe connecting plates to the manifold, in which water plugs could not form.

Similar to Experiment 1, matrix consistency was not achieved in Experiment 2 because of the error in the estimated bulk density of the pumice. The magnitude of the error, given by Equation 5.2, and plotted in Figure 5.2 is less than in Experiment 1 because of a narrower range and lower maximum pumice content than in Experiment 1, and because of a smaller difference between assumed and true pumice bulk density (0.5 to 0.7 gcm^{-3}, respectively).

$$R = \frac{1-\chi_c}{1-\chi_c+\chi_p(1-\frac{\rho_p}{\rho_p'})} \tag{5.2}$$

where χ_c is the intended total volumetric proportion of clasts (glass plus pumice = 0.3), and all other symbols are as of Equation 5.1. The ratio of actual matrix bulk density to intended ranges from 0.89 to 0.99 from the maximum (30%) to the minimum (3%) intended pumice volumetric proportion, respectively (Fig. 5.2).

In Experiment 2, no obvious sinking or cracking of the soil fines within the cores were observed, most likely because there was a smaller error in fines bulk density, and the volume of soil was generally less (70% of the cores), and hence there was a smaller absolute volume error.

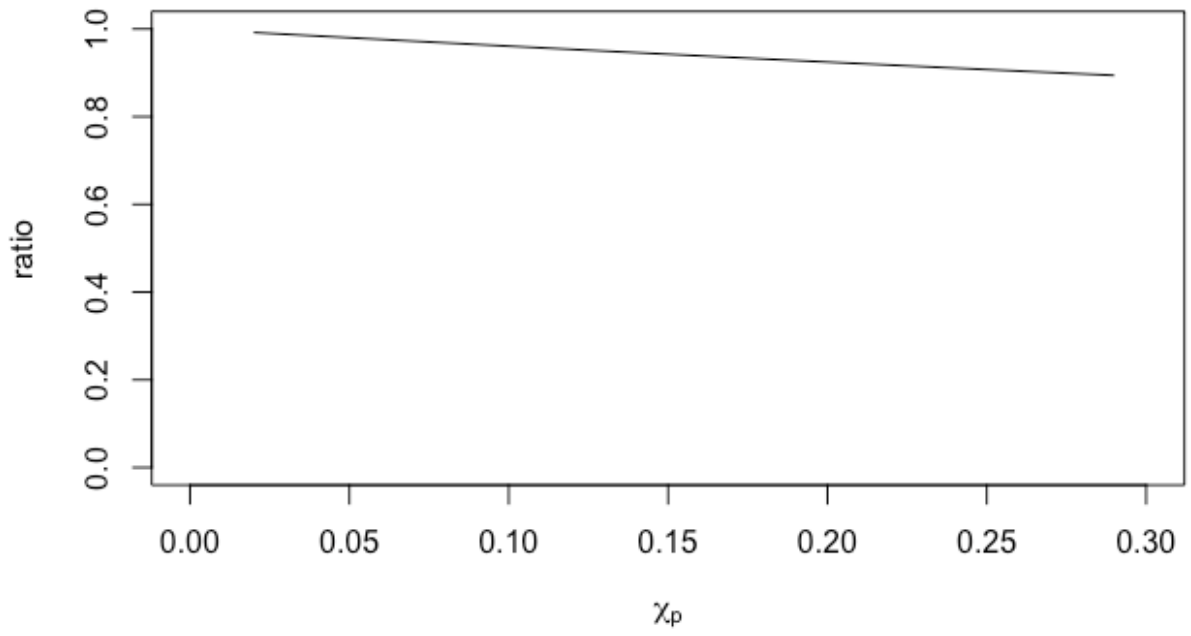

Figure 5.2: Estimated ratio of the true soil bulk density to the target soil bulk density against the proportion of pumice clasts for Experiment 2.

When estimating pumice water content, the error in pumice bulk density and the resulting inconstancy of the total clast content in the cores required an iterative numerical solution to applied. Stable solutions of high precision arose within 10 iterations, but the accuracy of the method remained uncertain. As a test, a numerical simulation of the experiment was conducted. This involved simulating water content of cores from assumed soil and pumice water contents, and soil and pumice volumetric proportions identical to the cores in the physical experiment. A random, normally distributed error of mean zero was added to each simulated core water content to generate regression R^2 values comparable to the experimental data. Next, the simulated data were processed according to the numerical iterative method, and derived water contents compared against the initial, assumed values. Multiple simulations showed distributions of estimated water contents of pumice and water were consistent with the assumed values within uncertainties. The simulations revealed that the uncertainties in the water contents we generated experimentally were a result of random experimental error and not systematic error related to inconsistent core packing.

When producing data for the pumice water-release curve beyond the suction the plates were capable of, a discrepancy occurred in the water content of the pumice clasts. The pumice water content measurement made with the use of the Dewpoint PotentiaMeter was 10% (v/v) higher than that inferred from the suction plate apparatus. It is possible that the water content of the pumice clasts, that were dried in a constant temperature chamber, had not reached equilibrium at -100 kPa. When this data point was removed, continuity of the data improved as did the fit of the Kosugi model to the water release curve. It appears that the combination of suction plates and the Dewpoint PotentiaMeter are suitable methods for developing the wet and dry ends of the soil water release curve.

5.1.3 Soil water release curve

A contrast in the water release behaviour was revealed in the suction plate experiment of Experiment 2. The soil matrix was observed to drain systematically from saturation up to 100 kPa suction, while the pumice clasts water content at 10 kPa was not significantly different from saturation. Only above 10 kPa of suction did the pumice clasts begin to drain. This suggests a hydraulic break (pore discontinuity) between the pumice clasts and the soil matrix and it is possible that a different matrix may yield a different mode of water release at low suctions (Figure 4.8).

The results produced in Experiment 2, Analysis 4 presented a unimodal pore distribution, which is best represented by the Kosugi (1996) model, presented below

$$S_e = Q\left[\frac{\ln(\frac{h}{h_m})}{\sigma}\right] \quad (5.1)$$

where σ is the standard deviation of the distribution, *h* is the matric potential, subscript *m* is a shape parameter, S_e represents the effective saturation, defined as

$$S_e = (\theta - \theta_r)/(\theta_s - \theta_r) \quad (5.2)$$

in which θ is the water content at *h*, θ_r is the residual water content and θ_s is the saturated water content. Q is the complementary normal distribution function, defined as

$$Q_{(x)} = 1 - \phi_{(x)} \quad (5.3)$$

where $\phi_{(x)}$ is a normalised form of the cumulative normal distribution function.

This log normal distribution equation is an adaptation of the popular van Genuchten model, presented below

$$S_e = \frac{\theta - \theta_r}{\theta_s - \theta_r} = [\frac{1}{1+(\alpha h)^n}]^m \quad (5.4)$$

where α and *n* are shape parameters, in which *n* relates to *m* as *m* is equal to 1 – 1/*n*.

Most studies on the water holding characteristics of pumice clasts carried out throughout the world have found the van Genuchten (1980) model provides the best fit. Adaptations of the van Genuchten model to provide a bimodal analysis of pumice clasts, without a soil matrix, have also been used (Blonquist et al., 2006; Dal Ferro et al., 2014; Fields, Owen, Zhang, & Fonteno, 2016; Gizas & Savvas, 2007; Raviv et al., 1999). In the study by Fields et al. (2016) in which evaporative methods were used to develop water release characteristic curves for soil-less substrates, the curves were fitted to the data using the SWRC Fit programme (Seki, 2007) with no concerns noted. The Kosugi (1996) model was used by Flores-Ramírez et al. (2018) to model capillary water retention in coarse porous growing

media, which included pumice clasts. Unimodal pore size distribution was modelled using Equation 5.1, while an adapted version was developed to model bimodal pore size distribution

$$S_e = \sum_{i=1}^{2} w_i S_{e_i} \quad (5.5)$$

where S_{ei} are weighted subfunctions expressed by the unimodal functions and w_i is the weighing factor for the subfunctions ($0 < w_i < 1$) (Flores-Ramírez et al., 2018).

Bimodal pore distributions have been commonly used to describe the pore distributions for pumice clasts where both intra and inter aggregate porosity is present. Bimodal, or dual porosity, does not appear to occur when a soil matrix, comprising soil fines <2 mm is present. For the experiment carried out, dual porosity is not present and as such, a bimodal model has not been fitted to the data.

5.2 Comparison to other studies of water release from Taupō pumice

The method developed in this research to determine the soil water release curve for pumice clasts in New Zealand Pumice Soils has produced a result that may be compared to the study by Will and Stone (1967) of the moisture storage capacity of different horizons of a Pumice Soil. The study by Will and Stone (1967) provides the most appropriate comparison as the materials studied were produced from the same volcanic eruption, although pumice from different phases of the eruption were used in the two studies. Will and Stone (1967) included a horizon of lapilli devoid of any fines from the Taupō plinian pumice phase of the 232 ± 10 AD Taupō eruption. This horizon of pure pumice should be comparable to the assessment of the water holding characteristics of pumice determined for the Hatepe plinian pumice.

Will and Stone (1967) aimed to determine the water holding capacity of Pumice Soils to support tree growth. This involved a combination of field, laboratory and greenhouse experiments. In the field experiment the pedon studied on the Kaingaroa plateau had 3028 L of water applied to an area measuring approximately 3 m by 6 m that had been cleared of 4 year old pine saplings. Following this extreme wetting event, the surface of the soil was covered and the profile was left to drain. Cores were taken from each soil horizon periodically between 2 and 69 days following the application of water. Samples were taken from a new pit that was excavated within the study area for each sampling day. The moisture content of each horizon was determined gravimetrically following sampling. For the greenhouse pot trials, composite samples from each horizon were mixed and

placed in pots with three dwarf sunflower seeds. The plants were watered and allowed to grow until they were 30 cm high when watering ceased and the plants were left to wilt. When the plants did not regain turgor overnight, PWP was assumed to have been reached and the water content of the soil was determined. In the laboratory experiment, samples were placed in a pressure plate apparatus at -1,500 kPa for 10 days to reach equilibrium before the water content of the samples was determined.

The FC values, at -10 kPa, determined in Experiment 2, Analysis 4, was 67% v/v (± 6%), higher than the field experiment value of 52% v/v, determined by Will and Stone (1967). The PWP values obtained in the two studies are more aligned than the FC values, with 5% determined for the Hatepe pumice, and 4.2% and 1.75% determined by Will and Stone (1967) using pressure plates and the pot trial, respectively. These FC and PWP values provide an AWC of 62% for Experiment 2, Analysis 4, 50% for the pot trial and 47.8% for the pressure plates. The differences in the AWC of the Hatepe pumice used in this thesis and the work done by Will and Stone (1967) may be attributed to the use of pumice from different deposits and the methods used to determine the water contents.

Differences in the bulk density of the Hatepe and Taupō pumice clasts used were found, which has the potential to impact the WHC of the clasts. Will and Stone (1967) recorded the bulk density of the clasts in the lapilli layer as 0.57 g cm^{-3}, while the Hatepe pumice has a bulk density of 0.7 g cm^{-3}. The Taupō lapilli in turn had a greater porosity than the Hatepe pumice. Differences in the bulk density and porosity of the clasts produced from the same eruption, and deposits of the same eruption phase in different locations and distances from the source, are not uncommon. Each phase of the eruptions that have produced material in which Pumice Soils formed have differences in the explosivity, magma composition and external interactions, which translate into differences in the material that is deposited (Nairn et al., 2004; Walker, 1981; Wilson & Walker, 1985). An increase in the bulk density of the clasts in deposits from the same eruption stage is often observed as the distance from the vent increases. With increasing distance from the source, clasts become smaller while bulk density increases. Walker (1981) documented an increase in the bulk density of the Hatepe clasts found near the vent having a bulk density from 0.5 g cm^{-3}, to 0.68 g cm^{-3} in distal exposures to the east of the vent. This aligns with the recorded bulk density value of 0.7 g cm^{-3} obtained for the Hatepe pumice 40 km to the north – northwest of the vent. The material produced in the Taupō pumice phase of the 232 ± 10 AD eruption is coarser than the material produced in the Hatepe pumice phase of the same eruption, with the coarser Taupō material having a lower bulk density than the finer Hatepe pumice (Wilson & Walker, 1985). This relationship between clast size and bulk density was also found in a study by Gizas and Savvas (2007), who found that smaller clasts had higher bulk densities and available water contents than larger clasts with lower bulk densities. While low bulk densities translate to higher porosity, in both the comparison of the Taupō and Hatepe eruption phases and the study by Gizas and Savvas (2007), the clasts with the higher bulk

densities and lower porosities had the greatest water holding capacity. This suggests the decrease in bulk density of coarser clasts involves an increase in large pores, which drain rapidly.

Will and Stone (1967) determined that FC was reached after 69 days of drainage following a significant wetting event. Field capacity was determined at 69 days of drainage as an increase in the water content of the clasts was recorded between days 9 and 27 following the saturation event, indicating that the profile took a significant period of time to saturate. No measure of the matric potential of the soil or pumice at this stage was recorded and it is possible that Will and Stone (1967) recorded the water content of the soil at a matric potential lower than -10 kPa.

Water was applied to the surface of the profile studied by Will and Stone (1967) and the layers were assumed to have saturated under these conditions. The Taupō lapilli gravel layer is was extremely coarse, and it is possible that the clasts did not fully saturate due to rapid water movement through the horizon. In my experiment on the Hatepe pumice, cores were packed with pumice clasts that had been saturating in water for 3 – 4 weeks before being packed into the cores. Once packed, the cores were placed in a water bath to saturate the soil matrix for 2 weeks. This provided confidence that the pumice clasts were completely saturated.

The Hatepe pumice failed to drain between 0 – -10 kPa, likely as a result of a hydraulic break. This does not appear to have occurred for the Taupō pumice and is another potential reason why the water content at FC for the Taupō pumice is lower than the FC water content for the Hatepe pumice.

The values obtained using pressure plates (Will & Stone, 1967) and the Dewpoint potentiometer for PWP at - 1,500 kPa were very similar to each other at 4.2% and 5% respectively. The water contents of the pumice clasts are higher than what was achieved using the sunflower pot trial, indicating that water retained by the pumice at this matric potential may still be plant available. Species-specific PWP values are likely to vary; however, the use of sunflower is a good proxy for the forestry species found in the pumice regions. *Pinus radiata* dominates the forestry species in the Central North Island (Selby, 1974; Will, 1974; Will & Stone, 1967) and have a root distribution that is similar to that of dwarf sunflower (*Helianthus annuus* L.). The roots of *H. annuus* L. is at a smaller scale to that of *P. radiata* and the plant is faster growing, making it more suited to pot trials (Angadi & Entz, 2002; Schneiter, 1992; Te Uru Rākau - Forestry New Zealand, 2019; Watson & O'Loughlin, 1990).

The variation between the pot trial results and those of the Dewpoint PotentiaMeter and pressure plate experiments raises question of how the water is able to be extracted by plants. In the pot trials by Will and Stone (1967), composite samples of each horizon were used for growing the sunflowers, while the dew point method used isolated pumice clasts. It is not clear if composite samples were used by Will and Stone (1967) in their suction plate experiment, or if material from each horizon was

analysed separately. There is little detail available on the composition of the samples used in the pot trial; however, the Taupō lapilli layer is likely to have been combined with the underlying or overlying horizons, both of which are classified as sands (Will & Stone, 1967). The pot trial, combining soil fines material and pumice clasts resulted in a lower water content at the PWP than what was achieved using isolated pumice clasts in the Dewpoint potentiometer and potentially on the pressure plates. While the matric potential at the PWP determined from the pot trial may not be at – 1,500 kPa, which was used in the laboratory experiments, the lower water content indicates potential interactions between the soil – root – water interfaces that are not present in the laboratory experiments. There is limited literature available on the interaction of roots with pumice clasts in the soil. In soil containing rock fragments of low porosity, such as the greywacke sandstone found in soils across the Canterbury Plains, macropores at the rock – soil interface form preferential flow paths through which water moves and plant roots accumulate (Sim, Brown, Teixeira, & Moot, 2017; Zhang, Niu, Zhang, Xiao, & Zhu, 2017). In Pumice Soils, the occurrence of macropores at the clast – soil interface is low, and water moves dominantly through the coarse textured, apedal matrix (McLeod, Aislabie, Ryburn, & McGill, 2008). Despite these soils supporting a large amount of agricultural and forestry activities (Ballingal & Pambudi, 2017; Nixon et al., 2017), there is little account of root distribution, particularly pasture, in soils containing pumice clasts to enable the relationships between roots, soil, water and clasts to be determined.

5.3 S-map

Based on the FC and PWP values determined for the Hatepe pumice it appears that the current assumption used by S-map, where the water contents of the pumice clasts and soil matrix are similar, is reasonable. For the Pumice Soil sibling,Taup_48, the first functional horizon contains 60 – 70% pumice, and has FC and PWP values of 17.2% and 3.2%, respectively (Landcare Research, 2020). The material included in this functional horizon at Acacia Bay, Lake Taupō, is from the Taupō ignimbrite of the 232 ± 10 AD Taupō eruption. These values are lower than what was obtained for the Hatepe Pumice; however, in this experiment pumice from only one deposit was used to develop a water release curve. There are likely to be a number of factors that have resulted in the higher FC and PWP values produced for the Hatepe pumice, including the eruption stage the materials were produced from, weathering environment and depth within the profile that the material was taken from.

Chapter 6

Conclusions

- Assessing the water holding characteristics of pumice based on the differences in water release between soil-pumice mixes and a soil-only medium does not produce accurate results. This is likely because pumice clasts have an influence on matrix water holding characteristics, which grows stronger the higher the pumice abundance. This finding must be qualified because the experiments in this study were affected by inconstant soil matrix bulk density due to an error in pumice bulk density.

- An experimental method which deconvolved pumice water content from changing core water content across cores of different pumice abundance showed promise. The most effective application of this approach minimised matrix variability by adding a glass fragment component in order to keep total coarse fragment abundance constant.

- The method produced volumetric water contents with standard errors of about 5 – 10%. Pumice water contents showed a systematic decline with increasing suction (decreasing matric potential), except over the range 0 to 10 kPa when the matrix drained but the pumice remained saturated. This behaviour is probably due to hydraulic breaks caused by contrasting pore-size distributions of pumice and matrix. Hence this method may yield results close to saturation that are dependent on the nature of the soil matrix employed.

- Dewpoint PotentiaMeter was successful in deriving water release characteristics for pumice at matric potentials less than -80 kPa.

- Water release appeared to reflect unimodal pore size distribution, and was best fit with the Kosugi model.

- Characterisation of water release was limited to a single pumice type (Hatepe plinain from Taupō eruption). However, the results suggest the current practice adopted by S-Map of assuming pumice and matrix water holding characteristics are similar appears to be reasonable. In future, a more rigorous approach could be adopted if different kinds of pumice in different weathering and soil forming environments are tested.

6.1 Limitations

A limitation of this study was the initial use of water displacement to determine the bulk density of the pumice clasts used in Experiment 1 and 2. This resulted in the incorrect proportions of pumice clasts being packed into the soil cores, reducing the bulk density of the soil fines. Remediation of this required scaling of the data points once the bulk density had been recalculated with the volume of the pumice clasts determined using glass beads.

This study determined the AWC from pumice collected from one location and while I am confident that this value is correct, it is not likely to be representative of all pumice that make up pumice soils. As such further experiments should include pumice clasts from a wide range of locations across the North Island.

6.2 Further research

In the research conducted, theoretical AWC and PAW values for the pumice clasts were determined. A plant growth study in Pumice Soils containing varying proportions of pumice clasts for the dominant plant species grown in these soil types would enable the actual plant available water contents to be determined and compared with the theoretical values. This could include perennial ryegrass, the most common pasture species used in the Waikato and Bay of Plenty Regions and dwarf sunflowers as a proxy for *Pinus radiata*, the dominant forestry species used (Charlton & Stewart, 1999; Popay & Crush, 2010; Tozer, 2014; White & Hodgson, 1999; Will, 1974).

In Experiment 1 Analysis 2, a poor linear fit was observed in the regression analysis when the 40% clast content core was included in the analysis. As such, in Experiment 2 the maximum clast content targeted was 30%; however, some profiles contain horizons that have clast contents greater than 30% (Landcare Research, 2019b). An investigation into the mechanics that result in this plateau effect when higher clast concentrations are included in the analysis and its implications in the field may provide useful insight in water movement and retention in different horizons of pumice soils.

Pumice clasts from across the North Island should be collected and water release curves developed to determine a representative value, or values, for use in New Zealand's soil information systems and nutrient budget modelling. This should involve pumice clasts collected from across the regions where Pumice Soils are present, including the andesitic pumice from Mt Taranaki, and clasts from different depths to ensure pumice from different eruptions and eruption stages throughout the soil profile are included. Pumice clasts are also the parent material of some Podzol and Allophanic Soils in the Central North Island. Clasts from these soils should be collected and analysed also. The method developed to determine the soil water release curve for pumice clasts in the course of this research has provided a result that is comparable to another study carried out on lapilli in a New Zealand

eruption. As a result of this, I would recommend its use in future studies for determining the water content of pumice clasts. Should future work on the water holding characteristics of pumice clasts in deposits across the North Island be undertaken I would recommend that a single matrix type be used for all clasts to eliminate inconsistencies between locations and soils, to ensure that the water content of the clasts remains the focus of the study.

References

Al-Kaisi, M. M., Lal, R., Olson, K. R., & Lowery, B. (2017). Chapter 1 - Fundamentals and Functions of Soil Environment. In M. M. Al-Kaisi & B. Lowery (Eds.), *Soil Health and Intensification of Agroecosytems* (pp. 1-23): Academic Press. Retrieved from http://www.sciencedirect.com/science/article/pii/B9780128053171000014. doi:https://doi.org/10.1016/B978-0-12-805317-1.00001-4

Allaby, M. (2013). *Dictionary of geology and earth sciences*. Oxford: Oxford University Press.

Andrews, E. D. (1974). Animal health problems. In N. E. Read (Ed.), *Yellow-brown pumice soils* (pp. 173-176). New Zealand: New Zealand Society of Soil Science.

Angadi, S. V., & Entz, M. H. (2002). Root system and water use patterns of different height sunflower cultivars [article]. *Agronomy Journal, 94*(1), 136-145. doi:10.2134/agronj2002.0136

Arriaga, F. J., Guzman, J., & Lowery, B. (2017). Chapter 5 - Conventional Agricultural Production Systems and Soil Functions. In M. M. Al-Kaisi & B. Lowery (Eds.), *Soil Health and Intensification of Agroecosytems* (pp. 109-125): Academic Press. Retrieved from http://www.sciencedirect.com/science/article/pii/B9780128053171000051. doi:https://doi.org/10.1016/B978-0-12-805317-1.00005-1

Ballingal, J., & Pambudi, D. (2017). *Dairy trade's economic contribution to New Zealand*. Wellington: NZIER. Retrieved from https://nzier.org.nz/static/media/filer_public/29/33/29336237-3350-40ce-9933-a5a59d25bd31/dairy_economic_contribution_update_final_21_february_2017.pdf

Banitalebi, G., Mosaddeghi, M. R., & Shariatmadari, H. (2019). Feasibility of agricultural residues and their biochars for plant growing media: Physical and hydraulic properties. *Waste Management, 87*, 577-589. doi:https://doi.org/10.1016/j.wasman.2019.02.034

Barnes, S., & Young, J. (2013). *Cap-and-trade of diffuse emissions of nitrogen in Lake Taupo Catchment. Reviewing the policy decisions and the market*. Retrieved from https://www.waikatoregion.govt.nz/assets/PageFiles/27778/TR201334.pdf

Barnes, S., & Young, J. (2013). *Cap-and-trade of diffuse emissions of nitrogen in Lake Taupo Catchment. Reviewing the policy decisions and the market*. Retrieved from https://www.waikatoregion.govt.nz/assets/PageFiles/27778/TR201334.pdf

Bay of Plenty Regional Council. (n.d). *Land*. Retrieved 31/07/2019, 2019,from https://www.boprc.govt.nz/landmanagement.

Bay of Plenty Regional Council. (n.d.). *General Good Management Practices - Nutrients*. Retrieved from https://www.boprc.govt.nz/media/796438/4975-land-management-good-management-practices-factsheet.pdf.

Beibei, Z., Ming'an, S., & Hongbo, S. (2009). Effects of rock fragments on water movement and solute transport in a Loess Plateau soil. *Comptes Rendus Geoscience, 341*(6), 462-472. doi:https://doi.org/10.1016/j.crte.2009.03.009

Bilardi, S., Calabrò, P. S., Caré, S., Moraci, N., & Noubactep, C. (2013). Improving the sustainability of granular iron/pumice systems for water treatment. *Journal of Environmental Management, 121*, 133-141. doi:https://doi.org/10.1016/j.jenvman.2013.02.042

Blok, C., De Kreij, C., Baas, R., & Weaver, G. (2008). Analytical methods used in soilless cultivation. In M. Raviv & J. Leith (Eds.), *Soilless culture theory and practice* (1st ed.. ed., pp. 245-286). Amsterdam: Elsevier.

Blonquist, J. M., Jones, S. B., Lebron, I., & Robinson, D. A. (2006). Microstructural and phase configurational effects determining water content: Dielectric relationships of aggregated porous media. *Water Resources Research, 42*. doi:10.1029/2005WR004418

Bloomer, D. J., Curtis, A., & Reese, P. (n.d.). *Irrigation Glossary*: Irrigation New Zealand. Retrieved from https://www.irrigationnz.co.nz/KnowledgeResources/COP/Attachment?Action=Download&Attachment_id=46

Boertje, G. A. (1995). Chemical and physical characteristics of pumice as a growing medium. *Acta Horticulturae, 401*(401), 85-87. doi:10.17660/ActaHortic.1995.401.9

Bouwer, H., & Rice, R. C. (1984). Hydraulic properties of stony vadose zones. *Hydraulic properties of stony vadose zones*(6), 696-705.

Brooks, R. H., & Corey, A. T. (1964). Hydraulic Properties of Porous Media and Their Relation to Drainage Design. *Transactions of the ASAE, 7*(1), 0026-0028. doi:10.13031/2013.40684

Brown, H., Martin, D., & Craigie, R. (2010). *Irrigation management for cropping - a grower's guide* (Vol. 4)

Campbell, G. S., & Campbell, C. S. (2005). WATER CONTENT AND POTENTIAL, MEASUREMENT. In D. Hillel (Ed.), *Encyclopedia of Soils in the Environment* (pp. 253-257). Oxford: Elsevier. Retrieved from http://www.sciencedirect.com/science/article/pii/B0123485304005026. doi:https://doi.org/10.1016/B0-12-348530-4/00502-6

Carter, R., Suren, A., Dare, J., Scholes, P., & Dodd, J. (2018). *Freshwater in the Bay of Plenty. Comparison against the recommended water quality guidelines*: Bay of Plenty Regional Council. Retrieved from https://atlas.boprc.govt.nz/api/v1/edms/document/A3155218/content

Celik, S., Family, R., & Menguc, M. P. (2016). Analysis of perlite and pumice based building insulation materials. *Journal of Building Engineering, 6*, 105-111. doi:https://doi.org/10.1016/j.jobe.2016.02.015

Challinor, P. F. (1996). *The use of pumice in horticulture*. Paper presented at the meeting of the Proceedings of 9th International Congress Soilless Culture, St Helier, Jersey.

Charlton, J. F. L., & Stewart, A. V. (1999). Pasture species and cultivars used in New Zealand -a list. *Proceedings of the New Zealand Grassland Association, 61*, 147-166.

Chow, T. L., Rees, H. W., Monteith, J. O., Toner, P., & Lavoie, J. (2007). Effects of coarse fragment content on soil physical properties, soil erosion and potato production. *Canadian Journal of Soil Science, 87*, 565-577. doi:10.4141/CJSS07006

Clare, N. T. (1999). The bush-sickness saga. In D. Hogan & B. Williamson (Eds.), *New Zealand is different: Chemical milestones in New Zealand history*. Christchurch: Clerestory Press.

Claydon, J. J. (1989). *Determination of particle-size distribution in fine-grained soils - pipette method*: DSIR.

Cooper, D. (2016). *Soil water measurement : a practical handbook*. Chichester, West Sussex, UK: John Wiley & Sons, Ltd.

Coppola, A., Dragonetti, G., Comegna, A., Lamaddalena, N., Caushi, B., Haikal, M. A., & Basile, A. (2013). Measuring and modeling water content in stony soils. *Soil and Tillage Research, 128*, 9-22. doi:https://doi.org/10.1016/j.still.2012.10.006

Council, W. R. (2011). *Waikato Regional Plan - 3 Water Module* (2007/21). Hamilton.

Cowie, J. D. (1974). Classification. In N. E. Read (Ed.), *Yellow-brown pumice soils* (pp. 9-10). New Zealand: New Zealand Society of Soil Science.

Dal Ferro, N., Pagliarin, C., & Morari, F. (2014). Pore network and water retention characteristics of volcanic porous media. *European Journal of Soil Science, 65*(5), 672-683. doi:10.1111/ejss.12163

Dane, J. H., & Hopmans, J. W. (2002). 3.3.2 Laboratory. In J. H. Dane, & Topp, G.C. (Ed.), *Methods of Soil Analysis. Part 4 - Physical Methods* (Vol. 4). Madison, Wisconsin, USA: Soil Science Society of America, Inc.

Davies, D. B., Eagle, D. J., & Finney, J. B. (1997). *Soil management* (5th ed.. ed.). Ipswich, England: Ipswich, England : Farming Press.

Day, P. R. (1965). Particle fractionation and particle size analysis In C. A. Black (Ed.), *Methods of Soil Analysis, Part 1* (pp. 545-567). Madison, Wiconsin: Americal Society of Agronomy.

Decagon Devices. (2013). *Operator's manual WP4C Dewpoint potentiaMeter*. Pullman, Washington: Decagon Devices Inc.

Deering, C. D., Bachmann, O., Dufek, J., & Gravley, D. M. (2011). Rift-Related Transition from Andesite to Rhyolite Volcanism in the Taupo Volcanic Zone (New Zealand) Controlled by Crystal melt Dynamics in Mush Zones with Variable Mineral Assemblages. *Journal of Petrology, 52*, 2243-2263.

Doran, J. W. (2002). Soil health and global sustainability: translating science into practice. *Agriculture, Ecosystems & Environment, 88*(2), 119-127. doi:https://doi.org/10.1016/S0167-8809(01)00246-8

ecoTech. (n.d.). *Plastic suction plates*. Retrieved 28/11/2019, 2019,from https://www.ecotech-bonn.de/en/produkte/bodenkunde/sickerwasser/saugplatten/kunststoff_saugplatten/.

Efford, J. T., Clarkson, B. D., & Bylsma, R. J. (2014). Persistent effects of a tephra eruption (AD 1655) on treeline composition and structure, Mt Taranaki, New Zealand. *New Zealand Journal of Botany, 52*(2), 245-261. doi:10.1080/0028825X.2014.886599

Ferrari, A., Favero, V., Marschall, P., & Laloui, L. (2014). Experimental analysis of the water retention behaviour of shales. *International Journal of Rock Mechanics and Mining Sciences, 72*, 61-70. doi:https://doi.org/10.1016/j.ijrmms.2014.08.011

Fields, J. S., Owen, J. S., Zhang, L., & Fonteno, W. C. (2016). Use of the evaporative method for determination of soilless substrate moisture characteristic curves. *Scientia Horticulturae, 211*, 102-109. doi:10.1016/j.scienta.2016.08.009

Fiès, J., C., Louvigny, N., D, E, & Chanzy, A. (2002). The role of stones in soil water retention. *European Journal of Soil Science, 53*(1), 95-104. doi:10.1046/j.1365-2389.2002.00431.x

Flint, A. L., & Childs, S. (1984). Physical properties of rock fragments and their effect on available water in skeletal soils. In J. D. Nichols, P. L. Brown & W. J. Grant (Eds.), *Erosion and productivity of soils containing rock fragments* (Vol. 13, pp. 91-103). Madison, WI: Soil Science Society of America. doi:10.2136/sssaspecpub13

Flores-Ramírez, E., Abel, S., & Nehls, T. (2018). Water retention characteristics of coarse porous materials to construct purpose-designed plant growing media. *Soil Science and Plant Nutrition, 64*(2), 181-189. doi:10.1080/00380768.2018.1447293

Fredlund, D. G., & Xing, A. (1994). Equations for the soil-water characteristic curve. *Canadian Geotechnical Journal, 31*(4), 521-532. doi:10.1016/0148-9062(95)96992-K

Gabriel, M. Z., Altland, J. E., & Owen, J. S. (2009). The Effect of Physical and Hydraulic Properties of Peatmoss and Pumice on Douglas Fir Bark Based Soilless Substrates. *HortScience, 44*(3), 874. doi:10.21273/hortsci.44.3.874

Gizas, G., & Savvas, D. (2007). Particle size and hydraulic properties of pumice affect growth and yield of greenhouse crops in soilless culture. *HortScience, 42*(5), 1274-1280. doi:10.21273/HORTSCI.42.5.1274

GNS. (n.d.). *New Zealand Geology Webmap*. Retrieved 11/10/19, from http://data.gns.cri.nz/geology/.

Gordon, R. B. (1971). *Soils and farming patterns of the central pumice region*. Paper presented at the meeting of the Proceedings of the New Zealand Grassland Association, Taupō. Retrieved from https://www.grassland.org.nz/publications/nzgrassland_publication_1599.pdf

Graham, I. J., Cole, J. W., Briggs, R. M., Gamble, J. A., & Smith, I. E. M. (1995). Petrology and petrogenesis of volcanic rocks from the Taupo Volcanic Zone: a review. *Journal of Volcanology and Geothermal Research, 68*(1), 59-87. doi:https://doi.org/10.1016/0377-0273(95)00008-I

Grzegorz, P., Tomasz, K., Katarzyna, S., Wojciech, O., Romuald, Ż., & Ryszard, P. (2018). Hydrological Performance and Runoff Water Quality of Experimental Green Roofs. *Water, 10*(9), 1185. doi:10.3390/w10091185

Gunnlaugsson, B., & Adalsteinsson, S. (1995). Pumice as environment-friendly substrate--comparison with rockwool. *Acta Horticulturae, 401*(401), 131-136. doi:10.17660/ActaHortic.1995.401.15

Haghverdi, A., Leib, B. G., Washington-Allen, R. A., Ayers, P. D., & Buschermohle, M. J. (2015). High-resolution prediction of soil available water content within the crop root zone. *Journal of Hydrology, 530*, 167-179. doi:https://doi.org/10.1016/j.jhydrol.2015.09.061

Hatfield, J. L., Parkin, T. B., Sauer, T. J., & Prueger, J. H. (2012). Chapter 28 - Mitigation Opportunities from Land Management Practices in a Warming World: Increasing Potential Sinks. In M. A. Liebig, A. J. Franzluebbers & R. F. Follett (Eds.), *Managing Agricultural Greenhouse Gases* (pp. 487-504). San Diego: Academic Press. Retrieved from http://www.sciencedirect.com/science/article/pii/B9780123868978000280. doi:https://doi.org/10.1016/B978-0-12-386897-8.00028-0

Hatfield, J. L., & Sauer, T. J. (2011). *Soil management: building a stable base for agriculture*. Madison, WI: American Society of Agronomy: Soil Science Society of America.

He, L., & Weber, D. (2019). *Monitoring soil moisture level for precision irrigation in apple orchards*. Retrieved from https://extension.psu.edu/monitoring-soil-moisture-level-for-precision-irrigation-in-apple-orchards.

Hewitt, A. E. (2010). *New Zealand Soil Classification*. Lincoln, New Zealand: Manaaki Whenua Press.

Hewitt, A. E., & J. R. Dymond. (2013). *Survey of New Zealand Soil Orders* [Ecosystem services in New Zealand – conditions and trends.]. Lincoln New Zealand: Manaaki Whenua Press.

Hillel, D. (2011). Chapter 1 - An overview of soil and water management: The challenge of enhancing productivity and sustainability. In J. L. Hatfield & T. J. Sauer (Eds.), *Soil management. Building a stable base for agriculture*. Madison, WI: American Society of Agronomy and Soil Science Society of America.

Hogg, A., Lowe, D. J., Palmer, J., Boswijk, G., & Ramsey, C. B. (2012). Revised calendar date for the Taupo eruption derived by 14C wiggle-matching using a New Zealand kauri 14C calibration data set. *The Holocene, 22*(4), 439-449. doi:10.1177/0959683611425551

Houghton, B. F., Carey, R. J., & Rosenberg, M. D. (2014). The 1800a Taupo eruption: "III wind" blows the ultraplinian type event down to Plinian. *Geology, 42*(5), 459-461. doi:10.1130/g35400.1

Jackson, R. J. (1974). Physical properties. In N. E. Read (Ed.), *Soil groups of New Zealand. Part 1, Yellow-brown Pumice Soils* (pp. 97-102). New Zealand: New Zealand Society of Soil Science.

Jacquelyne, W., & Tilling, R. I. (1999). *The ring of fire*. Retrieved from https://www.usgs.gov/media/images/ring-fire.

Kirkham, M. B. (2005). 8 - Field Capacity, Wilting Point, Available Water, and the Non-Limiting Water Range. In M. B. Kirkham (Ed.), *Principles of Soil and Plant Water Relations* (pp. 101-115). Burlington: Academic Press. Retrieved from http://www.sciencedirect.com/science/article/pii/B9780124097513500086. doi:https://doi.org/10.1016/B978-012409751-3/50008-6

Kosugi, K. i. (1996). Lognormal Distribution Model for Unsaturated Soil Hydraulic Properties. *Water Resources Research, 32*(9), 2697-2703. doi:10.1029/96wr01776

Lal, R., & Shukla, M. (2004). *Principles of soil physics*. New York: New York : Marcel Dekker.

Land Air Water Aotearoa. (n.d.). *Bay of Plenty region - Lakes*. Retrieved from https://www.lawa.org.nz/explore-data/bay-of-plenty-region/lakes/.

Landcare Research. (2010). FSL North Island (all attributes) (Publication no. 10.7931/L1FT0). from LRIS https://lris.scinfo.org.nz/layer/48136-fsl-north-island-all-attributes/

Landcare Research. (2018a). *S-map Online FAQ*. Retrieved from https://smap.landcareresearch.co.nz/support/faq/.

Landcare Research. (2018b). *Soil Orders; Pumice Soils [M]*. Retrieved from https://soils.landcareresearch.co.nz/describing-soils/nzsc/soil-order/pumice-soils.

Landcare Research. (2019a). *Hydrological pedotransfer functions for New Zealand soils*. Retrieved from https://smap.landcareresearch.co.nz/support/hydrological-pedotransfer-functions-for-new-zealand-soils/.

Landcare Research. (2019b). *S-map soil report. Taupof*: Landcare Research. Retrieved from https://api-factsheets-smap.landcareresearch.co.nz/reports?access=spatial&type=smap&gis=Waikato&rank=1&mapunitsymbol=KC%2FHn&confidence=L&xcoord=1864464&ycoord=5712535.5&region=Waikato&licence=

Landcare Research. (2020). *S-map soil report. Taupof*. Landcare Research. Retrieved from https://smap.landcareresearch.co.nz

Landcare Research. (2020). *Soil report. Kaingaroa_12a.1*. Retrieved from https://api-factsheets-smap.landcareresearch.co.nz/reports?access=spatial&type=smap-v2&gis=Waikato&rank=1&mapunitsymbol=KC%2FKgR&confidence=L&xcoord=1903986.090697139&ycoord=5700525.70387399&region=Bay%20of%20Plenty&licence=

Landcare Research. (n.d.-a). *NSDR viewer*. Retrieved from https://viewer-nsdr.landcareresearch.co.nz/search.

Landcare Research. (n.d.-b). *S-map online*. Retrieved from https://smap.landcareresearch.co.nz/app#.

Landman, M. J., Van Den Heuvel, M. R., & Ling, N. (2005). Relative sensitivities of common freshwater fish and invertebrates to acute hypoxia. *New Zealand Journal of Marine and Freshwater Research, 39*(5), 1061-1067. doi:10.1080/00288330.2005.9517375

Laubscher, N. (2014). *Improvement in soil water availability in pastures by excavating and mixing buried soil horizons from multilayered Pumice Soils (Vitrands) at Galatea, central North Island, New Zealand* (Masters). University of Waikato, Hamilton, New Zealand. Retrieved from https://hdl.handle.net/10289/8709

Leib, B., Grant, T., & McClure, A. (2019). The basics of soybean irrigation in Tennessee. https://extension.tennessee.edu/publications/Documents/W809-B.pdf

Leib, B., Grant, T., & Raper, T. (2019). The basics of cotton irrigation in Tennessee. https://extension.tennessee.edu/publications/Documents/W809-C.pdf

Lilburne, L. R., Hewitt, A. E., & Webb, T. W. (2012). Soil and informatics science combine to develop S-map: A new generation soil information system for New Zealand. *Geoderma, 170*, 232-238. doi:https://doi.org/10.1016/j.geoderma.2011.11.012

Lockwood, J. P., & Hazlett, R. W. (2010). *Volcanoes : global perspectives*. Hoboken, NJ: Hoboken, NJ : Wiley-Blackwell.

Lowe, D. J., Balks, M. R., & Laubscher, N. (2014). *Once despised now desired: innovative land use and management of multilayered Pumice Soils in the Taupo and Galatea areas, central North Island, New Zealand. Guidebook for field trip "Hot volcanic soils", New Zealand Society of Soil Science conference "Soil Science for Future Generations"*

Lowe, D. J., & King, C. M. (2015). A dramatic landscape. In C. M. King, D. J. Gaukrodger & N. A. Ritchie (Eds.), *The drama of conservation - The history of Pureora Forest, New Zealand* (pp. 1-17). Berlin: Springer. doi:10.1007/978-3-319-18410-4

Maloupa, E., Abou Hadid, A., Prasad, M., & Kavafakis, C. (2001). Response of cucumber and tomato plants to different substrates mixtures of pumice in substrate culture. *Acta Horticulturae, 559*, 593-600. doi:10.17660/ActaHortic.2001.559.87

Marco, B. (2010). Measuring Soil Water Potential for Water Management in Agriculture: A Review. *Sustainability, 2*(5), 1226-1251. doi:10.3390/su2051226

Marinou, E., Chrysargyris, A., & Tzortzakis, N. (2013). Use of sawdust, coco soil and pumice in hydroponically grown strawberry. *Plant, Soil and Environment, 10*, 452-459. doi:10.17221/297/2013-PSE

Maseyk, F., Brown, M., & Taylor, P. (2018). *Regional Council uses of OVERSEER. A review of the use of the OVERSEER nutrient budget model for nutrient management in regional planning.* (2018/140): The Catalyst Group. Retrieved from https://www.pce.parliament.nz/media/196490/regional-council-uses-of-overseer-catalyst-group-report.pdf

McLeod, M., Aislabie, J., Ryburn, J., & McGill, A. (2008). Regionalizing Potential for Microbial Bypass Flow through New Zealand Soils. *Journal of Environmental Quality, 37*(5), 1959-1967. doi:10.2134/jeq2007.0572

McLeod, M., McGill, A., Thronburrow, D., & Fitzgerald, N. (2016). *Soil data for Waikato Regional Council soil moisture monitoring network: sites 6 to 8 – 2015*: Landcare Research.

McNeill, S. J., Lilburne, L. R., Carrick, S., Webb, T. H., & Cuthill, T. (2018). Pedotransfer functions for the soil water characteristics of New Zealand soils using S-map information. *Geoderma, 326*(2018), 96-110. doi:https://doi.org/10.1016/j.geoderma.2018.04.011

METER Environment. (n.d.-a). Defining water potential - What it is. How to use it. https://www.metergroup.com/environment/articles/defining-water-potential/

METER Environment. (n.d.-b). *Soil moisture sensors - How they work. Why some are not research-grade.* Retrieved from https://www.metergroup.com/environment/articles/tdr-fdr-capacitance-compared/.

METER Group Inc. (2012). Instruction manual. Vacuum controller systems VS-single, VS-twin, VS-pro. http://library.metergroup.com/Manuals/UMS/VS:VSPro_Manual.pdf

METER Group Inc. (2019a). *5TM*. Retrieved from http://publications.metergroup.com/Manuals/20424_5TM_Manual_Web.pdf.
METER Group Inc. (2019b). *TEROS 21*. Retrieved from http://publications.metergroup.com/Manuals/20428_TEROS21_Manual_Web.pdf.
METER Group Inc. (2019c). *WP4C*. Retrieved from http://library.metergroup.com/Manuals/20588_WP4C_Manual_Web.pdf.
METER Group Inc. (n.d.-a). *Method A: Soil-specific callibrations for METER soil moisture sensors*. Retrieved 5 November, 2019,from https://www.metergroup.com/environment/articles/method-a-soil-specific-calibrations-for-meter-soil-moisture-sensors/.
METER Group Inc. (n.d.-b). *TensioVIEW*. [Software]. Retrieved from https://www.metergroup.com/de/environment/downloads/?download_category=software.
Microsoft. (n.d.). *LINEST function*. Retrieved from https://support.office.com/en-us/article/linest-function-84d7d0d9-6e50-4101-977a-fa7abf772b6d.
Milne, J. D. G., Clayden, B., Singleton, P. L., & Wilson, A. D. (1995). *Soil description handbook*. Lincoln, New Zealand: Manaaki Whenua Press. Retrieved from https://doi.org/10.7931/DL1JG6. doi:10.7931/DL1JG6
Ministry of Business Innovation and Employment. (2019). *Key Tourism Statistics*. Retrieved from https://www.google.com/url?sa=t&rct=j&q=&esrc=s&source=web&cd=11&ved=2ahUKEwjqrpzF7-LjAhVOX30KHXNbDE0QFjAKegQIBhAC&url=https%3A%2F%2Fwww.mbie.govt.nz%2Fdmsdocument%2F3438-key-tourism-statistics-pdf&usg=AOvVaw19VDgyEDdGzjOKvseOwinb
Morgenstern, U., Daughney, C. J., Leonard, G., Gordon, D., Donath, F. M., & Reeves, R. (2015). Using groundwater age and hydrochemistry to understant sources and dynaics of nutirent contamination through the catchment into Lake Rotorua, New Zelanad. *Hydrology and Earth System Sciences, 19*, 803-822. doi:10.5194/hess-19-803-2015
Murray, W., & Freeman, M. (2017). *Effective use of OVERSEER in regulation* (30): Fertiliser and Lime Research Centre. Retrieved from https://assets.ctfassets.net/bo1h2c9cbxaf/2dBtHlFzBjG5LoEvPdl9Af/c40508d6f099adaf66b2a7a89a81a4e7/Effective_Use_of_Overseer_in_Regulation..pdf
Nairn, I. A., Shane, P. R., Cole, J. W., Leonard, G. J., Self, S., & Pearson, N. (2004). Rhyolite magma processes of the ~AD 1315 Kaharoa eruption episode, Tarawera volcano, New Zealand. *Journal of Volcanology and Geothermal Research, 131*(3), 265-294. doi:https://doi.org/10.1016/S0377-0273(03)00381-0
Nanzyo, M., Shoji, S., & Dahlgren, R. (1993). Physical Characteristics of Volcanic Ash Soils. In S. Shoji, Nanzyo, M., & Dahlgren, R. (Ed.), *Volcanic Ash Soils. Genesis, Properties and Utilization* (pp. 189-207). Amsterdam: Elsevier.
NIWA. (2019). *NIWA's underwater health check*. Retrieved from https://www.niwa.co.nz/news/niwas-underwater-health-check.
NIWA. (n.d.). *Kōrua*. Retrieved from https://www.niwa.co.nz/our-science/freshwater/tools/kaitiaki_tools/species/koura.
Nixon, C., Gamperle, D., Pambudi, D., & Clough, P. (2017). *Plantation forestry statistics. Contribution of forestry to New Zealand*: NZIER. Retrieved from https://nzier.org.nz/static/media/filer_public/c6/a5/c6a55bbf-8f36-484e-82a0-91bb59211880/plantation_forestry_statistics.pdf
Noble, P. F. (1974). Moisture. In N. E. Read (Ed.), *Soil groups of New Zealand, Part 1, Yellow-brown Pumice Soils* (pp. 102-108). Wellington: New Zealand Society of Soil Science.
Nolz, R., Kammerer, G., & Cepuder, P. (2013). Calibrating soil water potential sensors integrated into a wireless monitoring network. *Agricultural Water Management, 116*, 12-20. doi:https://doi.org/10.1016/j.agwat.2012.10.002
Odeh, I. O. A., & McBratney, A. B. (2005). Pedometrics. In D. Hillel (Ed.), *Encyclopedia of Soils in the Environment* (pp. 166-175). Oxford: Elsevier. Retrieved from http://www.sciencedirect.com/science/article/pii/B0123485304000205. doi:https://doi.org/10.1016/B0-12-348530-4/00020-5

Overseer. (n.d.). *Overseer scientific model*. Retrieved from https://www.overseer.org.nz/our-model.
Özhan, S., Özcan, M., & Gökbulak, F. (2008). *Effect of pumice addition on available water capacity of different soil textural classes*. Paper presented at the meeting of the BALWOIS, Macedonia. Retrieved from http://balwois.com/wp-content/uploads/old_proc/ffp-912.pdf
Packard, R. Q. (1957). Some physical properties of Taupo pumice soils of New Zealand. *Soil Science, 83*, 273-289.
Papadopoulos, A. P., Bar-Tal, A., Silber, A., Saha, U. K., & Raviv, M. (2008). 12 - Inorganic and synthetic organic components of soilless culture and potting mixes. In M. Raviv & J. H. Lieth (Eds.), *Soilless Culture* (pp. 505-543). Amsterdam: Elsevier. Retrieved from http://www.sciencedirect.com/science/article/pii/B9780444529756500149. doi:https://doi.org/10.1016/B978-044452975-6.50014-9
Parajuli, K., Sadeghi, M., & Jones, S. (2017). A binary mixing model for characterizing stony-soil water retention. *Agricultural and Forest Meteorology, 244-245*, 1-8. doi:10.1016/j.agrformet.2017.05.013
Parliamentry Commissioner for the Environment. (2012). *Water quality in New Zealand: Understanding the science*. Wellington, New Zealand. Retrieved from www.pce.parliament.nz
Pérez-Urrestarazu, L., Fernández-Cañero, R., Campos-Navarro, P., Sousa-Ortega, C., & Egea, G. (2019). Assessment of perlite, expanded clay and pumice as substrates for living walls. *Scientia Horticulturae, 254*, 48-54. doi:https://doi.org/10.1016/j.scienta.2019.04.078
Platz, T. (2007). *Understanding aspects of andesitic dome-forming eruptions through the last 1000 yrs of volcanism at Mt. Taranaki, New Zealand : a dissertation presented in partial fulfilment of the requirements for the degree of Doctor of Philosophy in Earth Science, Massey University, Palmerston North, New Zealand* (Doctoral). Massey University. Retrieved from http://hdl.handle.net/10179/938
Pollacco, J. A. P. (2016). *Literature review of hydrological processes of soils with rock fragments* (LC2688). Lincoln, New Zealand: Manaaki Whenua Landcare Research.
Pollacco, J. A. P., Lilburne, L. R., Webb, T. H., & Wheeler, D. M. (2014). *Preliminary assessment and review of soil parameters in OVERSEER 6.1*. Retrieved from https://www.researchgate.net/publication/295906245_Preliminary_assessment_and_review_of_soil_parameters_in_OVERSEERR_6
Popay, A. J., & Crush, J. R. (2010). Influence of different forage grasses on nitrate capture and leaching loss from a pumice soil. *Grass and Forage Science, 65*(1), 28-37. doi:10.1111/j.1365-2494.2009.00717.x
Raviv, M., Wallach, R., Silber, A., & Bar-Tal, A. (2002). Substrates and their analysis. In D. Savvas & H. C. Passam (Eds.), *Hydroponic production of vegetables and ornamentals* (pp. 25-101). Athens, Greece: Embryo Publications. Retrieved from https://www.researchgate.net/profile/Michael_Raviv/publication/313419715_Substrates_and_their_analysis/links/5a61c0d2a6fdccb61c503f00/Substrates-and-their-analysis.pdf
Raviv, M., Wallach, R., Silber, A., Medina, S., & Krasnovsky, A. (1999). The effect of hydraulic characteristics of volcanic materials on yield of roses grown in soilless culture. *Journal of the American Society for Horticultural Science, 124*(2), 205-209. doi:10.21273/JASHS.124.2.205
Rawlings-Way, C., Atkinson, B., Bennett, S., Dragicevich, P., & Slater, L. (2016). *New Zealand's North Island : (Te Ika-a-Māui)* (4th edition.. ed.). Footscray, Victoria Oakland, CA: Lonely Planet Publications.
Rawls, W. J., Brakensiek, D. L., & Saxtonn, K. E. (1982). Estimation of soil water properties. *Transactions of the ASAE, 25*(5), 1316-1320. doi:10.13031/2013.33720
Read, N. E. (Ed.). (1974). *Yellow-Brown Pumice Soils*: New Zealand Society of Soil Science.
Regalado, C. M., Muñoz Carpena, R., Socorro, A. R., & Hernández Moreno, J. M. (2003). Time domain reflectometry models as a tool to understand the dielectric response of volcanic soils. *Geoderma, 117*(3), 313-330. doi:10.1016/S0016-7061(03)00131-9
Reicosky, D. C., Sauer, T. J., & Hatfield, J. L. (2011). Chapeter 2- Challenging balance between productivity and enviromental quality: Tillage impacts. In J. L. Hatfield & T. J. Sauer (Eds.), *Soil*

management: Building a stable base for agriculture. Madison, WI: American Society of Agronomy and Soil Science Society of America.

Ridler, B. (2017). *The feasibility of nutrient leaching reductions (N leaching) within the constraints of minimum impact on the profitability and production of three dairy farms in the Horizons Region*. Retrieved from http://www.horizons.govt.nz/HRC/media/Media/One%20Plan%20Documents/Ridler-Representative-Farm-Report-January-2018.pdf?ext=.pdf

Roberts, A., Wheeler, D. M., Ryan, D., Mathers, D., Power, I., Palmer, J., . . . Wilson, T. (2015). *Overseer 6.2.0 Best practice data input standards*.

Sahin, U., Ercisli, S., Anapali, O., & Esitken, A. (2004a). Regional distribution and some physico-chemical and physical properties of some substrates used in horticulture in Turkey. *Acta Horticulturae, 648*, 177-183. doi:10.17660/ActaHortic.2004.648.21

Sahin, U., Ercisli, S., Anapali, O., & Esitken, A. (2004b). Regional distribution and some physico-chemical and physical properties of some substrates used in horticulture in Turkey. *Regional distribution and some physico-chemical and physical properties of some substrates used in horticulture in Turkey*(648), 177-183.

Sahin, U., Ors, S., Ercisli, S., Anapali, O., & Eistken, A. (2005). Effect of pumice amendment on physical soil properties and strawberry plant growth. *Journal of Central European Agriculture, 6*(3), 361-366.

Schaetzl, R. J. (2015). *Soils : genesis and geomorphology* (Second edition. ed.). New York: Cambridge University Press.

Schmincke, H.-U. (2004). *Volcanism* (1st ed. ed.). Berlin: Springer.

Schneiter, A. A. (1992). Production of semidwarf and dwarf sunflower in the northern Great Plains of the United States. *Field Crops Research, 30*(3), 391-401. doi:https://doi.org/10.1016/0378-4290(92)90007-V

Seki, K. (2007). SWRC fit – a nonlinear fitting program with a water retention curve for soils having unimodal and bimodal pore structure. *Hydrol. Earth Syst. Sci. Discuss., 2007*, 407-437. doi:10.5194/hessd-4-407-2007

Selby, M. J. (1974). Erosion. In N. E. Read (Ed.), *Soil Groups of New Zealand, Part 1, Yellow-Brown Pumice Soils*. Wellington: New Zealand Society of Soil Science.

Seoane, A. P., Vence, L. B., Svartz, H. A., & Barbaro, L. A. (2018). Puyehue-Cordon caulle volcanic materials and their use for substrates formulations with sphagnum peat. *Ciencia del Suelo, 36*(1), 39-53.

Shepherd, M. A., Harrison, R., & Webb, J. (2002). Managing soil organic matter – implications for soil structure on organic farms. *Soil Use and Management, 18*(s1), 284-292. doi:10.1111/j.1475-2743.2002.tb00270.x

Shukla, M. (2014). *Soil physics : an introduction*: Boca Raton : CRC Press.

Silva, A. P., Kay, B. D., & Perfect, E. (1994). Characterization of the Least Limiting Water Range of Soils. *Soil Science Society of America Journal, 58*(6), 1775-1781. doi:10.2136/sssaj1994.03615995005800060028x

Sim, R. E., Brown, H. E., Teixeira, E. I., & Moot, D. J. (2017). Soil water extraction patterns of lucerne grown on stony soils. *Plant and Soil, 414*(1), 95-112. doi:10.1007/s11104-016-3112-x

Soil Survey Staff. (1999). *Soil taxonomy : a basic system of soil classification for making and interpreting soil surveys* (2nd ed. ed.). Washington, DC: U.S. Dept. of Agriculture, Natural Resources Conservation Service.

Soilmoisture equipment corp. (n.d.). *Ceramic plate extractor*. Retrieved from https://www.soilmoisture.com/EXTRACTOR15/.

Steiner, J. L. (1994). Crop residue effects on water conservation. In P. W. Unger (Ed.), *Managing Agricultural Residues* (pp. 41-76). Boca Raton, FL: Lewis Publishers.

Takahashi, T., & Shoji, S. (2002). Distribution and classification of volcanic ash soils. *Global Environmental Research, 6*(2), 83-98.

Te Puni Kōkiri. (n.d.). *Te Kāhui Māngi. Directory of Iwi and Māori organisations*. Retrieved 5/9/19, from http://www.tkm.govt.nz/map/.

Te Uru Rākau - Forestry New Zealand. (2019). *Getting started in farm forestry*. Retrieved from https://www.mpi.govt.nz/growing-and-harvesting/forestry/getting-started-in-farm-forestry/.

Tokunaga, T. K., Olson, K. R., & Wan, J. (2003). Moisture characteristics of hanford gravels: bulk, grain-surface, and intragranular components. *Vadose Zone Journal, 2*(3), 322-329. doi:https://doi.org/10.2136/vzj2003.3220

Tokunaga, T. K., Wan, J., & Olson, K. R. (2002). Saturation-matric potential relations in gravel. *Water Resources Research, 38*(10), 32-31-32-37. doi:10.1029/2001wr001242

Tomer, M. D., Clothier, B. E., Vogeler, I., & Green, S. (1999). A dielectric–water content relationship for sandy volcanic soils in New Zealand. *Soil Science Society of America Journal, 63*(4), 777-781. doi:10.2136/sssaj1999.634777x

Topp, G. C., Davis, J. L., & Annan, A. P. (1980). Electromagnetic determination of soil water content: Measurements in coaxial transmission lines. *Water Resources Research, 16*(3), 574-582. doi:10.1029/WR016i003p00574

Topp, G. C., & Ferré, T. P. A. (2005). Time-domain reflectometry. In D. Hillel (Ed.), *Encyclopedia of soils in the environment* (First ed., Vol. 4, pp. 174-181). Oxford, UK: Elsevier Ltd.

Topping, W. W. (1972). Burrell Lapilli eruptives, Mount Egmont, New Zealand. *New Zealand Journal of Geology and Geophysics, 15*(3), 476-490. doi:10.1080/00288306.1972.10422345

Tozer, K. N., Chapman, D.F., Bell, N.L., Crush, J.R., King, W.M., Rennie, G.M., Wilson, D.J., Mapp, N.R., Rossi, L., Aalders, L.T., & Cameron, C.A. (2014). Botanical survey of perennial ryegrass-based dairy pastures in three regions of New Zealand: implications for ryegrass persistence. *New Zealand Journal of Agricultural Research, 57*(1), 14-29. doi:10.1080/00288233.2013.863785

van Genuchten, M. T. (1980). A Closed-form Equation for Predicting the Hydraulic Conductivity of Unsaturated Soils. *Soil Science Society of America Journal, 44*(5), 892-898. doi:10.2136/sssaj1980.03615995004400050002x

Vant, W. N. (2013). Recent changes in the water quality of Lake Taupo and its inflowing streams. *New Zealand journal of forestry (New Zealand Institute of Forestry), 58*(2), 27-30.

Volterrani, M., & Magni, S. (2012). Hydrological characteristics of some volcanic materials as affected by particle size distribution and internal porosity. *Acta Agriculturae Scandinavica Section B - Soil and Plant Science, 62*, 150-154. doi:10.1080/09064710.2012.682161

Waikato Regional Council. (2011). *Waikato Regional Plan - 3 Water Module* (2007/21). Retrieved from https://waikatoregion.govt.nz/council/policy-and-plans/rules-and-regulation/regional-plan/waikato-regional-plan/3-water-module

Waikato Regional Council. (n.d.). *Regional Land Use*. Retrieved 31/07/2019, 2019,from https:// www.waikatoregion.govt.nz/Environment/Natural-resources/Land-and-soil/Land-use-in-the-Waikato/Regional-land-use/.

Walker, G. P. L. (1981). The Waimihia and Hatepe plinian deposits from the rhyolitic Taupo Volcanic Centre. *New Zealand Journal of Geology and Geophysics, 24*(3), 305-324. doi:10.1080/00288306.1981.10422722

Watkins, N., & Selbie, D. (2015). *Technical Description of OVERSEER for Regional Councils*. Retrieved from https://assets.ctfassets.net/bo1h2c9cbxaf/1KrtzjpuD9MugyieUPN3Bh/f8c7142467429be09dc89216ebd516d0/Technical_Description_of_OVERSEER_for_Regional_Councils.pdf

Watkins, N., Shepherd, M., & Ledgard, S. F. (2015). *OVERSEER nutrient budgets information base for the Rotorua catchment*: AgResearch. Retrieved from http://www.rotorualakes.co.nz/vdb/document/1408

Watson, A., & O'Loughlin, C. (1990). Structural root morphology and biomass of three age-classes of Pinus radiata. *New Zealand Journal of Forestry Science, 20*(1), 97-110.

Webb, T. H. (2003). Identification of functional horizons to predict physical properties for soils from alluvium in Canterbury, New Zealand. *Soil Research, 41*(5), 1005-1019. doi:https://doi.org/10.1071/SR01077

Wheeler, D. M. (2018). *OVERSEER technical manual. Characteristics of soils*. Retrieved from https://assets.ctfassets.net/bo1h2c9cbxaf/6I3Va3ErCbev7n1VaVjOa/46225ed53258a9c3c7add049aed33dd8/TMC_Characteristics_of_soils_v6.3_June_2018.pdf

White, J., & Hodgson, J. (1999). *New Zealand pasture and crop science*. Auckland, N.Z.

Oxford: Auckland, N.Z.
Oxford : Oxford University Press.
White, J. D. L., Manville, V., Wilson, C. J. N., Houghton, B. F., Riggs, N. R., & Ort, M. (2001). Settling and deposition of AD 181 Taupo pumice in lacustrine and associated environments. *Special Publication of the International Association of Sedimentologists, 30*, 141-150.
Wikaira, M. (2017). *Ngāti Tuwharetoa*. Retrieved from https://teara.govt.nz/en/ngati-tuwharetoa/print.
Will, G. M. (1974). Forestry. In N. E. Read (Ed.), *Yellow-brown pumice soils* (pp. 181-183). New Zeland: New Zealand Society of Soil Science.
Will, G. M., & Stone, E. L. (1967). Pumice soils as a medium for tree growth. 1. Moisture storage capacity. *New Zealand Journal of Forestry, 12*, 189-199.
Wilson, C. J. N. (1985). The Taupo eruption, New Zealand. II. The Taupo Ignimbrite. *Philisophical Transactions of the Royal Society of London A, 314*(1529), 229-310. doi:https://doi.org/10.1098/rsta.1985.0020
Wilson, C. J. N., Houghton, B. F., McWilliams, M. O., Lanphere, M. A., Weaver, S. D., & Briggs, R. M. (1995). Volcanic and structural evolution of Taupo Volcanic Zone, New Zealand: a review. *Journal of Volcanology and Geothermal Research, 68*(1), 1-28. doi:https://doi.org/10.1016/0377-0273(95)00006-G
Wilson, C. J. N., & Walker, G. P. L. (1985). The Taupo eruption, New Zealand I. Genral Aspects. . *Philisophical Transactions of the Royal Society of London A, 341*(1529), 199-228. doi:http://doi.org/10.1098/rsta.1985.0019
Wood, S. A., Hamilton, D. P., Paul, W. J., Safi, K. A., & Williamson, W. M. (2009). *New Zealand guidelines for cyanobacteria in recreational fresh waters. Interim guidelines*. Wellington: Ministry for the Environment; Ministry of Health. Retrieved from https://www.mfe.govt.nz/sites/default/files/nz-guidelines-cyanobacteria-recreational-fresh-waters.pdf
Woodward, S. J. R., Barker, D. J., & Zyskowski, R. F. (2001). A practical model for predicting soil water deficit in New Zealand pastures. *New Zealand Journal of Agricultural Research, 44*(1), 91-109. doi:10.1080/00288233.2001.9513464
Zhang, Y., Niu, J., Zhang, M., Xiao, Z., & Zhu, W. (2017). Interaction Between Plant Roots and Soil Water Flow in Response to Preferential Flow Paths in Northern China. *Land Degradation & Development, 28*(2), 648-663. doi:10.1002/ldr.2592

Appendix A

Core weight – Experiment 1

Table A.1: Soil weight at equilibrium - analysis 1 and 2

Suction (kPa)	0% Pumice	10% Pumice	20% Pumice	30% Pumice	40% Pumice
0	502.12	487.17	462.57	437.26	420.05
2	501.77	487.18	461.32	436.28	410.55
4	499.60	485.23	459.06	434.62	408.96
6	497.77	483.27	457.03	432.86	407.42
8	497.11	482.48	456.32	420.57	406.28
10	495.92	481.61	454.29	419.13	402.12
20	494.80	479.71	433.54	392.21	381.56
40	487.48	465.21	418.41	382.24	360.79
60	482.49	445.32	404.48	376.86	358.55
80	474.60	434.14	392.35	370.01	354.55

A.1 Analysis 1

Table A.2: Gravimetric water content of pumice clasts, determined using Equation 3.3. Proportion of pumice used in each core is presented gravimetrically (0.05 = 10%).

Suction (kPa)	0.05	0.10	0.15	0.22
0	1.37	1.07	0.94	1.01
2	1.39	1.04	0.92	0.85
4	1.39	1.02	0.92	0.85
6	1.37	1.00	0.91	0.84
8	1.36	1.00	0.63	0.83
10	1.37	0.96	0.62	0.77
20	1.31	0.29	0.01	0.43
40	0.77	-0.03	-0.10	0.15
60	-0.27	-0.37	-0.14	0.17
80	-0.55	-0.56	-0.17	0.18

Table A.3: Volumetric water content of pumice, determined using Equation 3.4.

Suction (kPa)	10%	20%	30%	40%
0	0.80	0.56	0.42	0.37
2	1.60	0.56	0.41	0.37
4	2.40	0.55	0.40	0.36
6	3.20	0.54	0.40	0.25
8	4.00	0.55	0.38	0.25
10	8.00	0.52	0.11	0.01
20	16.00	0.31	-0.01	-0.04
40	24.00	-0.11	-0.15	-0.06
60	32.00	-0.22	-0.23	-0.07
80	0.00	0.00	0.00	0.00

A.2 Analysis 2

Table A.4: Linear regression analysis of gravimetric water content of Pumice Clasts 10-40%.

10-40%	0	2	4	6	8	10	20	40	60	80
0.05	0.61	0.34	0.33	0.33	0.32	0.32	0.32	0.27	0.21	0.17
0.1	0.65	0.43	0.42	0.41	0.41	0.40	0.34	0.28	0.24	0.19
0.15	0.69	0.52	0.51	0.51	0.45	0.45	0.35	0.32	0.30	0.27
0.22	0.77	0.54	0.54	0.53	0.49	0.48	0.40	0.32	0.31	0.29
Slope	0.91	1.22	1.22	1.22	0.97	0.90	0.50	0.31	0.63	0.79
Intercept	0.56	0.30	0.29	0.29	0.29	0.30	0.29	0.26	0.18	0.13
Ws	0.56	0.30	0.29	0.29	0.29	0.30	0.29	0.26	0.18	0.13
Wp	1.47	1.52	1.51	1.51	1.26	1.20	0.79	0.57	0.81	0.92

Table A.5: Linear Regression analysis of gravimetric water content of Pumice Clasts 10-30%.

10-30%	0	2	4	6	8	10	20	40	60	80
0.05	0.61	0.34	0.33	0.33	0.32	0.32	0.32	0.27	0.21	0.17
0.1	0.65	0.43	0.42	0.41	0.41	0.40	0.34	0.28	0.24	0.19
0.15	0.69	0.52	0.51	0.51	0.45	0.45	0.35	0.32	0.30	0.27
Slope	0.80	1.81	1.80	1.80	1.28	1.26	0.38	0.45	0.87	1.00
Intercept	0.57	0.25	0.24	0.24	0.27	0.26	0.30	0.24	0.16	0.11
Ws	0.57	0.25	0.24	0.24	0.27	0.26	0.30	0.24	0.16	0.11
Wp	1.37	2.06	2.04	2.04	1.55	1.52	0.68	0.69	1.03	1.11

Table A.6: Statistical analysis of Linear Regression for 10-40% clast content. Ws – water content of the soil, Wp – water content of pumice, θw – gravimetric water content, SE – standard error, ρb – bulk density (of fines packed in core/pumice clasts), θv – volumetric water content.

	0 kPa		2 kPa		4 kPa		6 kPa		8 kPa		10 kPa		20 kPa		40 kPa		60 kPa		80 kPa	
A10-40%	Ws	Wp	Ws	Wp	Ws	Wp	Ws	Wp	Ws	Wp	Ws	Wp	Ws	Wp	Ws	Wp	Ws	Wp	Ws	Wp
θw	0.56	1.47	0.30	1.52	0.29	1.51	0.29	1.51	0.29	1.26	0.30	1.19	0.29	0.79	0.26	0.56	0.18	0.81	0.13	0.92
SE	0.01	0.06	0.04	0.29	0.04	0.28	0.04	0.28	0.03	0.18	0.03	0.20	0.01	0.06	0.01	0.09	0.02	0.14	0.03	0.19
ρb	1.04	0.43	1.04	0.43	1.04	0.43	1.04	0.43	1.04	0.43	1.04	0.43	1.04	0.43	1.04	0.43	1.04	0.43	1.04	0.43
SE	0.02	0.02	0.02	0.02	0.02	0.02	0.02	0.02	0.02	0.02	0.02	0.02	0.02	0.02	0.02	0.02	0.02	0.02	0.02	0.02
θv	0.58	0.63	0.31	0.65	0.31	0.65	0.30	0.65	0.31	0.54	0.31	0.51	0.30	0.34	0.27	0.24	0.19	0.35	0.13	0.39
SE	0.02	0.06	0.05	0.29	0.05	0.29	0.05	0.28	0.03	0.19	0.03	0.20	0.02	0.07	0.02	0.09	0.03	0.14	0.03	0.19

Table A.7: Statistical analysis of Linear Regression for 10-30% clast content. Ws – water content of the soil, Wp – water content of pumice, θw – gravimetric water content, SE – standard error, ρb – bulk density (of fines packed in core/pumice clasts), θv – volumetric water content.

	0 kPa		**2 kPa**		**4 kPa**		**6 kPa**		**8 kPa**		**10 kPa**		**20 kPa**		**40 kPa**		**60 kPa**		**80 kPa**	
A10-30%	Ws	Wp	Ws	Wp	Ws	Wp	Ws	Wp	Ws	Wp	Ws	Wp	Ws	Wp	Ws	Wp	Ws	Wp	Ws	Wp
θw	0.57	1.37	0.25	2.06	0.24	2.05	0.24	2.04	0.27	1.55	0.26	1.52	0.3	0.67	0.24	0.7	0.16	1.03	0.11	1.11
SE	0.00	0.04	0.00	0.04	0.00	0.04	0.01	0.05	0.03	0.26	0.02	0.22	0.00	0.03	0.01	0.12	0.02	0.19	0.04	0.39
ρb	1.01	0.43	1.01	0.43	1.01	0.43	1.01	0.43	1.01	0.43	1.01	0.43	1.01	0.43	1.01	0.43	1.01	0.43	1.01	0.43
SE	0.01	0.02	0.01	0.02	0.01	0.02	0.01	0.02	0.01	0.02	0.01	0.02	0.01	0.02	0.01	0.02	0.01	0.02	0.01	0.02
θv	0.58	0.59	0.25	0.89	0.24	0.88	0.24	0.88	0.27	0.67	0.26	0.65	0.30	0.29	0.24	0.30	0.16	0.44	0.11	0.48
SE	0.01	0.04	0.01	0.04	0.01	0.04	0.01	0.05	0.03	0.26	0.02	0.22	0.01	0.04	0.01	0.12	0.02	0.19	0.04	0.39

Appendix B

Experiment 2

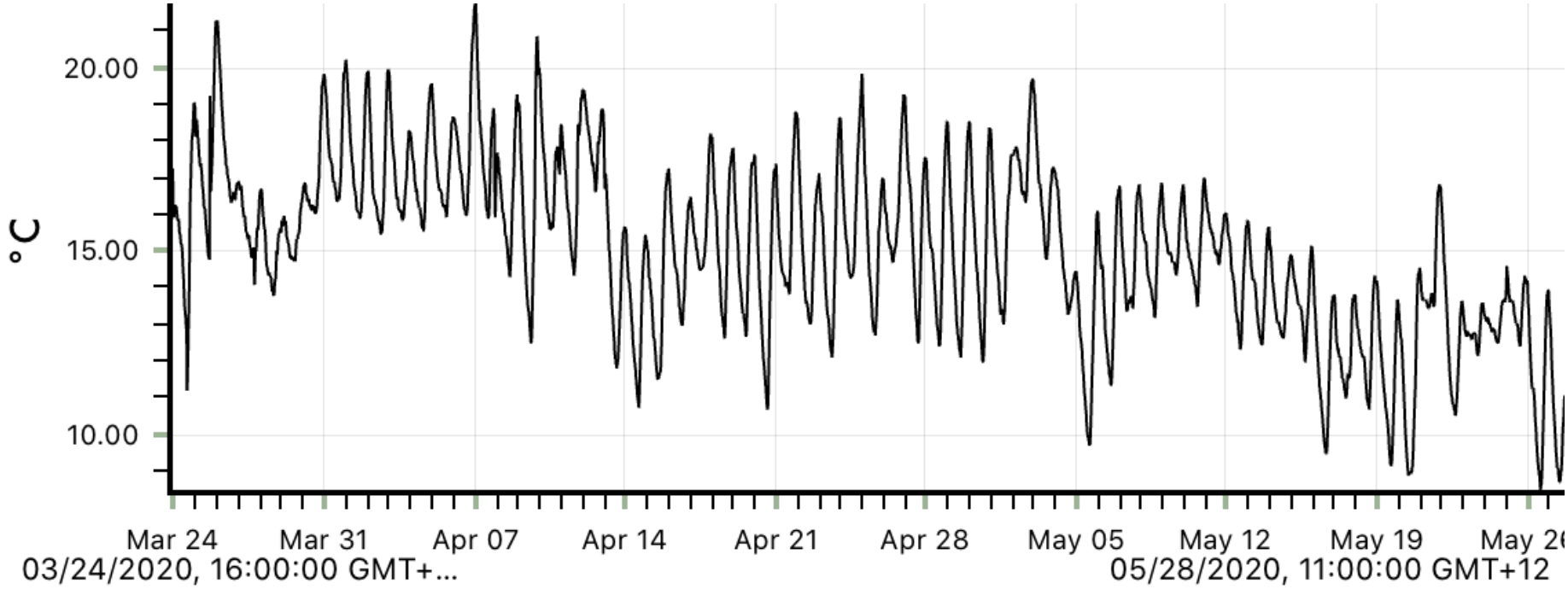

Figure B.1: Temperature of garage that Experiment 2 was run in from March 24 2020 to May 28 2020, recorded using HOBO datalogger. Temperature was recorded every 30 minutes for the duration of the time in the garage. Prior to relocation, the experiment was run in a temperature controlled room, kept at 22°C.

Table B.1: Soil weight at equilibrium for suction plate experiment.

Suction (kPa)	2% Pumice	4% Pumice	7% Pumice	9% Pumice	11% Pumice	13% Pumice	15% Pumice	18% Pumice	20% Pumice	22% Pumice
0	640.59	616.89	600.05	587.08	569.41	555.89	536.04	512.36	495.48	478.67
3	614.76	597.93	558.3	568.44	535.19	527.4	510.01	486.16	466.16	456.67
6	595.1	577.51	547.35	547.43	518.14	505.35	492.67	469.93	443.21	431.52
8	587.3	565.22	531.65	532.03	510.09	491.34	479.82	460.09	430.19	423.74
10	575.92	558.36	527.29	526.84	499.68	486.47	474.38	454.71	423.33	418.69
20	551.39	529.36	500.95	500.19	470.96	459.16	444.83	416.88	393.9	378.42
40	533.76	504.29	475.96	473.14	443.65	432.34	420.09	389.17	361.25	355.57
60	530	494.3	465.8	450.38	431.2	418.3	405.1	385.21	345.95	338.55
80	527.6	492.22	463.85	443.39	429.08	415.89	398.84	383.15	341.2	335.2

B.1 Analysis 4

Table B.2: Volumetric water content of the soil cores used on the suction plates and Dewpoint potentiometer.

Core	χp	0 kPa	3 kPa	6 kPa	8 kPa	10 kPa	20 kPa	40 kPa	60 kPa	80 kPa
1	0.02	0.42	0.35	0.29	0.27	0.24	0.18	0.13	0.12	0.11
2	0.04	0.42	0.37	0.31	0.28	0.26	0.18	0.11	0.09	0.08
3	0.07	0.48	0.35	0.32	0.28	0.27	0.19	0.12	0.09	0.08
4	0.09	0.47	0.42	0.36	0.32	0.31	0.23	0.16	0.09	0.07
5	0.11	0.50	0.40	0.35	0.33	0.30	0.22	0.14	0.10	0.09
6	0.13	0.51	0.43	0.37	0.33	0.32	0.24	0.17	0.13	0.12
7	0.15	0.53	0.45	0.40	0.36	0.35	0.26	0.19	0.15	0.13
8	0.18	0.54	0.46	0.42	0.39	0.37	0.26	0.18	0.17	0.17
9	0.20	0.55	0.47	0.41	0.37	0.35	0.27	0.17	0.13	0.12
10	0.22	0.59	0.52	0.45	0.43	0.41	0.30	0.23	0.18	0.17

Table B. 3: Volumetric water contents at matric potentials determined using the Dewpoint Potentiometer for pumice clasts and soil fines

kPa	**100**	**240**	**250**	**330**	**400**	**580**	**790**	**940**	**1050**	**1310**	**1510**
θ_p	0.45	0.27	0.31	0.20	0.20	0.13	0.09	0.07	0.07	0.06	0.05
kPa	**280**	**410**	**560**	**620**	**780**	**810**	**1020**	**1440**	**1600**	**1610**	
θ_s	0.075	0.057	0.034	0.050	0.033	0.023	0.030	0.020	0.024	0.019	

Table B.4: Statistical analysis of Analysis 4, where each data point was individually scaled.

	0 kPa	3 kPa	6 kPa	8 kPa	10 kPa	20 kPa	40 kPa	60 kPa	80 kPa
$\boldsymbol{\theta}$**p**	0.60	0.65	0.58	0.62	0.67	0.51	0.44	0.37	0.35
SE	0.04	0.06	0.04	0.05	0.06	0.04	0.06	0.08	0.09
t stat	14.787	10.645	13.518	11.347	12.087	12.726	7.000	4.690	4.102
p	0.000	0.000	0.000	0.000	0.000	0.000	0.000	0.002	0.003
$\boldsymbol{\theta}$**s**	0.575	0.464	0.401	0.351	0.318	0.229	0.143	0.107	0.097
SE	0.011	0.015	0.011	0.014	0.014	0.010	0.016	0.020	0.022

Appendix C

Equations relating to bulk density error

Ratio of true to intended soil bulk density

$$R = \frac{\rho_{s'}}{\rho_s} = \frac{\frac{M_s}{V_{s'}}}{\rho_s} = \frac{\cancel{\rho_s}(V_T - V_c)}{\cancel{\rho_s} V_{s'}} = \frac{V_T - V_c}{V_{s'}} = \frac{V_T - V_c}{V_T - V_{c'}}$$

$$= \frac{V_T - V_c}{V_T - V_g - V_{p'}} = \frac{V_T - V_c}{V_T - V_g + V_{p'} - V_p \frac{\rho_p}{\rho_{p'}}} = \frac{V_T - V_c}{V_T - V_g + V_{p'}\left(1 - \frac{\rho_p}{\rho_{p'}}\right)}$$

$$= \frac{V_T - \chi_c V_T}{V_T - \chi_c V_T + \chi_p V_T \left(1 - \frac{\rho_p}{\rho_{p'}}\right)} = \frac{1 - \chi_c}{1 - \chi_c + \chi_p \left(1 - \frac{\rho_p}{\rho_{p'}}\right)}$$

In Experiment 1 where there was no glass

$$\chi_c = \chi_p$$

$$R = \frac{1 - \chi_p}{1 - \chi_p + \chi_p \left(1 - \frac{\rho_p}{\rho_{p'}}\right)} = \frac{1 - \chi_p}{1 - \chi_p \frac{\rho_p}{\rho_{p'}}}$$

Derivation of equations for error introduced by incorrect pumice bulk density

$\boldsymbol{\rho}_s$ = target soil bulk density

$\boldsymbol{\rho}_{s'}$ = actual soil bulk density

$\boldsymbol{\rho}_p$ = apparent pumice bulk density

$\boldsymbol{\rho}_{p'}$ = true pumice bulk density

$\boldsymbol{\chi}_p$ = intended volumetric proportion of pumice

V_p = intended volume of pumice

$$V_p = \chi_p V_T$$

where V_T = total volume of core

$V_{p'}$ = actual volume of pumice

$$V_{p'} = V_p \frac{\rho_p}{\rho_{p'}}$$

V_c = intended volume of clasts (glass + pumice)

$$V_c = V_T \chi_c$$

where χ_c =volumetric proportion of clasts (pumice + glass)

$V_{c'}$ = actual volume of clasts

$$V_{c'} = V_g + V_{p'}$$

where V_g = volume of glass used

$$V_g = V_c - V_p$$

V_s = intended volume of soil

$$V_s = V_T - V_c$$

$V_{s'}$ = actual volume occupied by soil

$$V_{s'} = V_T - V_{c'}$$

M_s = mass of soil used

$$M_s = \rho_s (V_T - V_c)$$